AMIGO3 gene expression and function during oligodendrocyte differentiation in the central nervous system

By

Majed Almutairi

A thesis submitted to the University of Birmingham for the degree of

DOCTOR OF PHILOSOPHY

Neuroscience and Ophthalmology

Institute of Inflammation and Ageing

College of Medical and Dental Sciences

University of Birmingham

April 2024

UNIVERSITY OF
BIRMINGHAM

University of Birmingham Research Archive

e-theses repository

This unpublished thesis/dissertation is copyright of the author and/or third parties. The intellectual property rights of the author or third parties in respect of this work are as defined by The Copyright Designs and Patents Act 1988 or as modified by any successor legislation.

Any use made of information contained in this thesis/dissertation must be in accordance with that legislation and must be properly acknowledged. Further distribution or reproduction in any format is prohibited without the permission of the copyright holder.

Abstract

Demyelination causes disruption to neuronal signalling and occurs in many neurodegenerative diseases or in response to brain injury. There are no cures available for demyelinating diseases, including multiple sclerosis (MS), the most common autoimmune inflammatory disease in the central nervous system (CNS). Current approaches to treat MS focus on anti-inflammatory drugs, which prevent demyelination progression and reduce clinical relapses, but do not allow repair or replacement myelin. A natural repair process called remyelination can occur following demyelination. Remyelination can help to repair demyelinating plaques and protect axons from degeneration, but endogenous remyelination is inefficient and fails with ageing and disease progression, Improving remyelination is therefore an important for the focus for the development of MS therapies. Studies of animal models have to led to the discovery of new therapeutic targets which can promote endogenous remyelination. An example is the leucine rich repeat protein (LRRP) leucine rich repeat and immunoglobulin-like domain containing protein 1 (LINGO1). Inhibition of LINGO1 promoted remyelination in several animal models of demyelination, but clinical inhabitation of LINGO1 showed unsuccessful results in clinical trials. We considered the idea that the LINGO1 clinical trials failed due to compensation from another LRRP, amphoterin-induced gene and open reading fram-3 (AMIGO3). AMIGO3 is upregulated more rapidly than LINGO1 after spinal cord injury (SCI) in animal models, and also increases in expression rapidly after axotomy in culture of dorsal root ganglion neurons and retinal ganglion cells. Importantly, AMIGO3 expression is rapidly increased in the CNS during postnatal development when myelinating oligodendrocyte (OL) are generated, and decreases again quickly after myelination begins. AMIGO3 may therefore act a regulator of OL differentiation, and its inhibition could be an alternative therapeutic target for demyelinating diseases.

Considering the above, the first aim of this project was to study the function of AMIGO3 using in vitro models of OL differentiation. For this work, a primary mixed glial culture system was developed to study OL differentiation during early stage of CNS development. Using this system we found that AMIGO3 is downregulated in mixed glial cultures during OL differentiation. We also found that downregulation of AMIGO3 expression by siRNA resulted in the upregulation of OL maturation. On the other hand, increased AMIGO3 levels produced by treatment with recombinant AMIGO3 reduced OL maturation, and activated RhoA GTP activity, a molecule involved in AMIGO3 intracellular signalling. These findings suggest that AMIGO3 downregulates OL differentiation via RhoA GTP signalling.

AMIGO3 is known to engage in homotypic interactions, thus expression on different glial cells could allow cell to cell signalling. Also, AMIGO3 is expressed in cells of the OL lineage and astrocytes, thus AMIGO3 expression in non-OL glia could provide a signal to regulate OL differentiation. Considering this idea, the second aim in this thesis was to compare the expression of AMIGO3 and LINGO1 in primary cultures of astrocytes and microglia. Using Western blot and immunocytochemistry we found strong expression of AMIGO3 proteins in astrocytes, but not in microglia. Surprisingly, we also found that astrocytes express LINGO1 proteins. This work shows that astrocytes, but not microglia, are an abundant source of both AMIGO3 and LINGO1, which together could influence OL differentiation and myelin formation and repair.

Acknowledgements

I extend sincere thanks to my supervisors, Dr Daniel Fulton and professor Zubair Ahmed, for their relentless encouragement, guidance, support and motivation throughout my PhD project. Thanks for spent many hours during my PhD studies to discuss and provide the perfect scientist environment. Thank you, professor Zubair Ahmed, for helping, supporting and encouraging me to complete my PhD study. I cannot thank you enough, Dr Daniel for all time teaching me different lab techniques such as, brain dissection, co-culturing, cell isolation, Western blotting, knockdown and stimulating target genes, cells treatment, immunocytochemistry (ICC), immunohistochemistry (IHC), activating cell receptors assays and many other assays, data densitometry, data normalization, data analyzing and many scientific techniques throughout the years. I am grateful to Dr Daniel Fulton and professor Zubair Ahmed for the wonderful and amazing training in CNS myelination, demyelination, and remyelination studies. Thank you for your help and trust, allowing me deal with my project and discover the field of myelinating cells (OPC and OL), inhibitory factors and develop my scientific research. I believe this project would be impossible to complete without Dr Daniel Fulton and professor Zubair Ahmed involvement and I am deeply indebted to them for supporting and guidance. Thank you so much, I would not have the PhD qualification without my supervises help. Also, I am grateful and thankful past and present members of the Neuroscience and Ophthalmology lab who have supported and helped me during my PhD study.

Secondly, especial thank to Leah Bailey (PGR administrator) who supported and helped me with many official paperwork related to my PhD studies. Further, I would like to thank to other contributed members at University of Birmingham. Also, I would like to thanks all my past committee members Professor Andy Clark, Dr Graham Wallace, Dr Rachel Vincent who have been honesty and integrity to provide me with brilliant comments and suggestions throughout

my PhD years. Further, lovely thanks to Nadene Bryan (PA to Prof Tony Belli) and our grateful lab managers Sue Rhodes and Deb Croom-Carter thanks for all technical support in our lab. Especial thanks to Keven, Ashleigh Renelt and other members who extremely managed and provided me with all the materials were used in my lab work. Finally, I would like to thanks the Biomedical Services Unit (BMSU) at University of Birmingham for suppling and providing animals were dissected to preformed a primary cultures were fundamental used in myelination, demyelination and remyelination studies.

Declaration

This thesis is wholly dedicated to my wonderful and grateful parents ‘Mrs. Hallah Maziad Almutairi and Mr. Mutlaq Ammar Almutairi’ for being the happiness and success of my life. Further, this work is dedicated to my wonderful wife ‘Mrs. Lujain Almutairi’ who was patient with my difficulty time and to my lovely kids Miss Jana, Ghala, Deena, Ameirah Almutairi and Mr. Khaled Almutairi. Further, this thesis dedicated to my sister’s Mrs. Hassah, Mrs. Maha Almutairi and to my brother’s Mr. Fahad, Mr. Abdullah, Dr Khaled, and Mr. Abdulmajeed Almutairi, who were so generous during my PhD studies. Finally, to my best friends Mr. Majed Salem Al-Dosari, Mr. Fahad Halal Alharbi, Mr. Thamer Al-Tamimi, Mr. Ali Al-Tamimi, Mr. Salem Al-Tamimi, Mr. Osama Oudat and Mrs. Tamar Jagmaidze who helped and supported me a lot throughout my PhD years.

Majed Almutairi, April 2024

COVID-19 impact statement

The project was lab based and depended critically on a supply of brain tissues from the mouse colony in BMSU. The lab closed on 20th March and re-opened on 28th July and was therefore closed for 4 months. When our group went back to work we had to work part-time to meet the pandemic restrictions of the University, which we led to limitations in time for my experiments. Furthermore, BMSU stopped mouse breeding for all experiments during the closed period and did not restart this breeding until early July – it then took until 14th October to re-start my animal work. These delays slowed down my research at a time when I was gaining momentum in the lab.

Also my registration was extended during the Pandemic. However, the delays and extension had additional effects since I had to extend my visa to fit into the extension. This process was very complicated due to issues with the Home Office and the University administration. This process was stressful and required a lot of my attention that should have been used on my project.

Further, the COVID disruption delayed the breeding of an AMIGO-3 knockout mouse line imported from USA. It took BMSU many months to restart work to rederive imported mice, and once they finally started on our knockout line discovered that the imported material had been lost during the pandemic when they moved the frozen samples to storage. The line was re-ordered but could not be generated in time for this project. We attempted to replace this work using an AAV-shRNA vector but this work could not be completed in time. These issues were a big setback for my project as the knockout mouse formed a key part of my plans for an in vivo chapter. I also had additional caring responsibilities during the pandemic. My wife was pregnant and it was a tough time for her. During that time the women hospital services were

limited and most contact was by phone appointments. I admit it was difficult for me to manage my time between my online studies and supporting my wife through these health circumstances.

TABLE OF CONTENTS:

CHAPTER 1 INTRODUCTION ----------1

1.1 OVERVIEW OF THE CENTRAL NERVOUS SYSTEM (CNS) ----------2

1.1.1 Brain----------2

1.1.2 Spinal cord----------6

1.1.3 The role of blood brain barrier (BBB)----------8

1.2 OVERVIEW OF THE PERIPHERAL NERVOUS SYSTEM (PNS) ---------- 10

1.3 GLIAL CELLS IN CNS ---------- 11

1.3.1 Oligodendrocyte (OL)---------- 12

1.3.2 Astrocyte ---------- 14

1.3.3 Microglia ---------- 17

1.4 MYELINATION AND MAMMALIAN NERVOUS SYSTEM ---------- 18

1.4.1 Overview ---------- 18

1.4.2 Myelin structure and function---------- 18

1.5 MYELIN INJURY AND REPAIR ---------- 22

1.5.1 Demyelination---------- 22

1.5.2 Remyelination ---------- 23

1.5.3 Multiple sclerosis (MS) ---------- 24

1.5.3.1 Mechanisms of inflammatory demyelination in MS ---------- 28

1.5.3.2 Treatment of MS ---------- 28

1.5.3.2.1 Immunomodulation---------- 29

1.5.3.2.2 Stem cell transplantation---------- 32

1.5.3.2.3 Remyelination ---------- 32

1.5.3.2.4 Neuroprotection ---------- 32

1.6 BALO'S DISEASE (CONCENTRIC SCLEROSIS)---------- 33

1.7 NEUROMYELITIS OPTICA (NO)---------- 34

1.8 LEUCINE RICH REPEAT PROTEINS IN THE CNS ---------- 34

1.8.1 AMIGO3 and LINGO1 ---- *35*

1.8.2 LRRP in CNS injury ---- *38*

1.9 STUDY RATIONALE ---- 39

1.10 HYPOTHESIS AND AIMS ---- 40

CHAPTER 2 METHOD AND MATERIALS ---- 42

2.1 ANIMALS ---- 43

2.2 CELL LINE CULTURES *IN VITRO* ---- 43

2.2.1 Baby Hamster Kidney (BHK) culture ---- *43*

2.2.2 Freezing and storing BHK cells ---- *44*

2.3 PRIMARY CENTRAL NERVOUS SYSTEM (CNS) CULTURES ---- 45

2.3.1 Primary mixed glial culture ---- *45*

2.3.2 Astrocyte cultures ---- *47*

2.3.3 Microglial culture ---- *49*

2.3.4 Splitting and re-plating primary cells ---- *50*

2.4 EXPERIMENTAL TREATMENT OF MIXED GLIA AND BHK CELLS ---- 51

2.4.1 Recombinant Fc AMIGO3 treatment in BHK and primary mixed glial cultures ---- *51*

2.4.1.1 Principle of recombinant Fc AMIGO3 treatment ---- 51

2.4.1.2 Treatment procedure ---- 52

2.4.2 siRNA transfection in primary and BHK co-culture in vitro ---- *52*

2.4.2.1 Principle of siRNA ---- 52

2.4.2.2 siRNA transfection procedure in primary and BHK cultures ---- 53

2.5 WESTERN BLOT ---- 53

2.5.1 Overview of Western blotting ---- *53*

2.5.2 Protein extraction ---- *55*

2.5.3 Protein assay ---- *56*

2.5.4 Protein electrophoresis and transfer ---- *58*

2.5.5 Primary and secondary antibodies ---- *59*

2.5.6 Electrochemiluminescence detection ---- *60*

2.5.7 WB image quantification ---- *61*

2.5.8 Blot stripping ---- *62*

2.6 IMMUNOCYTOCHEMISTRY (ICC) ---- 63

2.6.1 principles of Immunocytochemistry (ICC) ---- *63*

2.6.2 Immunostaining of cell cultures ---- *64*

2.6.3 Imaging of ICC ---- *66*

2.7 RT-QPCR ---- 66

2.7.1 RNA isolation ---- *66*

2.7.2 RT-qPCR samples processing ---- *67*

2.7.3 RT-qPCR quantification ---- *68*

2.8 RHOA ACTIVATION ASSAY (G-LISA) ---- 69

2.8.1 Principles of RhoA activation assays ---- *69*

2.8.2 RhoA activation assays ---- *69*

2.8.3 RhoA activation assay quantification ---- *71*

2.9 STATISTICAL ANALYSIS ---- 72

CHAPTER 3 IN VITRO ANALYSIS OF AMIGO3 EXPRESSION AND FUNCTION DURING OL DIFFERENTIATION ---- 74

3.1 RATIONALE ---- 75

3.1.1 The NgR1 and p75 signalling pathway downregulates OL differentiation ---- *75*

3.1.2 Potential for AMIGO3-AMIGO3 homotypic signalling to influence OL differentiation *77*

3.2 HYPOTHESIS ---- 78

3.2.1 Aims ---- *78*

3.3 MATERIALS AND METHOD ---- 79

3.4 EXPERIMENTAL DESIGN ---- 79

3.4.1 Western blot ---- *79*

3.4.2 Immunocytochemistry ---- *79*

3.4.3 Cell cultures ---- *80*

3.4.3.1 Primary mixed glial culture ---- 80

3.4.3.2 BHK culture ---- 80

3.4.4 siRNA transfection ---- *80*

3.4.5 Recombinant AMIGO3 studies ---- *81*

3.4.6 RhoA activation assays ---- *81*

3.5 RESULTS ---- 81

3.5.1 Immunocytochemical analysis of OL differentiation in mixed glial culture ---- *81*

3.5.2 Western blot analysis of AMIGO3 and LINGO1 expression during OL differentiation in mixed glial cultures. ---- *86*

3.5.2.1 Analysis of OL differentiation in mixed glial cultures. ---- 87

3.5.2.2 AMIGO3 and LINGO1 expression during OL differentiation in mixed glial cultures 89

3.5.2.3 Summary of AMIGO3 and LINGO1 expression during OL differentiation in mixed glial cultures ---- 93

3.5.3 Studying AMIGO3 function in OL differentiation: siRNA studies ---- *94*

3.5.3.1 Optimizing knockdown of AMIGO3 in BHK cells ---- 95

3.5.3.2 siRNA knockdown of AMIGO3 in BHK cells ---- 96

3.5.3.3 siRNA knockdown of AMIGO3 in mixed glial cultures ---- 100

3.5.4 studying AMIGO3 function in OL differentiation: recombinant AMIGO3 studies ---- *104*

3.5.4.1 RhoA activation assay validation in BHK cells ---- 106

3.5.4.1.1 RhoA activation activator study ---- 106

3.5.4.1.2 Recombinant AMIGO3 stimulates RhoA in BHK: 1 and 2 µg/mL ---- 107

3.5.4.2 Effect of 2 µg/mL of recombinant AMIGO3 on RhoA activation in mixed glial cultures 109

3.5.4.2.1 Western blot Analysis of OL differentiation after treatment with recombinant AMIGO3 111

3.5.4.2.2 Immunocytochemical analysis of OL differentiation after treatment with recombinant AMIGO3 ---- 116
3.6 GENERAL DISCUSSION ---- 118
3.6.1 Western blot detection of AMIGO3 ---- *118*
3.6.2 Mixed glial cultures demonstrate OL differentiation ---- *118*
3.6.3 Mixed glial cultures showed a similar pattern of AMIGO3 and LINGO1 expression compared to previous studies in vivo ---- *119*
3.6.4 Evidence that AMIGO3 plays a role in regulating OL differentiation ---- *119*
3.6.5 Involvement of RhoA GTP pathway in AMIGO3 effects OL differentiation ---- *120*
3.6.6 Limitations ---- *121*
3.6.7 Future studies ---- *121*
3.7 CONCLUSION ---- 123
CHAPTER 4 AMIGO3 AND LINGO1 EXPRESSION IN ASTROCYTES ---- 124
1.1 RATIONALE ---- 125
4.1.1 AMIGO3 expression in astrocytes ---- *125*
4.1.2 LINGO1 expression in astrocytes ---- *126*
4.1.3 AMIGO3 and LINGO1 expression in microglia ---- *126*
4.2 HYPOTHESIS ---- 127
4.2.1 Aims ---- *127*
4.3 METHOD AND MATERIALS ---- 128
4.4 EXPERIMENTAL DESIGN ---- 128
4.4.1 Cell cultures ---- *128*
4.4.1.1 Astrocyte cultures ---- 128
4.4.1.2 Microglial cultures ---- 129
4.4.2 Western blot ---- *130*
4.4.3 RT-qPCR ---- *130*
4.4.4 Immunocytochemistry ---- *130*

4.5 RESULTS ---- 131
4.5.1 Confirming GFAP antibody in astrocyte cultures ---- 131
4.5.2 AMIGO3 expression in primary astrocyte cells ---- 132
4.5.3 LINGO1 expression in primary astrocyte cultures ---- 135
4.5.4 RT-qPCR of AMIGO3 and LINGO1 mRNA. ---- 138
4.5.5 AMIGO3 and LINGO1 expression in primary microglial cultures ---- 141
4.6 GENERAL DISCUSSION ---- 143
4.6.1 Western blot and ICC detection of AMIGO3 and LINGO1 in astrocytes ---- 143
4.6.2 Western blot and ICC detection AMIGO3 and LINGO1 in microglia ---- 143
4.6.3 Limitations ---- 144
4.6.4 Future study ---- 144
4.7 CONCLUSION ---- 146
CHAPTER 5 GENERAL DISCUSSION ---- 147
5.1 AMIGO3 IN MIXED GLIAL CULTURES ---- 148
5.1.1 AMIGO3 in mixed glial culture ---- 148
5.1.2 siRNA (suppression) ---- 149
5.1.3 Recombinant human AMIGO3 ---- 149
5.1.4 The roles of leucin-rich repeat protein in mixed glial cell cultures ---- 151
5.1.5 AMIGO3 mechanism of action in OL ---- 152
5.1.6 AMIGO3 role in multiple sclerosis ---- 153
5.2 LIMITATION AND FUTURE STUDIES ---- 153
5.2.1 Models of myelination ---- 153
5.2.2 Astrocytes and AMIGO3 expression ---- 154
5.3 FINAL CONCLUSIONS ---- 155

TABLE OF FIGURES:

FIGURE 1.1: DIAGRAM SHOWING THAT THE CNS CONSISTS OF THE BRAIN AND SPINAL CORD. ...5

FIGURE 1.2: THE ANATOMY OF THE SPINAL CORD AND SPINAL MENINGES. ...8

FIGURE 1.3: THE MAIN TYPE OF GLIAL CELLS IN THE PNS AND CNS. ...12

FIGURE 1.4: THE STAGES OF OL DEVELOPMENT AND THE DIFFERENT MORPHOLOGICAL FEATURES OF OPC. ...14

FIGURE 1.5: FORMATION OF THE GLIAL SCAR. ...16

FIGURE 1.6: COMPARISON OF PNS AND CNS MYELINATION. ...19

FIGURE 1.7: THE FUNCTION OF MAJOR MYELIN PROTEINS AND THE STRUCTURE OF MYELIN. ...20

FIGURE 1.8: LOCATION AND STRUCTURE OF NODES OF RANVIER. ...21

FIGURE 1.9: THE DISTINCTION BETWEEN A HEALTHY MYELINATED AXON AND AN AXON AFTER DEMYELINATION. ...23

FIGURE 1.10: HISTOLOGY OF MS LESION DEMONSTRATING DEMYELINATION AND IMMUNE CELL ACTIVITY ...27

FIGURE 1.11: STRUCTURAL DIFFERENCES AND SIMILARITIES BETWEEN AMIGO3 AND LINGO1. ...36

FIGURE 1.12: AMIGO3 AND LINGO1 SIGNALLING IN NEURONS. ...38

FIGURE 2.1: TYPICAL BHK CULTURE THAT HAS REACHED AROUND 60% CONFLUENCY. ...44

FIGURE 2.2: PRIMARY MIXED GLIAL CULTURE AT 9 DAYS IN VITRO (DIV). ...47

FIGURE 2.3: ASTROCYTES ISOLATED FROM MIXED GLIAL CULTURE BY SHAKING THE FLASK OVERNIGHT. ...48

FIGURE 2.4: IMAGE SHOWS MICROGLIAL CELLS ISOLATED FROM PRIMARY MIXED GLIAL CULTURES. ...50

FIGURE 2.5: PROTEIN ELECTROPHORESIS SETUP. ...55

FIGURE 2.6: PROTEIN ASSAY SETUP. ...57

FIGURE 2.7: BOVINE SERUM ALBUMIN CALIBRATION CURVE. 58

FIGURE 2.8: DENSITOMETRY IN IMAGE J. 62

FIGURE 2.9: PRINCIPLE OF IMMUNOCYTOCHEMISTRY. 63

FIGURE 2.10: A SAMPLE RT-QPCR PLATE DEPICTING NTC AND CDNA SAMPLES FOR VARIOUS PRIMERS. 68

FIGURE 2.11:RHOA ACTIVATION ASSAY EXAMPLE. 71

FIGURE 3.1: DIAGRAM SHOWING THE AMIGO3/LINGO1/P75/TROY AND NGR1 SIGNALLING PATHWAY WITH LINKS TO THE ACTIN CYTOSKELETON. 77

FIGURE 3.2: DIFFERENT MARKERS PROTEINS FOR OL LINAGE DEVELOPMENT USED IN THIS STUDY. 83

FIGURE 3.3: REPRESENTATIVE POSITIVE STAINING FOR OLIG2 AND CC1 IN PRIMARY MIXED GLIAL CULTURE. 85

FIGURE 3.4: QUANTIFICATION OF OLIG2 AND CC1 STAINING IN PRIMARY MIXED GLIAL CULTURE. 86

FIGURE 3.5: (A) REPRESENTATIVE BLOTS OBSERVED WITH ANTI-CNPASE . (B) QUANTIFICATION OF THE CNPASE EXPRESSION IN PRIMARY MIXED CELLS GROUPS 88

FIGURE 3.6: (A) REPRESENTATIVE WB OF BIOTECHNE-MAB ANTI-AMIGO3 AB . (B) QUANTIFICATION OF AMIGO3 EXPRESSION IN PRIMARY MIXED GLIAL CULTURE GROUPS 90

FIGURE 3.7: (A) REPRESENTATIVE BLOTS OBSERVED WITH ABCAM ANTI-LINGO. (B) QUANTIFICATION OF LINGO1 EXPRESSION IN PRIMARY MIXED GLIAL CULTURES. 92

FIGURE 3.8: SUMMARY OF CNPASE, AMIGO3 AND LINGO1 PROTEIN 94

FIGURE 3.9: REPRESENTATIVE AMIGO3 STAINING IN BHK CELLS. 95

FIGURE 3.10: (A) REPRESENTATIVE BLOT OF ANTI-AMIGO3 BANDS . (B) QUANTIFICATION OF AMIGO3 EXPRESSION IN BHK CELL TRANSFECTED WITH 30 NM OF NEGATIVE CONTROL AND AMIGO3 SIRNA. 97

FIGURE 3.11: (A) REPRESENTATIVE BLOT OF AMIGO3 BANDS . (B) QUANTIFICATION OF AMIGO3 EXPRESSION IN BHK CELLS, TRANSFECTED WITH EITHER 50 NM OF NEGATIVE CONTROL OR AMIGO3 SIRNA. 99

FIGURE 3.12: (A) REPRESENTATIVE WB OF ANTI-AMIGO3 AND ANTI-CNPASE EXPRESSION FOLLOWING TREATMENT WITH 30 NM AMIGO3 SIRNA. (B-C) QUANTIFICATION OF AMIGO3 (B) AND CNPASE (C) EXPRESSION IN MIXED GLIAL CULTURES TRANSFECTED WITH 30 NM NEGATIVE CONTROL AND AMIGO3 SIRNA. 101

FIGURE 3.13: (A) REPRESENTATIVE WB WITH ANTI-AMIGO3 AND ANTI-CNPASE IN PRIMARY MIXED GLIAL CULTURE FOLLOWING TRANSFECTION WITH 50 NM OF CONTROL OR AMIGO3 SIRNA. (B-C) QUANTIFICATION OF AMIGO3 (B) AND CNPASE (C) EXPRESSION IN MIXED GLIAL CULTURES TRANSFECTED WITH 50 NM OF AMIGO3 OR CONTROL SIRNA. 103

FIGURE 3.14: SCHEMATIC SHOWING HYPOTHESISED ACTION OF AMIGO3 ON THE AMIGO3/P75/NGR1 SIGNALLING COMPLEX 105

FIGURE 3.15: QUANTIFICATION OF RHOA ACTIVITY IN BHK SAMPLES TREATED WITH A RHOA ACTIVATOR (CALPEPTINTUKEY'S 107

FIGURE 3.16: QUANTIFICATION OF RHOA ACTIVITY IN BHK CELLS. 109

FIGURE 3.17: QUANTIFICATION OF RHOA GTP ACTIVITY IN PRIMARY CULTURES. 111

FIGURE 3.18: (A) REPRESENTATIVE WB OF AMIGO3 AND CNPASE PROTEINS IN MIXED GLIAL CULTURES. (B-C) QUANTIFICATION OF AMIGO3 (B) AND CNPASE (C) EXPRESSION IN MIXED GLIAL CULTURES TREATED WITH 1 μG/ML OF RECOMBINANT AMIGO3 OR LEFT UNTREATED (CONTROL). 113

FIGURE 3.19: (A) REPRESENTATIVE WB OF AMIGO3 AND CNPASE IN MIXED GLIAL CULTURES. (B-C) QUANTIFICATION OF AMIGO3 (B) AND CNPASE (C) EXPRESSION IN MIXED GLIAL CULTURES TREATED WITH 2 μG/ML OF RECOMBINANT AMIGO3 OR LEFT UNTREATED (CONTROL). 115

FIGURE 3.20: RECOMBINANT AMIGO3 TREATMENT IN PRIMARY MIXED GLIAL CULTURE..... 117

FIGURE 4.1: IMAGE FROM A PRIMARY ASTROCYTE CULTURE DEMONSTRATES ASTROCYTE CELLS 24 HOURS FOLLOWING THE ISOLATION. 129

FIGURE 4.2: EXPRESSION OF GFAP IN ASTROCYTE CULTURES..... 132

FIGURE 4.3: DETECTION OF AMIGO3 IN PRIMARY ASTROCYTE CULTURE. 134

FIGURE 4.4: QUANTIFICATION OF THE NUMBER OF CELLS EXPRESSING AMIGO3 IN PURIFIED ASTROCYTE CULTURES 135

FIGURE 4.5: DETECTION OF LINGO1 IN PRIMARY ASTROCYTE CULTURE. 137

FIGURE 4.6: QUANTIFICATION OF THE NUMBER OF CELLS EXPRESSING LNGO1 IN PURIFIED ASTROCYTE CULTURES 138

FIGURE 4.7: RT-QPCR ANALYSIS OF GFAP, CD11B AND PDFRA EXPRESSION IN PRIMARY ASTROCYTE CULTURES. RNARNA 139

FIGURE 4.8: RT-QPCR ANALYSIS OF AMIGO3 AND LINGO1 EXPRESSION IN PRIMARY ASTROCYTE CULTURE. MRNA 140

FIGURE 4.9: DETECTION OF MAB-2375 ANTI-AMIGO3, AB-23631 ANTI-LINGO1 AND ABCAM-133357 ANTI-CD11B EXPRESSION IN PRIMARY MICROGLIA CULTURE..... 142

LIST OF TABLES:

TABLE 1-1: INTERFERON BETA THERAPIES THAT HAVE BEEN APPROVED FOR THE TREATMENT OF RELAPSING MS.....31

TABLE 2-1: BRAIN DISSECTION MEDIUM COMPONENTS. 45

TABLE 2-2: SHOWS PRIMARY MIXED GLIAL SERUM MEDIUM COMPONENTS.....46

TABLE 2-3: PRIMARY AND SECONDARY ANTIBODIES USED FOR DETECTING PROTEINS IN WB ...59

TABLE 2-4: PRIMARY AND SECONDARY ANTIBODIES WERE USED FOR STAINING AND DETECTING PROTEINS IN IMMUNOCYTOCHEMISTRY 65

TABLE 2-5: LIST OF PRIMERS USED IN THIS INVESTIGATION. 69

LIST OF ABBREVIATIONS:

AB	Antibody
AMIGO3	Amphoterin-induced gene and open reading frame 3
BBB	Blood brain barrier
BHK	Baby Hamster Kidney
BMSU	Biomedical Services Unit
CC1	Adenomatous polyposis coli
cDNA	Complementary DNA
CD11b	Leukocyte specific receptor
CNPase	2', 3'-cyclic-nucleotide 3'-phosphodiesterase
CNS	Central nervous system
DAPI	4', 6-diamidino-2-phenylindole
DIV	Days in vitro
DMEM	Dulbecco's modified Eagle's medium
DNA	Deoxyribonucleic acid
GFAP	Glial fibrillary acidic protein
HRP	Horse radish peroxidase
ICC	Immunocytochemistry
IFN	Interferon
Ig	Immunoglobulin
IHC	Immunohistochemistry
IL	Interleukins
LIMK	LIM-domain containing protein kinases
LINGO1	Leucine rich repeat and immunoglobulin-like domain-containing protein 1
LRR	Leucin-rich repeat
LRRP	Leucin-rich repeat protein
MBP	Myelin basic protein
MOG	Myelin oligodendrocyte glycoprotein
mRNA	Messenger RNA
MS	Multiple Sclerosis
NgR1	Neurite outgrowth inhibitor-66 receptor 1
NG2	Neurone/glial antigen 2

OL	Oligodendrocyte
OPC	Oligodendrocyte precursor cell
PBS	Phosphate buffer saline
PDGF	Platelet-derived growth factor
PDGFRa	Platelet-derived growth factor α receptor
PNS	Peripheral nervous system
p75	Neurotrophin receptor
RhoA	Ras homolog gene family member A
RhoA GTP	RhoA guanosine triphosphate
RNA	Ribonucleic acid
ROCK	Rho-associated protein kinase (ROCK)
RT	Room temperature
RT-qPCR	Reverse transcription quantitative polymerase chain reaction
SCI	Spinal cord injury
SDS	Sodium dodecyl sulphate
siRNA	Short interfering RNA
TBST	Tween-Tris buffered saline
TROY	Tumor necrosis factor receptor superfamily, member 19
Th	T helper
VZs	Ventricular zones

Chapter 1 Introduction

1.1 Overview of the central nervous system (CNS)

The nervous system is the master controller, regulating body functions and communication throughout the whole body. The nervous system is composed of two main systems, the central nervous system (CNS), which includes the brain and spinal cord (Figure 1.1), and the peripheral nervous system (PNS), which is located outside of the CNS (Cross, 2005). The nervous system is responsible for all body functions such as, reflexes, cognition, emotion, moving, breathing, pain sensation, vision and sensory processing (Figure: 1.1) (Tata, Ruhrberg and Fantin, 2015). The main function of the PNS is to connect the CNS to limbs and organs and essentially detect peripheral stimuli and carry the signals towards the brain (Catala and Kubis, 2013). Additionally, the PNS and CNS have different functions, different physiologies, and use different transmitters to transmit information. Furthermore, the CNS is separated by a layer of ependymal cells that produce the cerebral spinal fluid (CSF) and form the blood-cerebrospinal fluid barrier, and by the blood brain barrier (BBB), formed from epithelial cells and various glia, which supports the brain, and stops the buildup of toxic substances, pharmaceuticals, and pathogens from entering the brain (Patel *et al.*, 2009). Further, tight-junctions between epithelial cells in the BBB maintain CNS homeostasis and protect the CNS from pathogens (Newell and Tessa Hedley-Whyte, 2003).

1.1.1 Brain

The human brain is the most complex and delicate organ in the body. The brain is responsible for controlling all of the bodies functions including movement, interpreting sensory information and controlling behavior. It has many different components with each being responsible for specific functions. The major divisions of the brain are the cerebrum, brainstem, and the cerebellum (Figure 1.1) (Raichle *et al*., 2010). The cerebrum is the biggest

part of the vertebrate brain, constituting about 90% of the brain volume, and being composed of two cerebral hemispheres (Figure 1.1). The cerebrum contains more neurons than any other part of the brain, and through connections with other regions of the brain and spinal cord control key functions such as somatosensation, hearing, memory, cognition, language, emotions, motor, and vision (Glickstein et al., 2007). The two hemispheres of the cerebral cortex, consisting of grey matter (containing neuronal cell bodies, dendrites and axons) remain in contact and communication with one another via a thick band of white matter (containing bundles of myelinated fibers) called the corpus callosum (Chauhan *et al.*, 2021). Each hemisphere is divided into a frontal, parietal, occipital, and temporal lobe, and each lobe is involved in a range of different functions (Figure 1.1) (Bui and Das, 2022).

The brainstem is the lower part of the brain that connects the brain to the spinal cord (Figure 1.1). The major function of the brainstem is to connect the input signals from the body to specific target in the brain such as, thalamus, amygdala and hypothalamus. These processes are important for basic physiological functions such as breathing and cardiovascular activity, and modulation of states such as awareness, consciousness and sensitivity to pain via somatosensory function (Vila-Pueyo, Hoffmann, Romero-Reyes and Akerman et al., 2018). Brainstem connections are mediated via multiple systems including the posterior column-medial lemniscus pathway, corticospinal track for motor signals, vibration sensation and proprioception, spinothalamic tract for temperature, and the trigeminothalamic track for touch and pain signals from the head and face. The brainstem's major division are the midbrain, pons and medulla oblongata, which is the lowest part of brainstem and connected to the spinal cord (Figure 1.1). The midbrain, also known as the tectum, is the smallest part of the brainstem and contains various regions, important for body functions, such as dopaminergic modulation of movement, appetite and the reward system, and auditory and visual pathways.

Furthermore, the superior and inferior colliculus nuclei, red nucleus, substantia nigra, oculomotor nuclear complex, and trochlear nucleus are all part of the midbrain and play important roles in brain function (Ruchalski and Hathout *et al*., 2012).

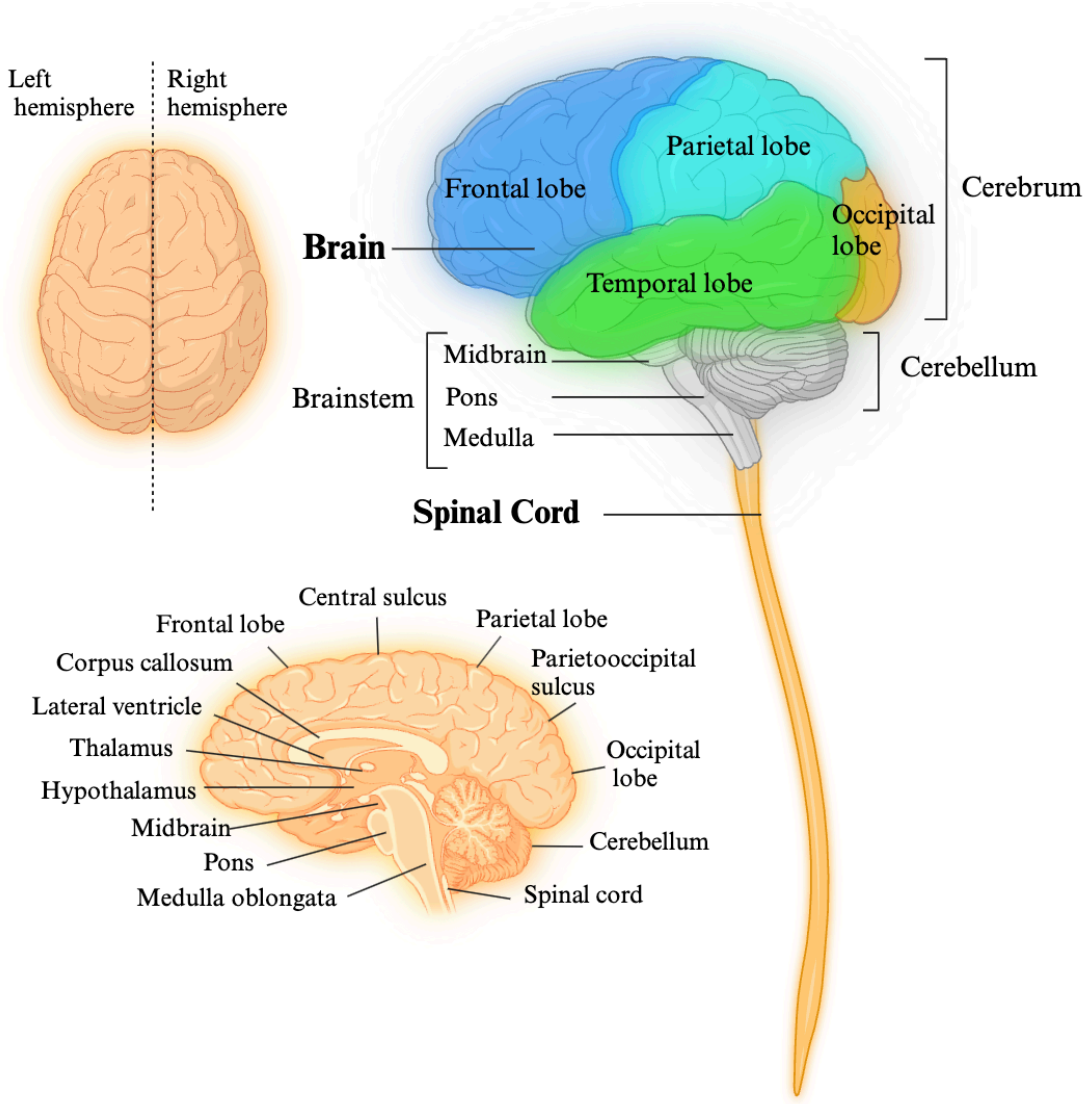


Figure 1.1: Diagram showing that the CNS consists of the brain and spinal cord. Top left: The cerebrum is divided into two hemispheres. Right: Each hemisphere is divided into four lobes (frontal lobe, parietal lobe, occipital lobe and temporal lobe), with the cerebellum and brainstem (midbrain, pons and medulla) located below the cerebrum. Bottom: Cross section of brain showing key structures of cerebrum and brain stem. This figure was generated by BioRender.

1.1.2 Spinal cord

The spinal cord is the lower part of the CNS, located below the brainstem and extending from the medulla oblongata until the lumbar region of the vertebral column. The spinal cord plays an essential role in all communication between the brain and the rest of the body. Signals are sent from the brain to skeletal and visceral muscles via motor neurons in the spinal cord, and sensory information from the bodies organs and skin are sent to the brain via spinal cord sensory neurons (Brodal, 2010). The spinal cord in human is an elongated cylinder shape of about 40 to 45 cm long. The spinal cord consists of white matter in the outer zone and grey matter in the center in an H structure (Figure 1.2). White matter in the spinal cord (and other CNS regions) consists of myelinated axon fiber paths, whose high lipid content provides the white appearance responsible for the name white matter. In contrast, grey matter consists mainly of neuronal and glial cells bodies and dendrites (Brodal, 2010), and lacks organized bundles of myelinated fibers. The spinal cord contains nervous tissue protected by the bony structures of the vertebral column and surrounded with three membranes, the dura mater, arachnoid mater and pia mater (Cramer and Darby, 2013). These membranes are protective layers playing a similar role to the meninges within the brain. The dura mater is the outer layer, while the arachnoid mater is thinner and located between dura mater and the inner pia matter, which all covers the spinal cord for protection (Figure 1.2) (Nógrádi and Vrbová, 2006). The bony vertebrae are essential for protection and support in the spinal cord. The vertebrae consist of 31 segments divided into 5 different regions: 8 cervical, 12 thoracic, 5 lumbar, 5 sacral and 1 coccygeal segment. Six to eight motor and sensory nerve root branches exit and enter the cord, with each group identified depending on their location. For example, the cervical nerves control the head, neck and arms, while the thoracic nerve controls abdominal muscles, and the lumbar and sacral nerves control the lower parts of the body (Diaz and Morales, 2016).

Each spinal nerve branches to supply motor fibers for glands and muscles, and sensory fibers to tissues in the body. Each nerve is linked to the spinal cord by two grey matter roots, one carrying sensory fiber from the PNS is called the dorsal horn, while the ventral horn carries the motor fibers (Nógrádi and Vrbová, 2006; Diaz and Morales, 2016).

The white matter of the spinal cord contains myelinated axons that transmit information upwards and downwards within the spinal cord. The white matter consists of three regions called the dorsal, ventral and lateral columns, while the spinal cord grey matter comprises of the posterior horn, lateral horn, and anterior horn. In addition to these tissues, the spinal cord contains a central canal located inside the grey matter that is filled with cerebrospinal fluid and is connected to the ventricular systems of the brain (Diaz and Morales, 2016).

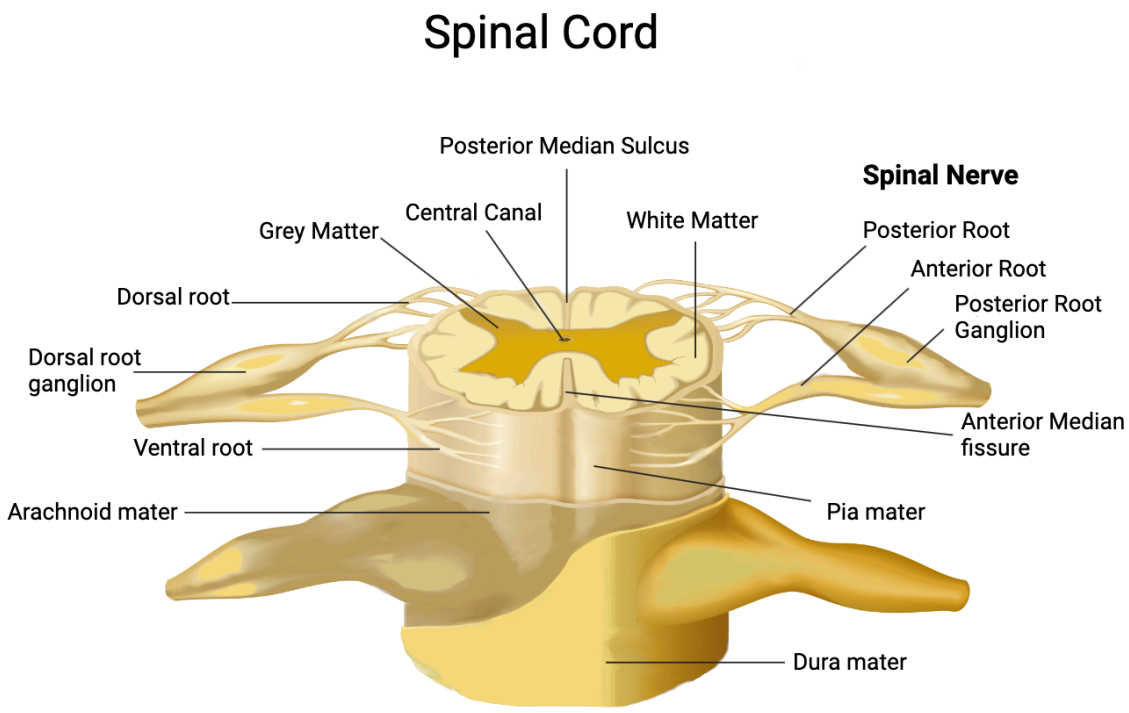


Figure 1.2: The anatomy of the spinal cord and spinal meninges. The spinal cord is composed of a central core of grey matter surrounded by white matter. Spinal nerves consist of a dorsal root carrying sensory fibers from the PNS, and a ventral root carrying motor fibers. The spinal meninges include the pia matter associated with the spinal cord surface, a middle layer called the arachnoid matter, and a tough outer layer called the dura matter. This figure was generated using Biorender and the Image Manipulation Programme.

1.1.3 The role of blood brain barrier (BBB)

Blood vessels are essential for delivering oxygen, ions, and nutrients to organs and tissue throughout the body. The blood vessels that vascularize the brain have special properties, and interactions with glial cells, that allow them to form the blood brain barrier (BBB), which tightly regulates the movement of molecules, ions, and cells from the blood into the brain. The BBB therefore provides s stable environment to support neuronal function and prevent pathogens and toxins from entering the CNS tissues (Daneman and Prat, 2015). Brain

endothelial cells that form the BBB are connected by tight junction proteins which allow the separation of the molecules between the cerebral blood vessels and brain interstitial fluid (Dotiwala, McCausland and Samra, 2023). The BBB is comprised of three cellular barriers which highly adhere between each other. These include the endothelial cell tight junctions, endothelial basement membranes, and the glial podocytes (astrocyte endfeet) (Serlin *et al.*, 2015). In addition, pericytes, another type of glial cell, are highly attached to the endothelial cells and embedded in the basement membrane. Together, these cells help to control and regulate immune cells entry to the CNS, and via contact with astrocytes, play an important role in CNS blood flow regulation (Attwell *et al.*, 2016).

The BBB helps to maintain the extracellular environment surrounding neural cells within the brain, and protects these tissues from toxins and pathogens within the peripheral circulation. BBB dysfunction is implicated in numerous disease states, including inflammatory demyelinating diseases (section 1.5.3), thus BBB properties are important for the diagnosis and the progression of neurological diseases, and are therefore essential to understanding the different functions of the brain during health and disease (Daneman and Prat, 2015).

The complex tight junctions that form between endothelia cells, basement membrane and glial podocytes, results in a capillary wall that forbids the movement of polar and lipid-insoluble compounds across the BBB. As well as protecting the CNS from pathogens, this property of the BBB also prevents the delivery of therapeutic drug to that the CNS diseases (Khaledian et al., 2022). For example, the BBB is largely impermeable to therapeutic monoclonal antibodies with around only 0.1% of antibodies delivered systemically reaching the brain (Kouhi *et al.*, 2021).

Drug delivery across the BBB is therefore a major clinical challenge, and one that needs consideration when a brain targeting drug is being developed. Various approaches have been studied to allow therapeutics to cross the BBB more effectively. Some of these approaches take into consideration existing physiological transportation mechanisms such as, cell-medicated endocytosis, receptor-medicated transport, adsorptive-mediated transcytosis, inhibition of active efflux pumps and the peptide vectors (Khaledian *et al*., 2022). In addition, lipid-based systems such as liposomes and solid lipid nanoparticles, and recombinant viral vectors such as the adeno-associated viral vectors, provide options to achieve the delivery of drugs across the BBB.

1.2 Overview of the peripheral nervous system (PNS)

The PNS is made up of two different systems: somatic nervous system, and autonomic nervous system. The somatic nervous system consists of sensory nerves (afferent nerve fibers) which transfer sensory nerve impulses from the body to the CNS, and motor nerves (efferent nerve fibers) carrying motor signals from CNS to stimulate muscle contraction in various body tissues and skeletal muscles. The somatic nervous system controls the functions we can consciously influence, like the movements of the body such as legs or arms (Akinrodoye and Lui *et al*., 2020). On the other hand, the autonomic nervous system regulates the unconscious functions in the body, such as heart rate, digestion, respiratory rate, urination, and pupillary response. The autonomic nervous system is divided into two different branches, the sympathetic and parasympathetic systems. The sympathetic nervous system controls the response in the body to stressors, and the parasympathetic nerve system dominates in resting situations including feeding, slowing of the heart rate, and dilation of the blood vessels (McCorry, 2007).

Myelin is formed in the PNS by cells called Schwann cells (or neurilemma cells) named after Theodor Schwann who discovered this type of cells in the 19th century. Schwann cells can only myelinate one axon, while in CNS oligodendrocytes (OL) can extend their process to myelinate over 50 axons. Schwann cells are divided into two different types, myelinating and non-myelinating. During development immature Schwann cells first give rise to myelinating Schwann cells, before generating the non-myelinating Schwann cells. Myelinating Schwann cells myelinate axons of both motor and sensory neurons within the PNS, while non-myelinating Schwann cells provide metabolic, physiological and physical support to unmyelinated axons (Mirsky *et al.*, 2002; Monk, Feltri and Taveggia, 2015).

1.3 Glial cells in CNS

The nervous system is built from two types of cells, glial and neurons. Glia, or neuroglia, are the nervous system cells discovered by a group of scientists, Rudolf Virchow, Theodor Schwann, and Robert Remak in the mid 1800s. The main functions of these cells is to provide support and protection to neurons, maintain homeostasis of ions, metabolites and signalling molecules in CNS tissues, and generally support neuronal function (Ndubaku and de Bellard, 2008). Glial cells are typically smaller than neurons, occur in similar number to neurons (e.g., 1:1 ratio), and are estimated to provide around 33% to 60% of the brain mass. Glial cells are therefore the second major component of the CNS.

The main type of glial cells in the CNS are astrocytes, OLs, and microglia (Figure 1.3) (Jessen, 2004). These cells play diverse roles in supporting CNS development and neuronal function, such as the regulation of synaptic functions, maintaining CNS barriers (e.g., BBB), enhancing axonal conduction velocity, and protecting the CNS from infection (Ceprian and Fulton *et al*., 2019).

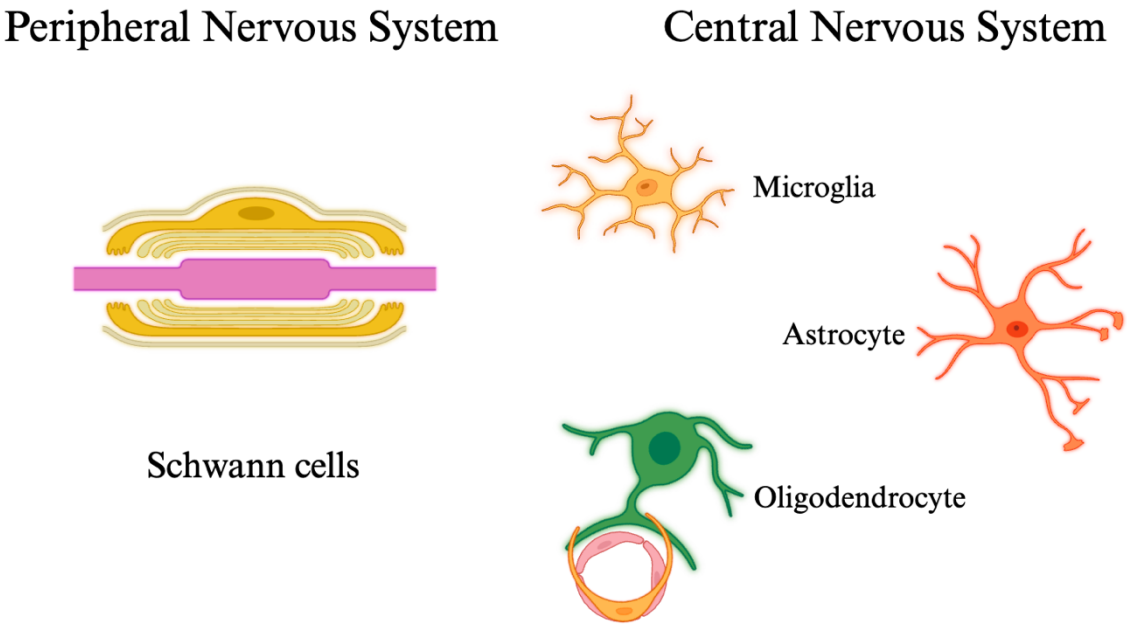


Figure 1.3: The main type of glial cells in the PNS and CNS. This figure was generated using BioRender.

1.3.1 Oligodendrocyte (OL)

The name OL, and the alternative name of oligodendroglia, mean cell with a few branches or processes. These cells are a major type of glial cell in the CNS whose function is to produce the myelin sheaths surrounding neuronal axons. OL extend their process to myelinate up to 50 axons providing up to 1 μm of myelin sheaths around each axon. OLs are derived in the developing embryo from oligodendrocyte precursor cells/progenitors (OPCs) in the ventricular zones of the brain and spinal cord. During embryonic development these OPCs proliferate and then migrate to populate different regions of the spinal cord and the hind and the mid regions of the brain. Later on these OPC will differentiate to form mature myelinating OL cells (Figure 1.4) (Bradl and Lassmann, 2010). The forebrain is supplied by a different source of OPC that develop from forebrain ventricular zones (Richardson, Kessaris and Pringle, 2006). Many growth factors have been found to influence OPC development.

These factors include platelet derived growth factor (PDGF), fibroblast growth factor, hepatocyte growth factor, epidermal growth factor, and insulin-like growth factor 1 (Bergles and Richardson, 2016). Studies on the endocannabinoid system also suggested that endocannabinoid elements such as cannabinoid receptors CB1 and CB2, and endocannabinoid 2-arachidonoylglycerol, may play roles in different stages of OL differentiation, for example promoting OPC proliferation and differentiation to mature OL and myelinating OL (Ceprian and Fulton, 2019). OPCs migration can be regulated by contact mediated mechanisms which involve extracellular matrix proteins, N-cadherins, Netrin-1, Semaphorin, and Ephrins (Bradl and Lassmann, 2010; Bergles and Richardson, 2016). Neuronal signals may also influence OPCs differentiation and maturation. In line with this, pharmacological blockade of neuronal activity influences OPC proliferation and differentiation *in vitro* (Fannon, Tarmier and Fulton, 2015) and *in vivo* (Gibson et al., 2014). OPC are also found in the adult CNS where they can divide and proliferate to produced new mature OL (Levine, Reynolds and Fawcett, 2001; Bergles and Richardson, 2016). OPC therefore have important functions in restoring myelin sheaths after myelin loss (Arnett *et al.*, 2004).

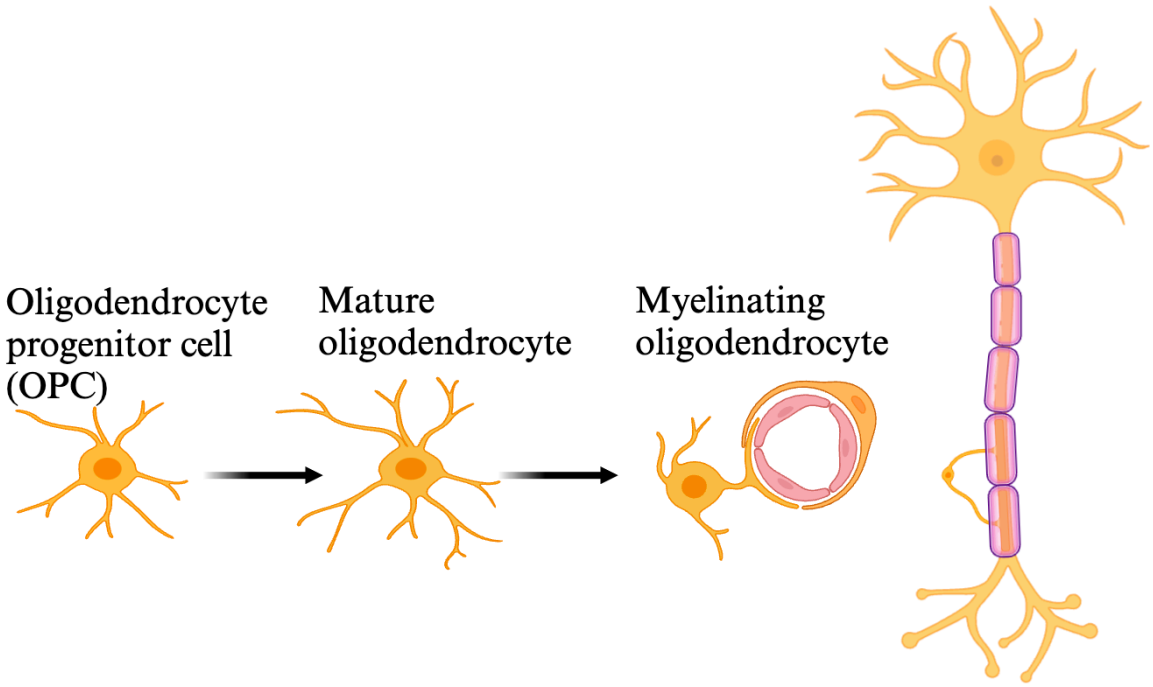


Figure 1.4: The stages of OL development and the different morphological features of OPC, mature OL and myelinating OL. This figure was generated by BioRender.

1.3.2 Astrocyte

Astrocyte, also called astroglia, are one of the major glial cell types in the CNS. The name derives from their typical star-shaped structure which is formed by processes that extended from the cell body (Sofroniew and Vinters, 2010). Astrocyte functions are essential to maintain extracellular homeostasis by regulating extracellular levels of neurotransmitters, via membrane expressed neurotransmitter transporters, and ions via ion channels and ion pumps, e.g., NA+/K+ ATPase (Ceprian and Fulton, 2019). Astrocytes also provide metabolic support to axons by transferring lactate as a fuel for glycolysis (Mason *et al*., 2017), contributing to regulating CNS inflammatory responses (Linnerbauer, Wheeler and Quintana, 2020), and playing an important role in phagocytosing synapses (Kim, Park and Choi, 2019; Linnerbauer, Wheeler and Quintana, 2020).

There are four types of astrocytes existing within the human CNS: protoplasmic, fibrous, interlaminar and varicose projection astrocytes (Wei and Morrison, 2019). Protoplasmic astrocytes possess a high number of process branches compared to the other types of astrocytes. This type of astrocyte is formed widely in the grey matter where they interact with blood vessels and synapses. This organization suggests they play a role in linking blood flow to neuronal activity (Wei and Morrison, 2019). Protoplasmic astrocytes also play an important role in regulating synapse function by secreting neurotransmitters (e.g. glutamate and ATP) at excitatory and inhibitory synapses (Farhy-Tselnicker and Allen, 2018). Fibrous astrocytes are larger than protoplasmic astrocytes and are located in white matter tracts while protoplasmic astrocyte located in grey matter. Fibrous astrocytes have fewer branches processes compare to other types of astrocytes. Interestingly, most axonal nodes of Ranvier receive contact from astrocyte processes (Serwanski, Jukkola and Nishiyama, 2017). Nodes of Ranvier are abundant in white matter because it consists mostly of axonal fibers, therefore axonal nodes of Ranvier are a key target for fibrous astrocytes involved in neuronal regulation.

Interlaminar astrocytes, first described by Retzius and Andriezen in the 1890s, are glia possessing a small cell body and large long processes which measure up to 1 mm (Colombo, 2018). Interlaminar astrocyte cell bodies are located in the cortical lamina layer 1, and the long interlaminar process project down from this layer to connect several cortical layers (Falcone *et al.*, 2021). Varicose projection astrocyte are similar to interlaminar astrocytes and contain long processes (Vasile, Dossi and Rouach, 2017).

Astrocyte also play an important role in CNS injury responses by forming glial scars (Yang *et al.*, 2020). This scar, formed by newly proliferated cells expressing high levels of glial

fibrillary acid protein (GFAP), interfaces between CNS neural parenchyma and non-neural inflammatory cells at the sites of CNS tissue damage. During CNS injury and inflammation, high levels of immune and inflammatory cells migrate into sites of infection, stroke, and autoimmune and neurodegenerative lesions. The astrocyte scar helps to seal the injury site via regulatory signals between immune and inflammatory cells, limiting the spread of inflammation from sites of injury, and reducing secondary injury processes (Figure 1.5) (Yang *et al.*, 2020).

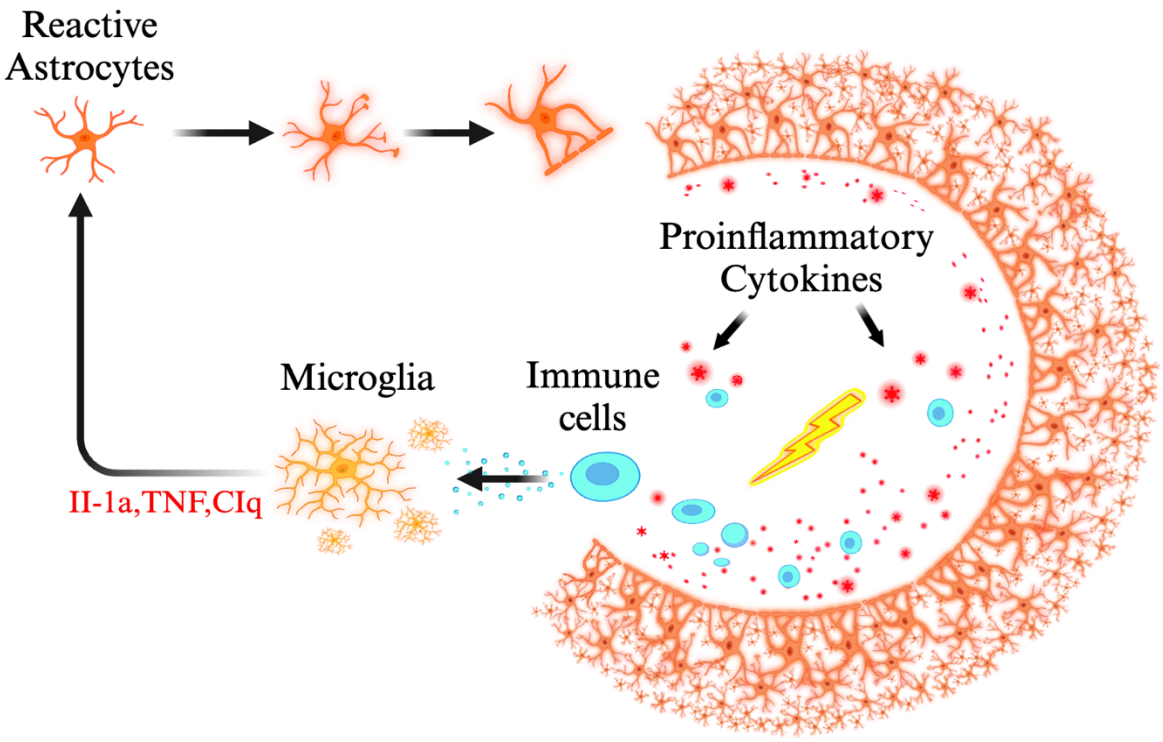


Figure 1.5: Formation of the glial scar. Astrocyte cells are activated by inflammatory cues from injury and disease-related innate peripheral immune cells and resident microglial cells. Reactive astrocytes proliferate and migrate to the injury site to seal of the site of injury. This figure was generated by using Image Manipulation Programme and Biorender.

1.3.3 Microglia

Microglia are the third major from of glial cell in the CNS. Microglia, as described by Pio del-Hortega in 1920s, are smaller than the other main glia and represent about 10-15% of CNS cells (Colonna and Butovsky, 2017). Microglia are considered to be the immune cells of the CNS with similar roles to macrophage cells in the periphery. Microglia are derived from yolk sac macrophages that arise during embryonic hematopoietic development. During early development they migrate to the CNS through the bloodstream after the blood brain barrier has formed (Speicher *et al.*, 2019). Microglia have two main phenotypes, resting (or homeostatic) microglia, which have a small cell body and multiple motile processes, and activated microglia, with fewer shorter processes and a large swollen cell body (Wake *et al.*, 2013). Microglia are the immune cells within CNS contributing to both innate and adaptive immune responses by releasing pro and anti-inflammatory factors to recruit immune cells and other glial cells such as OLs and astrocytes. Microglia are activated via cluster of differentiation, 200 receptors, which enable interactions with CD200 expressed on the surface of many neurons (Kierdorf and Prinz, 2013). Microglia also express many pattern-recognition receptors (PRRs) such as, Toll-like receptor (TLRs), CD14 and NLRP3 inflammasomes, which detect pathogen- associated molecular patter (PAMPs) and also tissue damage-associated molecular patterns (DAMPs) (Colonna and Butovsky, 2017). These receptors allow microglia to play an important role in detecting and fighting CNS infection and mediating and resolving CNS inflammation. Microglia are also involved in homeostatic processes within the CNS (Ginhoux *et al.*, 2013). For example, microglia regulate and control neuronal proliferation and differentiation and are involved in the formation of synaptic connections within the CNS (Ginhoux *et al.*, 2013).

1.4 Myelination and mammalian nervous system

1.4.1 Overview

Myelin forms part of the sheath that covers axons in the PNS and CNS of vertebrates. Myelin was discovered by Antoni Van Leeuwenhoek in 1717 (Boullerne *et al*., 2016). It is formed from multiple layers of lipid-rich glial cell membrane that wrap tightly around the axon. The myelin sheath provides several benefits to the axon, including electrical insulation, and physical and metabolic support and protection. OLs are the source of myelin in the CNS (Cantile and Youssef, 2016), while Schwann cells perform this role in the PNS.

1.4.2 Myelin structure and function

The main function of myelin is to increase the conduction velocity of action potentials. Myelin is composed of myelin basic protein (MBP), myelin oligodendrocyte glycoprotein (MOG) and proteolipid protein (PLP) (Min *et al.*, 2009; Bonetto, Belin and Káradóttir, 2021; Kister and Kister, 2022). Effects on conduction velocity depend on the composition and structure of myelin. Myelin is comprised of 80% of lipid, 20% of specialized proteins (myelin proteins), and a low water content (Morell *et al*., 2013). OL can extend their processes to contact 50 axons, wrapping them with up to 1 μm thickness of myelin sheath. In contrast, in the PNS Schwann cells only wrap one axon (Figure 1.6) (Bradl and Lassmann, 2010). MBP is the second principal component of myelin protein's myelin composition, and is responsible for attachment and binding of the cytosolic surface of the myelin multimembrane. PLP is also abundant in myelin and is responsible for the formation and maintenance of the multi-layer membrane (myelin) (Figure 1.7) (Gudz *et al.*, 2002; Boggs, 2006; Fulton, Paez and Campagnoni, 2010).

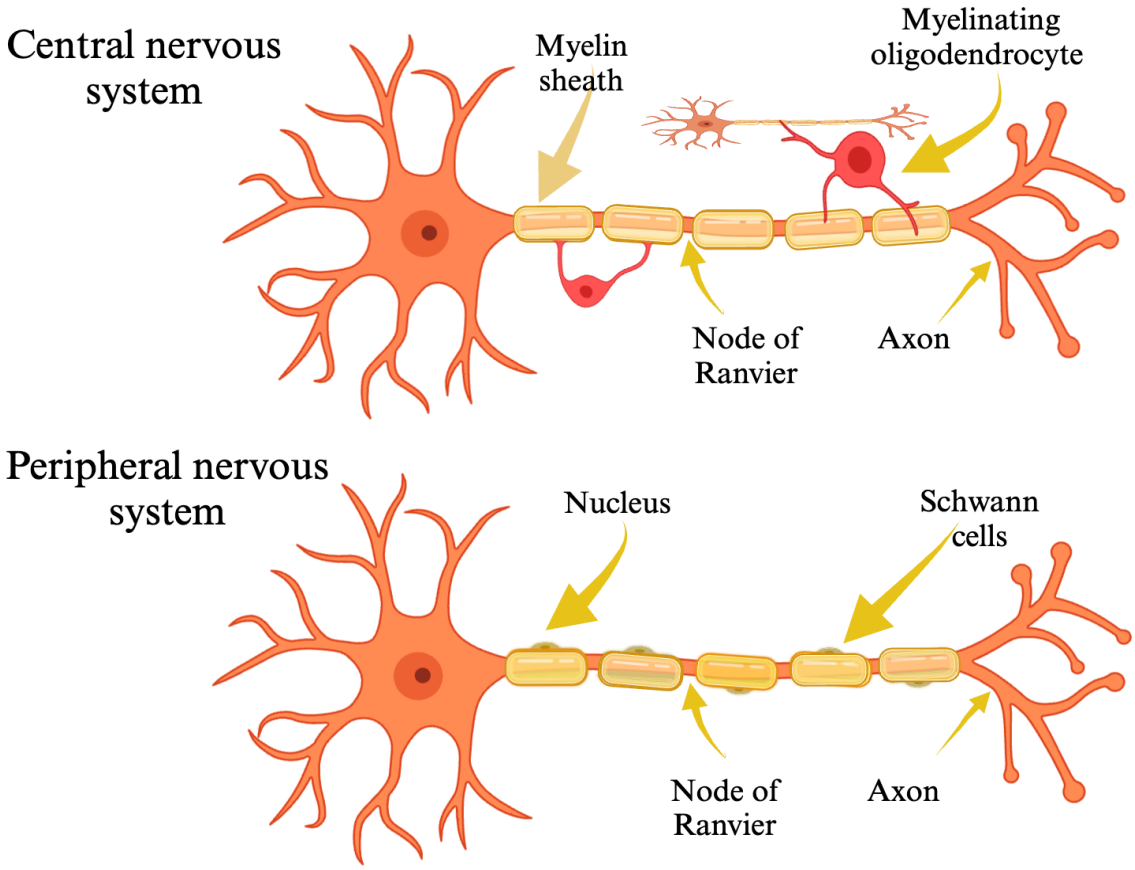


Figure 1.6: Comparison of PNS and CNS myelination. In the PNS, Schwann cells myelinate only one axon. In the CNS, OL myelinate more than one axon, with each axon potentially having multiple myelin sheaths from a single OL. This figure was generated by BioRender.

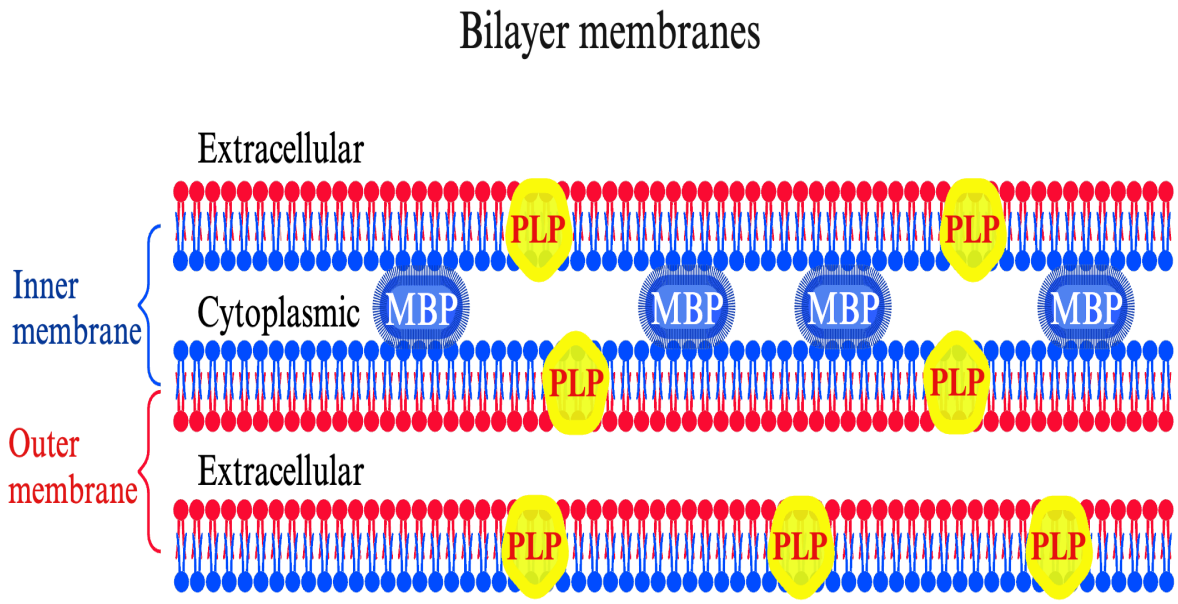


Figure 1.7: The function of major myelin proteins and the structure of myelin. MBP is located within the cytosolic membrane surface where it plays a role in the compaction of the myelin wraps. PLP resides in the membrane where it plays a role in stabilizing interactions between adjacent myelin wraps. This figure was generated by using Image Manipulation Programme and Biorender.

Myelin increases the speed of action potential conduction by increasing axonal membrane resistance and lowering axonal membrane capacitance. Furthermore, myelination regulates the organization of ion channels along the axon, resulting in the spatial separation of Na+ and K+ channels to the nodes of Ranvier. Action potential generation occurs only at the node, thus the action potential travels by saltatory conduction (effectively jumping from node to node). At each of the internodes, the myelin sheath forms a tight junction, known as the paranode region (Figure 1.8). The axonal junctions at the paranode are formed by the

interaction of axonal proteins such as Caspr (contactin-associated protein), and glial proteins. K+ channels are concentrated at the region adjacent to the paranode (juxtaparanode), and Na+ channels are concentrated within the node itself (Lim and Rasband, 2020). In addition, the Na+ K+ ATPase is located at the nodes of Ranvier, contributing to stabilization of membrane potential and the generation of the action potential (Figure 1.8) (Young *et al.*, 2008).

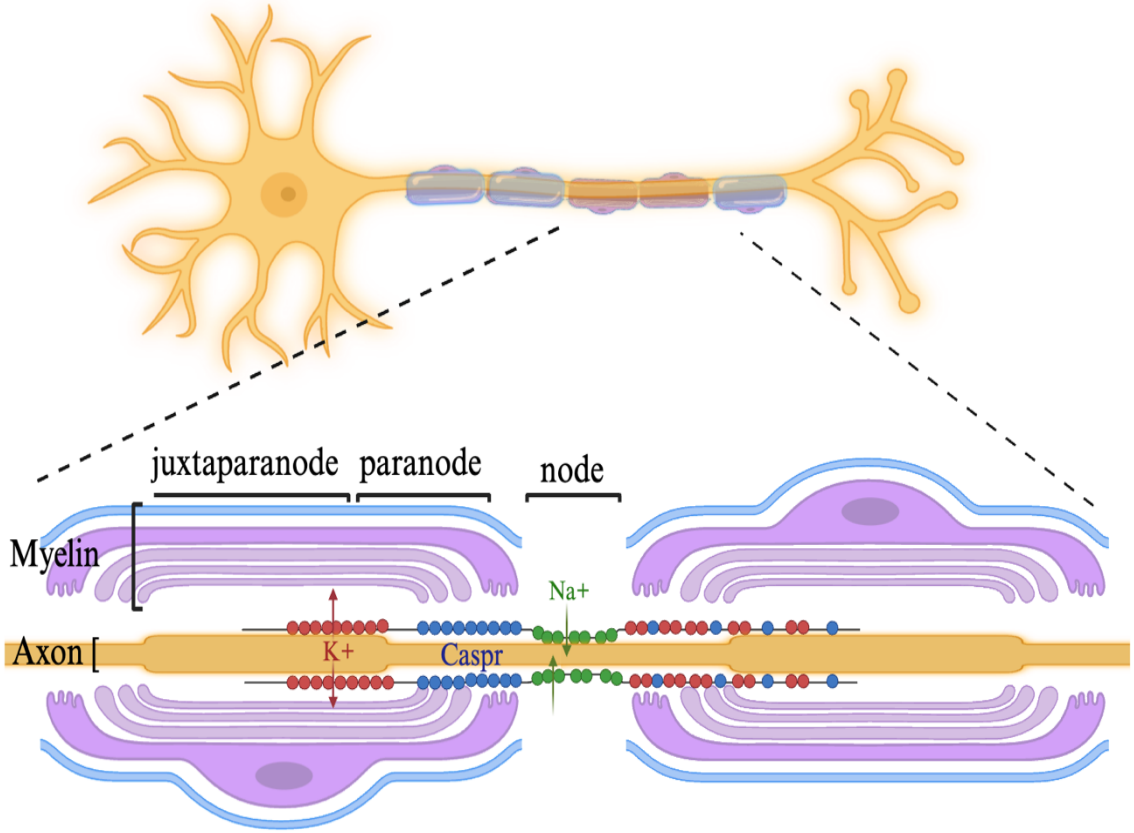


Figure 1.8: Location and structure of nodes of Ranvier. Nodes are discrete gaps formed between adjacent myelin segments. Nodes of Ranvier feature three domains: the node itself contains high densities of Na+ channels; the paranode contains the axon/myelin junctions formed by axonal Caspr proteins interacting with glial proteins; the juxtaparanode contains high densities of K+ channels. This figure was generated by BioRender.

1.5 Myelin injury and repair

1.5.1 Demyelination

OLs form and maintain the myelin surrounding axons in the CNS allowing the electrical impulses to travel efficiently and quickly throughout nerve cells (Mayo, Quintana and Weiner, 2012). The thickness and length of myelin internodes influence the speed of action potential conduction (Waxman and Swadlow, 1977; Wu *et al.*, 2013). Therefore, myelin can regulate conduction velocity along axons of different lengths allowing coordinated activation of large target structures (e.g., different CNS regions). Myelin is therefore essential for healthy CNS function. Demyelinating disease is characterized by damage to OL and the protective myelin sheath that they wrap around nerve fibers in the brain and spinal cord. This damage changes the electrical properties of the axonal membrane (increasing axonal capacitance charge / reducing axonal resistance), and also disrupts the nodal ion channel organization, resulting in a disruption of electrical impulse conduction and coordinated axonal activity. These effects cause neurological dysfunction in disease such as Multiple Sclerosis (MS) and Neuromyelitis Optica (NO) (Williamson and Lyons, 2018).

Demyelinating disease or CNS injury can result in damage to myelin, or OL death, which results in axonal dysfunction, axonal degeneration, leading to the loss of sensory and motor functions (Figure 1.9) (Alizadeh, Dyck and Karimi-Abdolrezaee, 2015). In MS, myelin injury and OL damage occurs as a results of CNS inflammation (Dobson and Giovannoni, 2019). Demyelinating diseases can also cause damage to the myelin sheaths of Schwann cells in the PNS such as Guillain-Barre Syndrome (GBS) which is an autoimmune demyelinating disease of the PNS (Figure 1.9) (Willison, Jacobs and van Doorn, 2016).

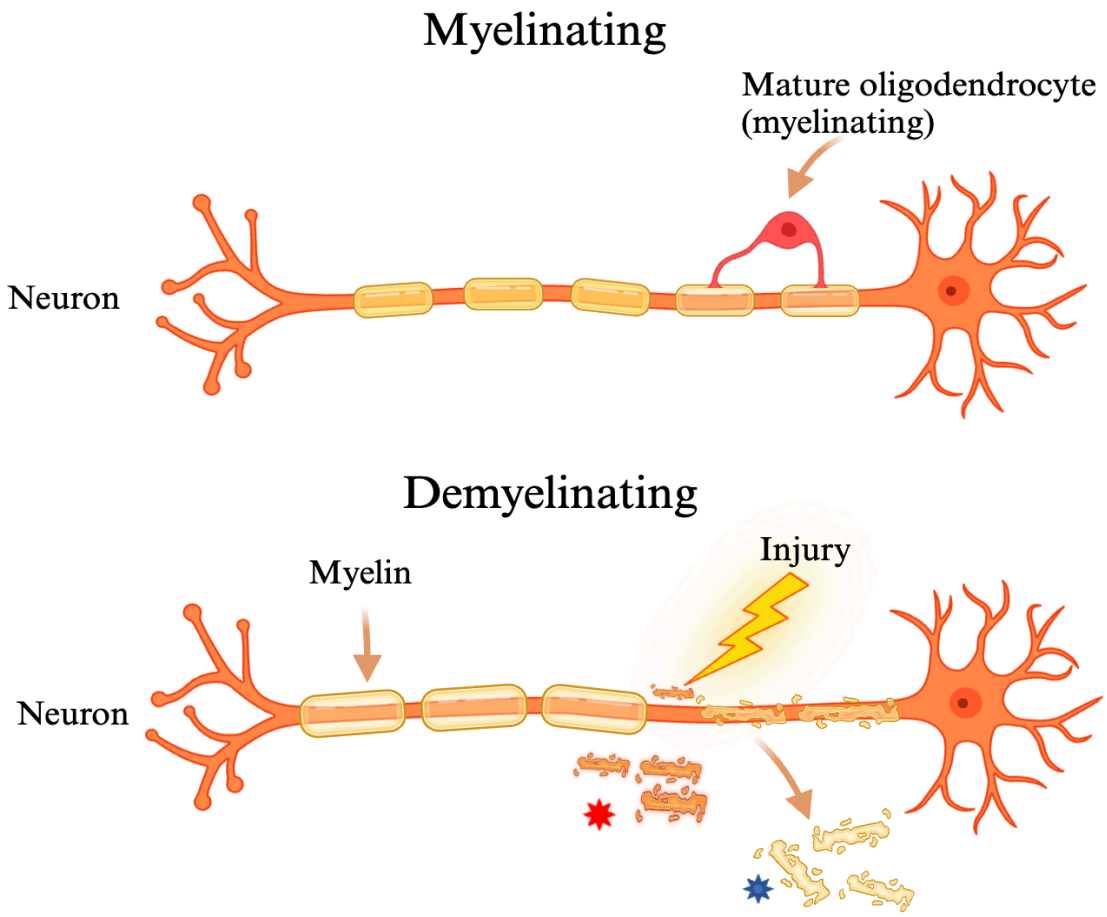


Figure 1.9: The distinction between a healthy myelinated axon (top) and an axon after demyelination (bottom). Demyelination results in the degeneration of the myelin sheath and axonal damage (indicated by blue and red stars respectively). This figure was generated by BioRender.

1.5.2 Remyelination

Remyelination is the process of creating new myelin sheaths for axons that have lost myelin due to injury or diseases such as MS. Remyelination processes occur in both clinical diseases and experimental animal models. Remyelination occurs within the CNS, with OL creating new myelin sheaths for unmyelinated axons, and in the PNS via Schwann cells (Franklin and Kotter, 2008). In the CNS, OPCs migrate to the injury site, differentiate into mature OL, and

began to produce myelin sheaths (Li and Leung, 2015). Remyelination processes are limited in demyelinating diseases such as MS, particularly after disease progression, due to a failure of OPC to differentiate into myelinating OL. Furthermore, genes that are involved in OPC regulation and differentiation also play important roles within CNS remyelination (Skaper, 2019). These genes therefore represent potential therapeutic targets. Growth factors are involved in CNS remyelination, and astrocytes produce many of the growth factors that are essential to the OL lineage. Reactive astrocytes produce the remyelination-associated growth factors such as PDGF, fibroblast growth factor 2, and insulin-like growth factor 1 during remyelination (Molina-Gonzalez and Miron, 2019). Axonal Nfasc186 play roles in the node of Ranvier by localizing the high density of voltage gated Na^+ channels through the node which is essential to transmit the signals in both CNS and PNS. Nfasc155 is specific for oligodendroglia and also essential for the paranodal junctions where it separates the Na^+ channel and K^+ channels at the juxtaparanode. Both Nfasc186 and Nfasc155 expressions are essential during remyelination processes in animal models (Howell et al., 2006).

1.5.3 Multiple sclerosis (MS)

MS is the most common autoimmune disease affecting the CNS. In MS, immune mediated inflammation attacks and destroys myelin, resulting in focal lesions and clinical symptoms (Dyment, Ebers and Sadovnick, 2004). MS lesions are often spread throughout the CNS, including the optic nerves, brainstem, cerebellum, spinal cord and periventricular white matter. In active lesions, microglia and macrophages are present and predominate, with variable degree of T cell inflammation (Hu and Lucchinetti, 2009). Fatigue, numbness, muscle weakness and spasms and other common neurological symptoms are often associated with MS (Eckstein, Saidha and Levy, 2011). Additionally, neuropathic pain in the arms or

legs, painful spasms, and trigeminal neuralgia are also features of MS (Rice and Cameron, 2017).

MS most commonly presents in people between the ages of 20 and 30 and affects women more than men. MS is diagnosed based on symptoms, radiographic evidence such as magnetic resonance imaging (MRI), and laboratory findings such as oligoclonal bands in cerebrospinal fluid (McGinley, Goldschmidt and Rae-Grant, 2021). The pathology of MS appears as a focal areas of myelin loss in the CNS, which are referred to as plaques or lesions (Figure 1.10). MS is classified as relapsing remitting MS, primary progressive MS, secondary progressive MS or progressive relapsing MS with 85% of MS patients having the relapsing remitting form of the disease. Relapsing remitting MS is characterized by acute relapse followed by partial or complete recovery. Moreover, approximately two-thirds of untreated patients progress to secondary progressive MS. Primary progressive MS affects approximately 15% of MS patients. This form is characterized by increasing clinical worsening with no attacks from the beginning (Mayo, Quintana and Weiner, 2012). Interestingly a small number of patients with primary progressive MS experience relapses and are diagnosed as progressive relapsing MS. Overall, the clinical course of progressive relapsing MS is similar to primary progressive MS, and the condition is characterized by a progressive worsening of the condition from the start (Rejdak, Jackson and Giovannoni, 2010).

MS lesions appear differently as the disease progresses, and different plaque types appear at different stages. Acute active plaques are the most common pathologic substrate of the clinical attacks in both acute and relapsing remitting MS (Popescu, Pirko and Lucchinetti, 2013). These plaques are demyelinated areas (Figure 1.10 A) with high level of immune cells

including macrophages/microglia (Figure 1.10 B,C,D) and clear BBB damage with perivascular inflammatory cell infiltrates. The macrophage/microglia often contain particles suggesting phagocytosis of myelin and axonal components (Popescu, Pirko and Lucchinetti, 2013). Chronic plaques are divided into two types. Chronic active, where demyelination is accompanied by signs of ongoing inflammation at lesion borders, and chronic inactive, where demyelinated areas show little evidence of inflammation (absence of immune cells), but do have signs of axonal and OL loss. Chronic inactive plaques typically show an intact BBB and can present an astroglia scar (Popescu, Pirko and Lucchinetti, 2013). Chronic plaques are the most common features of progressive form of MS.

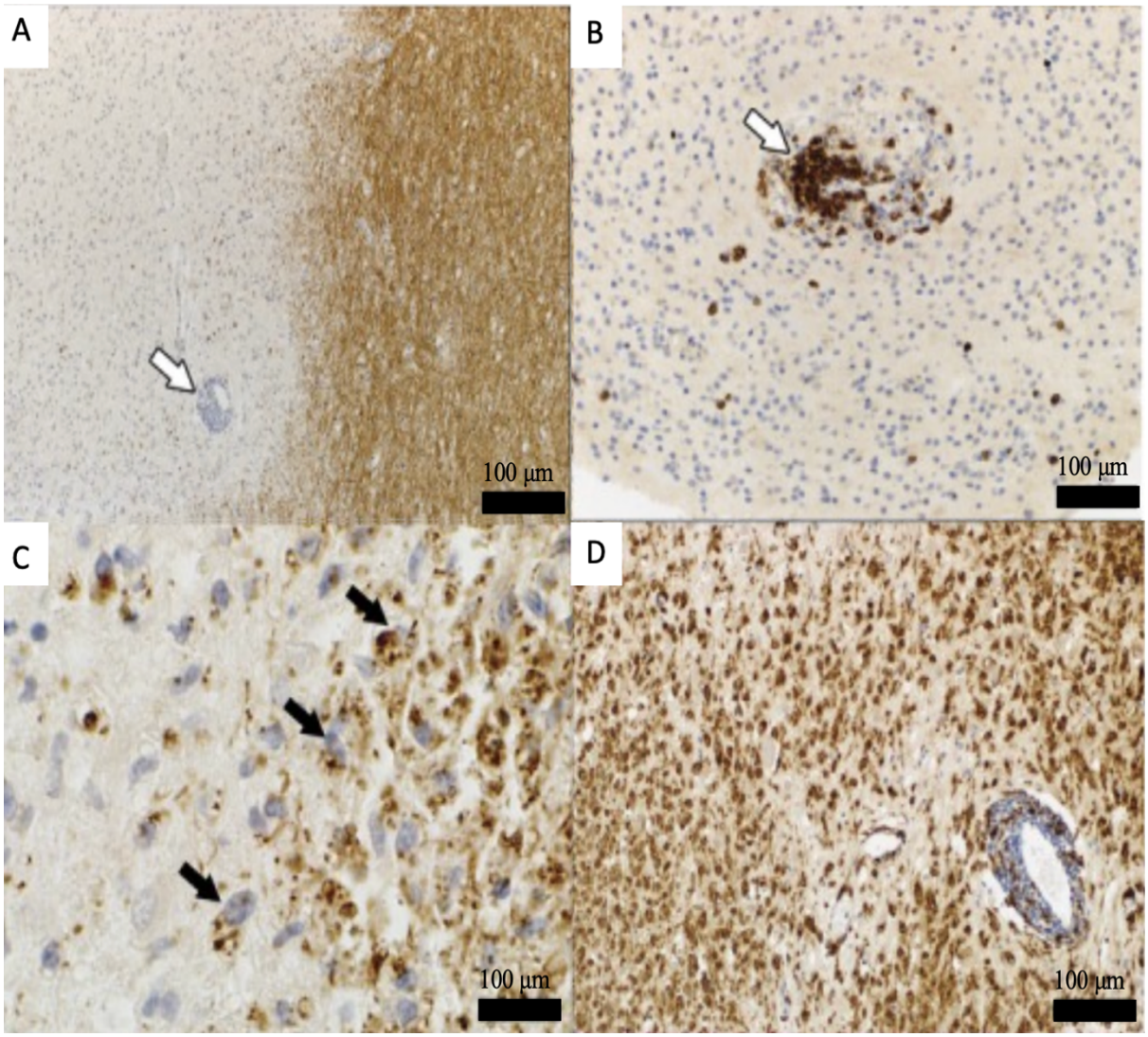


Figure 1.10: Histology of MS lesion demonstrating demyelination and immune cell activity. (A) PLP immunohistochemistry indicating MS plaques. (B) T cell infiltrates observed within an MS lesion. (C) and (D) indicating a high number of macrophages/microglia surrounding MS lesion. Note macrophage/microglia in C contain fragments suggesting phagocytosis (Popescu, Pirko and Lucchinetti, 2013).

1.5.3.1 Mechanisms of inflammatory demyelination in MS

MS has been classified a T cell mediated autoimmune disease (Popescu, Pirko and Lucchinetti, 2013). For example, T helper (Th) cells or $CD4^+$ T cells interact with antigen presenting cells (APCs) and orchestrate damage to oligodendrocytes through interaction with $CD8^+$ T cells and release of perforin and granzyme (Kaskow and Baecher-Allan, 2018). Further, the pathogen-associated molecules bind to the APC receptor stimulating APCs to release a specific interleukins (IL) cytokines like IL-12, IL-4 and IL-23 which induce $CD4^+$ T cell to differentiation into Th2 and Th17 cells (Ghasemi, Razavi and Nikzad, 2017). The innate immune systems also plays a role in pathogenesis and recovery in MS. The innate system, acting through cells such as microglia, macrophages, and monocytes, affect both demyelination and remyelination processes by breaking down myelin during the injury phase, and cleaning up myelin debris (via phagocytosis) and dead cells, which both affect OL and neurons growth (Mayo, Quintana and Weiner, 2012). When microglia are activated, they release potentially cytotoxic molecules like pro-inflammatory cytokines, proteinases like matrix metalloproteinases, reactive oxygen intermediates and completement proteins (Block and Hong, 2005). The innate system also drives demyelinating disease by activating and modulating cells from the adaptive immune system, such as CD8+ cytotoxic T cells and B cells. For example, microglia attract leukocytes by secreting chemokines (Mayo, Quintana and Weiner, 2012).

1.5.3.2 Treatment of MS

The aetiology of MS is not fully understand. There are no cures available and the available treatments for MS aim only to reduce the number of relapses, and slow the progression of the disease. There are a wide range of treatment options and these therapies target immune cells such as T cells and B cells to reduce inflammation (Hauser and Cree, 2020).

1.5.3.2.1 Immunomodulation

Immunomodulation is one of the available approaches to reduce the number of autoimmune attacks and slow the disease progression. Recombinant interferon (IFNβ) has been used as treatment for MS. IFNβ leads to an increase in the expression of anti-inflammatory cytokines IL-4, IL-5, IL-10, IL-13, IL-27 and transforming growth factor β. IFNβ also downregulates the expression of proinflammatory cytokines such as, IL17, IFNγ and tumour necrosis factor alpha which together helps to control and stabilize dysregulated CNS inflammation. Moreover, the IFNβ-mediated shift away from Th1/Th17 may prevent neuronal damage by reducing neuronal demyelination. Also, IFNβ plays a role in T cell regulation by reducing T cell activation, adhesion, and penetration into the CNS via the BBB. Moreover, IFNβ can also disrupts antigen presentation by B cells and other antigen-presenting cells. Overall, IFNβ therapy seems to promote the brain immune balance from proinflammatory (Th1/Th17) to anti-inflammatory (Th2) responses, and reduce the number of inflammatory cells which are able to cross the BBB (Filipi and Jack, 2020). Interferon drugs suppress immune system functions via effect on T cells and B cells, hence their use may increase the opportunities for infection (Lalive *et al.*, 2011). Despite these risks five IFNβ drugs have been approved by the US food and drug administration for the treatment of relapsing remitting MS (Table 1.1) (Filipi and Jack, 2020).

Glatiramer acetate (GA) has been used as immunomodulatory therapy agent in MS (Ramos González *et al.*, 2021). GA is a synthetic peptide of 40-100 residues randomly of four amino acids (Avila *et al.*, 2019). GA shifts cytokine secretion of CD4 + Th cells. Studies in the animal model experimental autoimmune encephalomyelitis show that GA treatment has effects on cells in both the innate and adaptive immune system. GA interacts with APC such as dendritic cells and monocytes, and lymphocytes including Foxp3+ regulatory T cells,

CD4+Th cells and CD8+T cells. In addition, some investigations suggest GA also plays a role in regulating B cells. Studies in mouse models demonstrated that GA treatment lead to an increase in B cell anti-inflammatory cytokines such as, IL-6, IL-12 and tumour necrosis factors (Lalive et al., 2011). The beneficial effects of GA is to reduce neuronal damage and also, to reduce demyelination and promote the neuronal and myelin repair. GA may produce some of these effects through the activity of brain-derived neurotrophic factor (BDNF) (Kasindi *et al.*, 2022). Fingolimod is other treatment has been used with MS patients, which inhibit the lymphocyte cells to reduce the inflammation resulting from MS (Hjorth, Dandu and Mellergård, 2020).

Table 1-1: Interferon beta therapies that have been approved for the treatment of relapsing MS (Filipi and Jack, 2020).

Drug type	**Name**	**Route of administration**	**Dosing**	**Frequency**
Interferon beta-1b	Betaseron	Subcutaneous	0.25 mg	Every other day
Interferon beta-1b	Extavia	Subcutaneous	0.25 mg	Every other day
Interferon beta-1a	Avonex	Intramuscular	30 μg	Once weekly
Interferon beta-1a	Rebif	Subcutaneous	22 or 44 μg	3 times weekly
Interferon beta-1a	Plegridy	Subcutaneous	125 μg	Once every 2 weeks

Immunomodulators therapy of MS has been issued by the MS Therapy Consensus Group, and recommended in primary and secondary progressive MS disease (Wiendl *et al.*, 2008). Immunomodulatory drugs slow the progression of MS and reduce the number of relapses with MS. Interferon drugs are more effective in early stage but show less benefit in the later stages of MS. Plaque formation and disability still occurs with MS despite treatment (Lalive et al., 2011).

1.5.3.2.2 Stem cell transplantation

More potent treatment approaches include intense immunosuppression followed by autologous hematopoietic stem-cell transplantation. This approach has been used over the last few years as a therapeutic strategy with MS (Mancardi and Saccardi, 2008).

1.5.3.2.3 Remyelination

Remyelination or myelin regeneration is the process of restoring myelin that has been lost due to various pathological diseases. In the early stages of MS demyelination is frequently followed by spontaneous remyelination (Lubetzki *et al.*, 2020). For remyelination to occur OPC must migrate to the lesion, differentiate into mature OL, and then grow new myelin sheaths. However, this recovery process eventually fails following CNS trauma or demyelinating disease, resulting in progressive and irreversible functional deficits (Zhang et al., 2015). Importantly, remyelination declines with age and in the chronic stages of demyelinating diseases such as MS. In addition, remyelinated segments are thinner than original myelin (Franklin and Ffrench-Constant, 2008). OPCs have emerged as a promising therapeutic target in demyelinating diseases such as MS due to their ability to migrate to the injury site and differentiate into mature OL cells. Moreover, remyelination is limited in demyelinating diseases due to the failure of adult OPCs to differentiate into myelinating mature OL cells (Franklin and Ffrench-Constant, 2008; Skaper, 2019). Therapies aiming to boost the supply of OPC are being investigated (Franklin and Ffrench-Constant, 2008).

1.5.3.2.4 Neuroprotection

Neuroprotection is a therapeutic approach that aims to prevent neural cell death (neurons and OLs), and reduce the number of cells lost over the time (Kuehn, Fingert and Kwon, 2005). The treatment action of neuroprotection therapy is to inhibit the pathogenic cascades (e.g.

caspases, oxidative stress, excitotoxicity) that result in cell dysfunction and eventual death (Zhang et al., 2005). Furthermore, while treatment will not repair damaged axons caused by demyelinating diseases, it may prevent and reduce further axon damage. This type of treatment is likely to be beneficial in conjunction with other therapeutics, such as drugs that suppress the immune system, in order to limit axonal damage within the CNS. There are numerous neuroprotective therapeutic drugs available, and these drugs frequently target oxidative stress and excitotoxicity, which are common mechanisms in neuronal injury and demyelinating diseases. The primary treatment used to control oxidative stress levels are antioxidants (Villoslada, 2016). Acetylcysteine, crocin, minocycline, pyrroloquinoline quinone, vinpocetine are examples of antioxidant drugs used for neuroprotection. In addition, cannabidiol, a major psychoactive component of cannabis, may have neuroprotectant effects in MS, with anti-inflammatory and antioxidant effects being possible (Nouh *et al.*, 2024). Moreover, other neuroprotection treatments, such as selegiline, nicotine, and caffeine, have been shown to potentially delay and slow the progression of Parkinson's disease. Furthermore, caspase inhibitors, trophic factors, therapeutic hypothermia, erythropoietin, nithium, and neuroprotection D1 have all been reported and used for neuroprotection in CNS disorders (Villoslada, 2016). Despite research into these therapies there are currently no neuroprotective therapies available for use in MS.

1.6 Balo's disease (concentric sclerosis)

Balo's Disease, which is considered a variant of MS, is a rare demyelinating disorder within CNS which cause damage to the myelin sheaths that surround the axons. Balo's disease is distinguished by alternating rings of demyelination and myelin preservation. MS lesions are frequently found in Balo disease along with many hypertrophic astrocytes coexisting in demyelinated areas with OL, which often exhibit apoptotic features (Kira, 2011).

Importantly, the ring pattern appearance seen frequently on MRI scans in Balo disease is not common in MS (Amini Harandi et al., 2018).

1.7 Neuromyelitis Optica (NO)

Neuromyelitis Optica (NO), also known as Devic's disease, is a CNS demyelinating disease that affects the optic nerve and spinal cord. NO was previously thought to be a variant of MS due to considerable clinical overlap (e.g. relapsing symptoms) (Wingerchuk et al., 2007), but pathological, clinical, immunological, and laboratory findings differ from those of MS. Importantly, NO is not progressive, and detection of autoantibody marker (NMO-IgG) in NO distinguishes it from MS, and has helped to classify the NO spectrum of disorders (Wingerchuk et al., 2007). The interaction of NMO-IgG with the water channel aquaporin 4, results in complement activation and damage to the inflammatory target. There is currently no cure for NO, which is similar to MS and other demyelinating diseases. However, therapeutic treatments are available for NO (Trebst et al., 2013). Azathioprine has been shown to reduce relapses in NO, and other therapies for NMO include Fingolimod, Methotrexate, and Cyclophosphamide (Wingerchuk et al., 2007).

1.8 Leucine rich repeat proteins in the CNS

A leucine-rich repeat is a protein structural motif that is composed of repeating 20-30 amino acid stretches that are unusually rich in the hydrophobic amino acid leucine (Bella *et al.*, 2008). Leucine-rich repeat (LRR) proteins (LRRP) are made up of various lengths of consensus sequences repeats (Kajava *et al.,* 1998). LRRP are expressed in various cell types within the CNS including neurons and glial cells, with numerous studies indicating important roles for these proteins in shaping CNS function (de Wit and Ghosh, 2014). For example, in

neurons LRRP located at the postsynaptic membrane play an important role in circuit formation and function by coordinating pre- and postsynaptic differentiation, and regulating activity-dependent plasticity (de Wit and Ghosh, 2014), and as discussed below (section 1.8.1) LRRP in OL lineage cells play an important role in regulating myelination and remyelination (Mi *et al.*, 2005; Foale, 2019).

1.8.1 AMIGO3 and LINGO1

Amphoterin-induced gene and open reading frame-3 (AMIGO3) and immunoglobulin-like domain-containing protein 1 (LINGO1) are both LRRP with an IgG-like domain. However, a key difference between AMIGO3 and LINGO1 structure is the number of domains, with AMIGO3 having 6 domains and LINGO1 having 12 domains (Foale *et al.*, 2017) (Figure 1.11). Furthermore, LINGO1 is only expressed in the CNS where it is found in axons and OLs, but is reported to be absent from astrocytes (Mi *et al.*, 2005). In contrast, AMIGO3 is found in tissues outside of the CNS including liver and lungs (Kuja-Panula *et al.*, 2003), as well as within CNS OL (Foale *et al*., 2019) and neurons (Ahmed *et al.*, 2013). To date there are no published reports describing AMIGO3 expression in astrocytes or microglia.

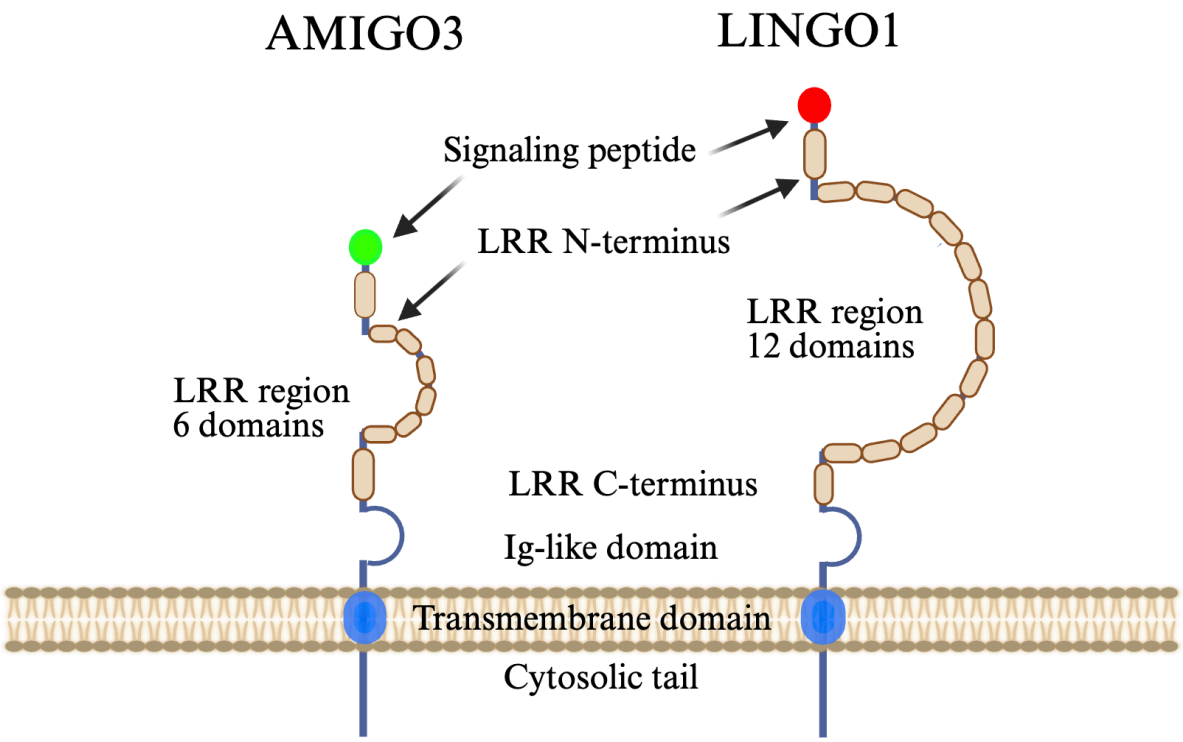


Figure 1.11: Structural differences and similarities between AMIGO3 and LINGO1. AMIGO3 possess 6 LRR domains while LINGO1 has 12 LRR domains. Each protein contains a signalling peptide, a small cytosolic tail, and a transmembrane domain. This figure was generated by BioRender.

AMIGO3 and LINGO1 can form complexes in the plasma membrane with neurite outgrowth inhibitor-66 receptor 1 (NgR1) and p75 neurotrophin receptor (p75), allowing the complex to activate when bound to ligands such as myelin-derived proteins (e.g. neurite outgrowth inhibitor, oligodendrocyte myelin glycoprotein and myelin-associated glycoprotein) (Figure 1.12). Tumor necrosis factor receptor superfamily, member 19 (TROY) is able to substitute for p75 in this complex (Ahmed *et al.*, 2013). Importantly, previous studies from our lab identified the presence of both p75 and NgR1 proteins in primary OPC (Foale, 2019), suggesting that AMIGO3 could form a functional receptor complex with these proteins. Importantly, in neurons this complex activates ras homolog gene family member A (RhoA),

causing Rho-associated protein kinase (ROCK) signalling, and activating LIM-domain containing protein kinases (LIMK) and myosin light chain (MLC) on the actin filament (Ahmed *et al.*, 2013). This signalling pathway in axons allows AMIGO3 and LINGO1 to promote growth cone collapse in injured axons that are exposed to myelin fragments (Figure 1.12) (Mi *et al.*, 2004; Ahmed *et al.*, 2013). Interestingly, LINGO1 activates the RhoA pathways in OPC leading to a block in differentiation and myelination (Mi *et al.*, 2005). Considering their structural similarity, and overlapping functions following axonal injury (Ahmed et al., 2013; Mi et al., 2004), the possibility exists that AMIGO3 has a similar function to LINGO1 during OL differentiation and myelination (Foale *et al.*, 2017).

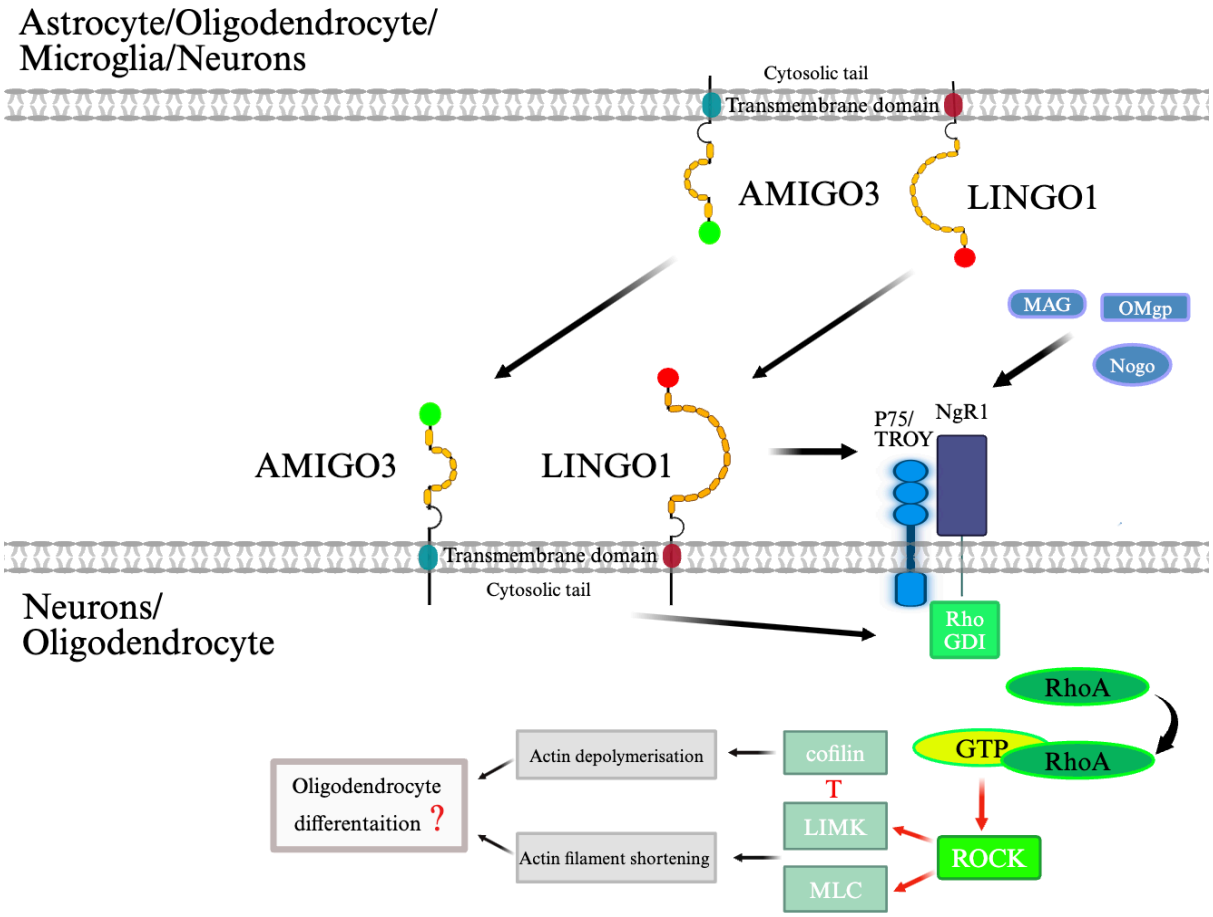


Figure 1.12: AMIGO3 and LINGO1 signalling in neurons. AMIGO3 and LINGO1 interact with NgR1/p75 (or TROY) complexes leading to the activation of the RhoA / ROCK pathway and eventual actin depolymerisation and axonal growth cone collapse. This figure was generated by BioRender.

1.8.2 LRRP in CNS injury

LRRP play an important role after CNS injury. LINGO1 expression is induced following CNS injury, suggesting that LINGO1 may play a role in axonal regeneration and in demyelinating diseases like MS. In support of this, LINGO1 expression is increased in rat spinal cord after injury (Mi, Sandrock and Miller, 2008), and inhibition of LINGO1 promotes OPC differentiation and myelination (Mi *et al.*, 2005), and promotes remyelination

(Ji *et al.*, 2006; Mi, Blake Pepinsky and Cadavid, 2013). Moreover, both LINGO1, and structurally similar AMIGO3, expression increased significantly after seizure induction in mice, with level of AMIGO3 and LINGO1 maintained for 20 days after induction (Li *et al.*, 2021). Similarly, in a rat model of spinal cord injury,AMIGO3 expression was induced rapidly, and interestingly, this response was earlier than the increase in expression of LINGO1 (Ahmed *et al.*, 2013). LINGO1 is a negative regulator of retina ganglion cell survival, and it is overexpressed after optic nerve injury in vivo (Quan *et al.,* 2020). Thus, both LINGO1 and AMIGO3 appear to be associated with various CNS injury and disease conditions where they inhibit axonal and myelin development and repair. Importantly, a monoclonal LINGO1 antibody boosted remyelination in the experimental autoimmune encephalomyelitis model of demyelination (Mi, Sandrock and Miller, 2008), but failed to meet clinical endpoints in subsequent clinical trials for optic neuritis and MS (Ahmed, Fulton and Douglas, 2020). The failure of the anti-LINGO1 therapy could be explained by several factors. First, LINGO1 may exhibit a cytoplasmic localization keeping it away from therapeutic antibodies (Meabon *et al.*, 2015). Second, therapeutically reduced levels of LINGO1 could be compensated for by the structurally and functionally similar protein AMIGO3. Therefore, a clearer understanding of the function of AMIGO3 in OL could inform future trials involving therapeutic targeting of LINGO1 and other LRRP.

1.9 Study rationale

LRRP are primarily involved in synaptic functions within the CNS and are negatively regulated in CNS injury and demyelinating diseases. LINGO1 expression is increased during spinal cord injury and demyelinating disease, and knocking down LINGO1, or inhibiting its function, promoted axonal regeneration and myelination (Mi *et al.*, 2004, 2005). Both LINGO1 and AMIGO3 belong to the LRRP family, and have a similar structure, and share

functions such as preventing axon regeneration (Ahmed *et al.*, 2013). AMIGO3 is expressed more widely than LINGO1 within the CNS (Mi *et al.*, 2004) with LINGO1 being absent from astrocytes (Mi *et al.*, 2004). In addition, like LINGO1, AMIGO3 can interact with the p75/NgR1 complex to induce RhoA signalling in axons (Ahmed *et al.*, 2013), and recent data from primary OPC suggest that all of the required proteins for this signalling complex are present in these cells (Foale *et al.*, 2017). Importantly, AMIGO3 protein expression in the developing CNS shows a peak that coincides with the initiation of myelination (Foale *et al*., 2019). Specifically, AMIGO3 expression peaks around postnatal day 7 in mouse forebrain, and then declines at the same time that MBP expression increases. This suggests that AMIGO3 may play a role in regulating CNS myelination. AMIGO3 structural and functional similarities with LINGO1 (e.g. inhibition of axon regeneration), and the timing of its expression in development, suggests that AMIGO3 is likely to play an important role in OL differentiation and myelination (Foale *et al.*, 2017). The wider CNS expression of AMIGO3, potentially involving astrocytes (Tickle *et al*., 2013), suggests AMIGO3 may be a more significant regulator of myelination as compared to LINGO1, and may substitute for LINGO1 function during therapeutic inhibition of LINGO1 (Foale *et al.*, 2017).

1.10 Hypothesis and aims

We hypothesize that AMIGO3 is expressed by the major glial cells: astrocyte and OL, and this expression is negatively correlated with the onset of OL differentiation. We also hypothesize that AMIGO3 inhibits OL differentiation and maturation, and that knockdown of AMIGO3 gene expression will promote OL differentiation. Finally, we predict that AMIGO3 stimulates the activation of RhoA signal in CNS glial cells.

In this study we aim to examine the expression of AMIGO3 and LINGO1 during OL differentiation and maturation *in vitro* using mixed glial cultures, and to clarify the wider expression of these proteins in glia by studying their expression in isolated cultures of astrocytes and microglia. The study also aims to examine the function of AMIGO3 by measuring OL differentiation following knockdown of AMIGO3 by short interfering ribonucleic acid (siRNA), and after stimulation of endogenous AMIGO3 signalling using recombinant AMIGO3 proteins. Finally, this project aims to explore the signalling pathways activated by AMIGO3 in glial cells by studying the activation of RhoA in primary mixed glial after stimulation with recombinant AMIGO3.

Chapter 2 Method and materials

2.1 Animals

In this study, animals used were bred by the Biomedical Services Unit (BMSU) at University of Birmingham. Animals were provided with food and water freely and kept in a 12-hours light-dark cycle. Animals were killed using methods approved by the UK Home Office, and in accordance with the Animals (scientific procedures) Act (1986).

2.2 Cell line cultures *in vitro*

2.2.1 Baby Hamster Kidney (BHK) culture

Baby Hamster Kidney (BHK) cells were obtained by Dr Fulton from the University of Warwick School of life Sciences. BHK cells were stored at – 80 °C. All experiments completed with BHK cells were performed in a class 2 biological safety cabinet. BHK were cultured in medium containing GMEM (Glasgow Modified Essential Medium, Sigma-Aldrich, Dorset, UK) with 10% of Fetal Bovine Serum BFA (Sigma; Sigma-Aldrich) and gentamicin (50 mg/mL, Thermo Fisher Scientific). Cells were grown in T 75 cm^2 tissue-culture flask, and maintained in a humidified incubator set at 5% CO_2 and 37 °C (Greiner Bio-One Frickenhausen, Germany). Following 80% cells confluency, 2 ml of trypsin-EDTA solution (Sigma; Sigma-Aldrich) was applied to detach the cells. Trypsin was incubated with the cells for 5 mins, then the flask was tapped to remove the cells. Cells were then centrifuged (300 x g, 5 min) into a pellet. Cells were then resuspended in 1 mL of media and counted with a haemocytometer. Each experiment required different numbers of cells to be seeded, for example 150.000 cells per 6-well plate, and 250,000 per T-25 flask. During culture BHK cells were examined under the microscope (Figure 2.1) (Haq *et al.*, 2003; Suárez-Patiño *et al.*, 2019).

2.2.2 Freezing and storing BHK cells

BHK-21 cells trypsinised after reaching 80% confluence, were stored at – 80 °C. First, trypsinised cells were collected in 10 ml of high serum medium. Cells were then centrifuged at 300 x g, 10 °C for 5 minutes, then spare medium was removed from the pellet. Pellets were re-suspended with freezing medium (90% of serum medium (20% foetal bovine serum) and 10% of DMSO). Samples were then aliquoted into 0.5 uL cryovials, before aliquots were placed in the freezing container (Mr Frosty). Samples were then transferred to a -80 °C freezer for long-term storage.

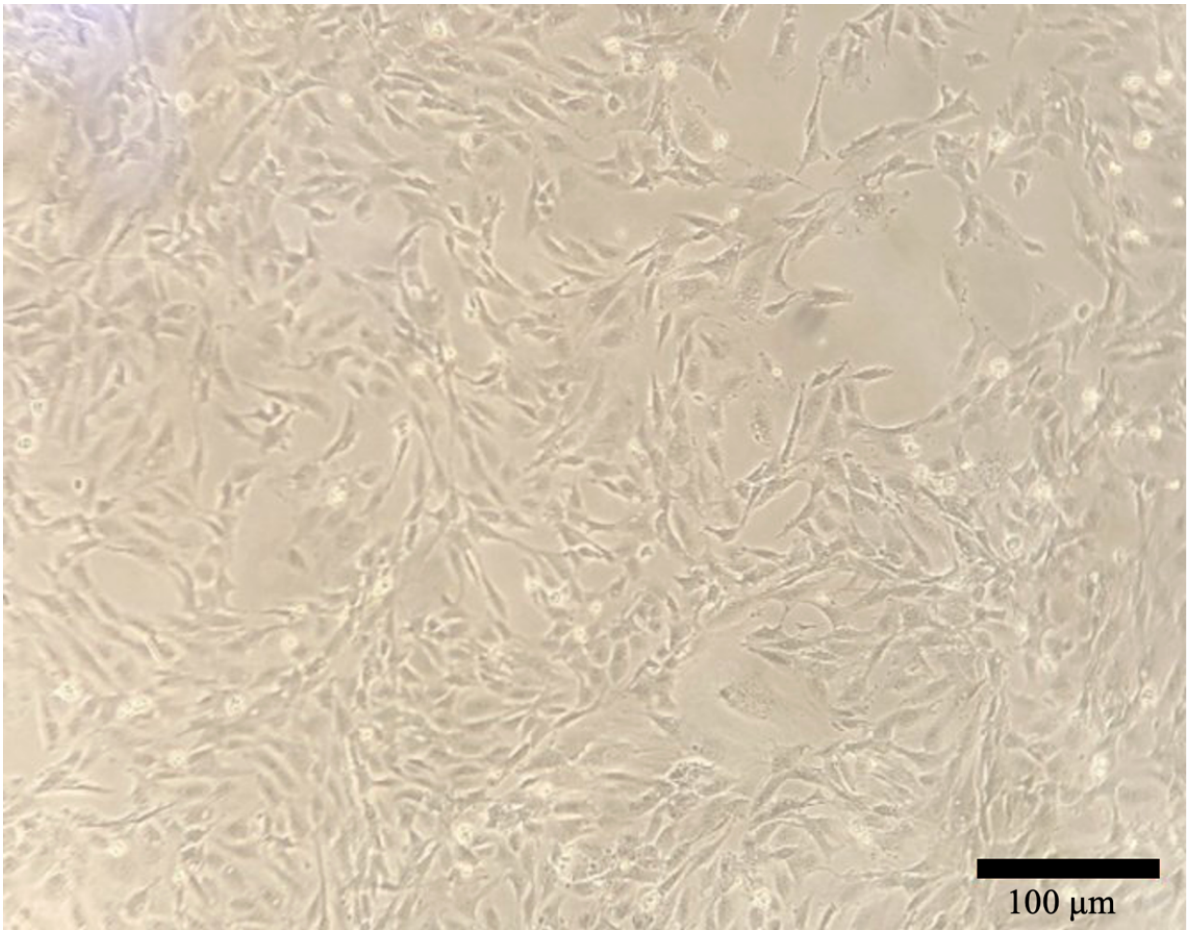


Figure 2.1: Typical BHK culture that has reached around 60% confluency. Note cells have flattened shape on the surface of the T75 flask.

2.3 Primary central nervous system (CNS) cultures

2.3.1 Primary mixed glial culture

Primary mixed glial cultures were obtained from the forebrains of FVB/N mice at postnatal 3-day P3. These cultures were used to observe oligodendrocyte (OL) differentiation in vitro. P3 has been reported to be the optimal age to obtain a high number of glial cells (Petrović *et al.*, 2021). The mouse pup heads were collected from the BMSU team and delivered to our lab on ice. To remove the brain the scalp was opened from the center of the posterior part of the skull along the midline by using a fine spring scissor. Brains were removed from the skull using a small spatula and placed into an ice-cold 100x15 mm petri dish, containing 5 ml of ice-cold filtered dissection medium (Table 2.1). Under the dissection microscope the meninges were removed and disrupted by slicing with forceps.

Table 2-1: Brain dissection medium components.

Component	ml
Dulbecco's modified Eagle's medium (DMEM-F12)	50
L-glutamine	0.5
Penicillin and streptomycin	0.5

After mincing, cortex tissue was collected into a 15 ml tube contained 5 ml of dissection medium. The tissue was then enzymatically digested by adding 0.5 mL of trypsin-EDTA (0.25%). DNAsel (0.2% v/v: Thermo Fisher Scientific) was added to avoid cells aggregation in the culture. Cells were then incubated at 37 °C for 20 mins with regular agitation. Cells were then strained with a cell strainer (mesh size: 70µm), before cells were centrifuged at 300

x g, at 10 °C, for 5 mins. Cells were then counted with a haemocytometer and seeded into Poly-L-lysine (PLL; Sigma-Aldrich) coated T 75 cm^2 tissue flask, or 6-well plate. Cells were seeded into each T 75 cm^2 flask, and 1.5 pups cortices used for T 25 cm^2 flasks. For 6-well-plates cells were seeded at 500.000 cells per well.

Table 2-2: Shows primary mixed glial serum medium components.

Component	%
DMEM (DMEM; Life Technologies)	89
Fetal bovine serum	10
Penicillin and streptomycin	1

Mixed glial cells were incubated at normal growth conditions, (5% of CO_2 , at 37 °C). Following 24 hours, 1/3 of medium was replaced with fresh medium containing 2 mg/mL of insulin (Sigma- Aldrich). Then, at the following change medium was fully changed to medium with 2 mg/mL of insulin. Cells were regularly checked under the microscope to confirm viability of cultures by confirming the appearance of flattened cells attached to the surface of the flask (astrocyte), and small round cells growing on the top of astrocyte cells (oligodendrocyte precursor cell (OPC) and microglia) (Figure 2.2).

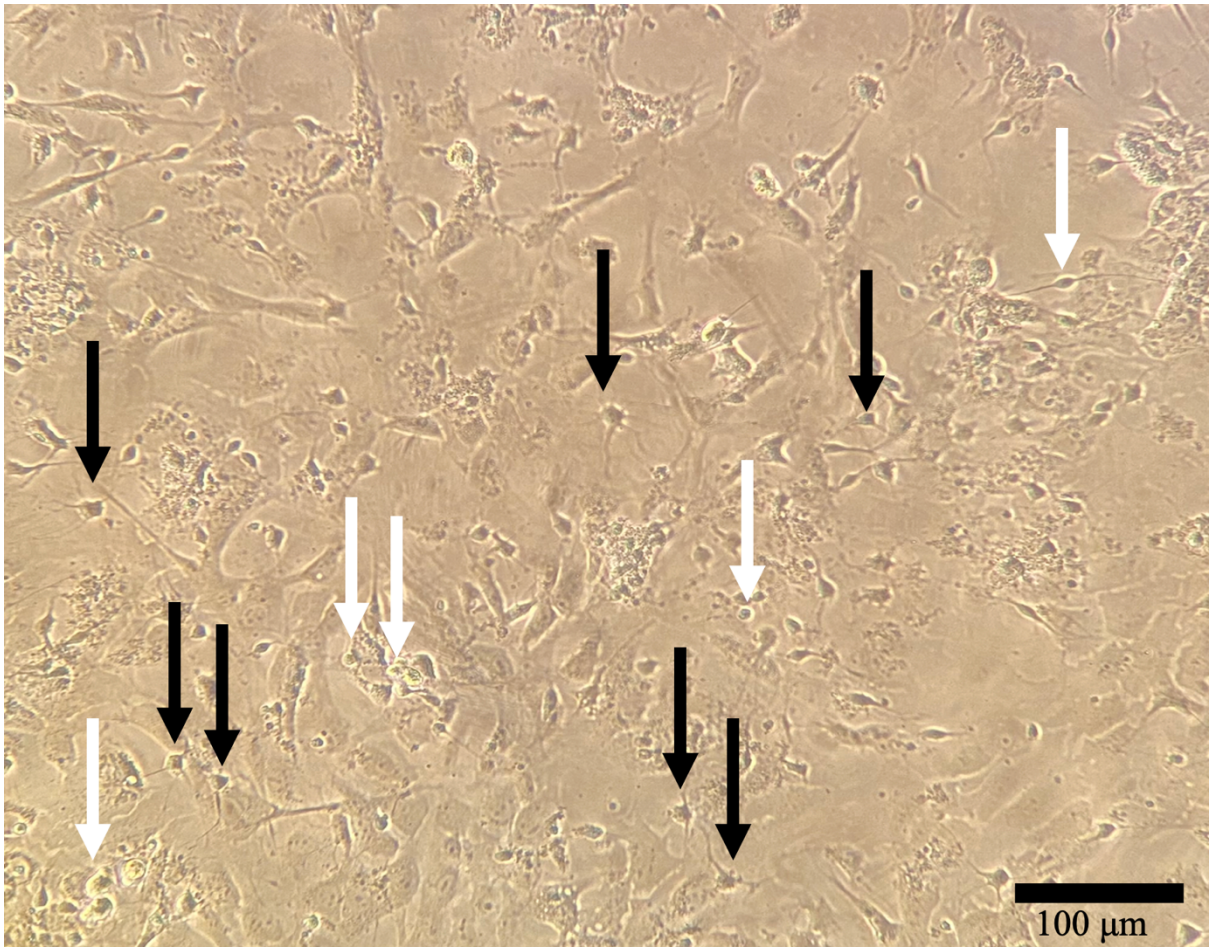


Figure 2.2: Primary mixed glial culture at 9 days in vitro (DIV). Image indicates flattened astrocytes attached to the bottom of the flask with OPCs and microglia growing on top. The arrows indicated other glia (microglia and OPCs) as small cells with multiple processes. Black arrows indicated mature OLs which have more processes then OPCs and microglia.

2.3.2 Astrocyte cultures

Astrocyte cells were isolated from primary mixed glial cultures (described above in section 2.3.1). At 9 DIV primary mixed glial cultures have formed monolayers of astrocyte cells growing on the bottom of the flask, with microglia and OL cells growing on top of astrocyte cells (Figure 2.2). For these mixed glial cultures, either three pups cortex tissues were seeded in each T 75 cm^2 tissue culture flask, or 1.5 pup cortex tissue were used for T 25 cm^2 tissue culture flasks. To isolate astrocytes, cultures were removed from the incubator to the culture

hood, and cells were washed with warmed sterile phosphate buffer saline (PBS) once before adding fresh serum medium (Table 2.2). Primary mixed glial culture flasks were then secured onto an orbital shaker and shaken for 18 hours at 300 rpm inside an incubator maintained at 5% of CO_2 and 37 °C (Migliaccio *et al.*, 2022). Following the shaking, medium was disposed of and cultures were washed three times with warmed PBS to remove floating cells (microglia and OPC). Medium was then added to the remaining astrocyte monolayer, which was then used for different studies of isolated astrocytes (Figure 2.3).

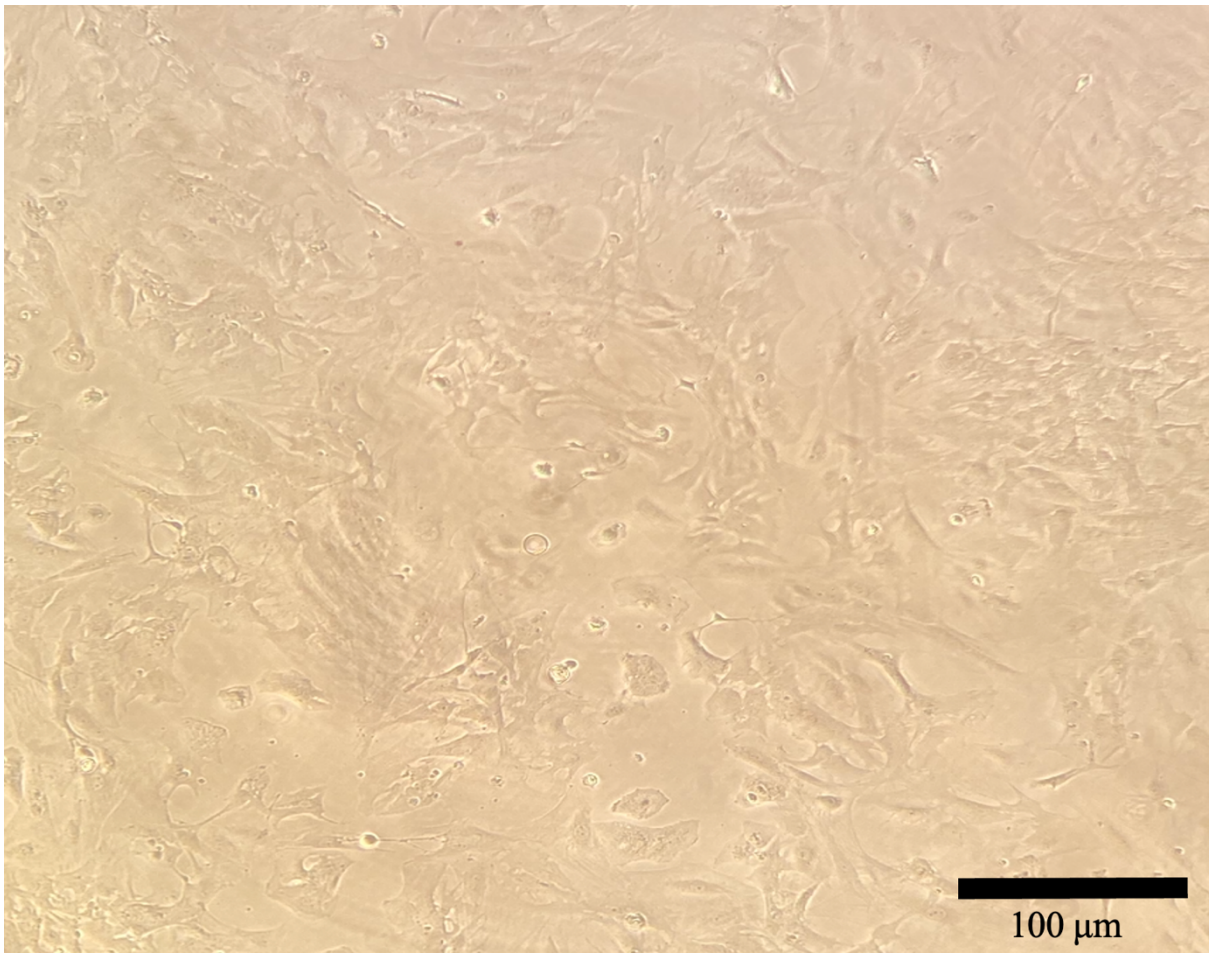


Figure 2.3: Astrocytes isolated from mixed glial culture by shaking the flask overnight.

2.3.3 Microglial culture

Microglial cells were isolated from primary mixed glial cultures at 9 DIV. At this stage Microglial cells are seen as small round cells on top of the astrocyte layer (Figure 2.2). Microglia have a weak attachment to the astrocyte layer. They can be removed by tapping the flask 8 to 10 times on each side. Two rounds of tapping was used to obtain a high number of microglial cells (Scott, Witt and Schober, 2022). Following the tapping process, detached microglial cells were visualized as floating cells under the microscope. These cells were then collected in the medium, centrifuged at 300 rpm, 10 °C, for 10 minutes, re-suspended in medium and then seeded in Poly-L-lysine (PLL; Sigma-Aldrich) coated 12-well-tissue culture plate (Figure 2.4). After 3 hours, medium was replaced to remove contamination of other cells such as OPC.

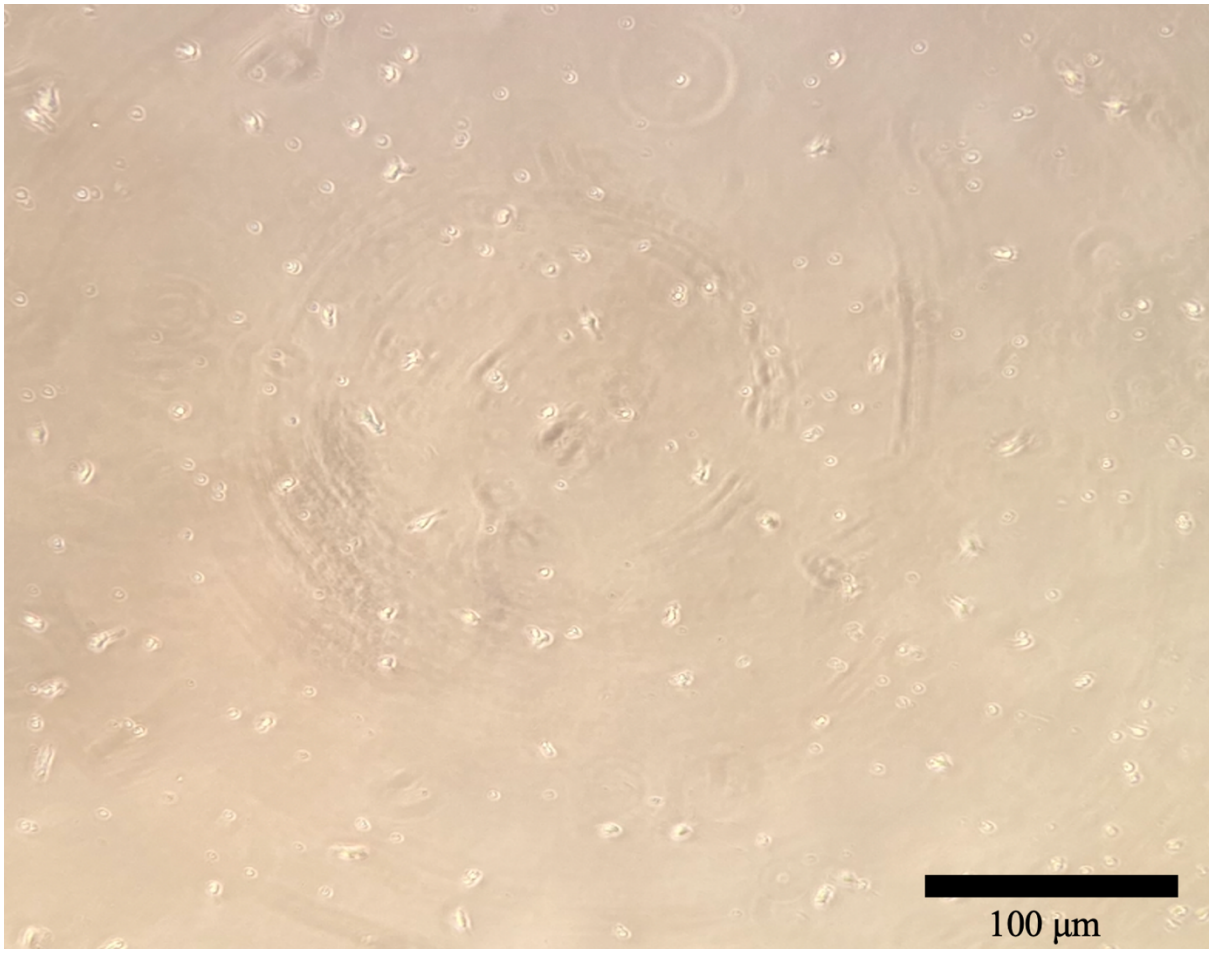


Figure 2.4: Image shows microglial cells isolated from primary mixed glial cultures. Microglia are seen as small round cells.

2.3.4 Splitting and re-plating primary cells

Mixed glial cultures were collected from flasks and seeded to different tissue culture containers as follows. First, cells were washed with warm PBS (5 ml), and then trypsin-EDTA solution (0.25%) was added to the tissue culture flask. Cultures were incubated for 5 minutes in the incubator. Following incubation, 5 ml of serum was added to inhibit the trypsin and cells were collected and centrifuge at 300 rpm for 5 minutes at 10 °C. Cells were resuspended with 1 ml of serum medium and cell count was performed before cells were seeded into Poly-L-lysine (PLL; Sigma-Aldrich) coated tissue culture plates containing serum

medium. Cells were then grown at 5% of CO_2 37 °C in the humidified incubator (Calvo-Garrido *et al.*, 2021).

2.4 Experimental treatment of mixed glia and BHK cells

Different treatments designed to manipulate amphoterin-induced gene and open reading frame-3 (AMIGO3) were applied to BHK cells and mixed glia in this study. Recombinant AMIGO3 was used to stimulate endogenous AMIGO3 signalling, while AMIGO3 knockdown via short interfering ribonucleic acid (siRNA) was used to inhibit AMIGO3 function in BHK cell lines and mixed glial cultures. Cultures were seeded with specific numbers of cells according to the procedure of the treatment. Treatment time-courses depended on the experimental protocol, with some treatments used for 24 hours and other treatments for up to one week.

2.4.1 Recombinant Fc AMIGO3 treatment in BHK and primary mixed glial cultures

2.4.1.1 Principle of recombinant Fc AMIGO3 treatment

Recombinant AMIGO3 (Recombinant Human AMIGO3 Fc chimera Protein, R&D systems), was used to stimulate ras homolog gene family member A (RhoA) activity and OL differentiation in mixed glial cultures. BHK cells were also stimulated with recombinant AMIGO3 to validate the RhoA activation assays. Bovine serum albumin has been added to the protein by the manufacturer as a carrier protein.

2.4.1.2 Treatment procedure

Cultures of primary mixed glial were moved from cell growth conditions (37°C, 5% CO_2) and two different concentration of recombinant AMIGO3 were added to the serum medium. Cells were treated with either 1 ug/mL or 2 ug/mL of recombinant AMIGO3, or a control protein (mouse isotype IgG, Sigma). Mixed glial cultures were treated from 7 DIV until 11 DIV, and the treatment was refreshed at 9 DIV. To prepare the treatments, the total amount of protein (recombinant AMIGO3, isotype control IgG) was diluted with PBS in an Eppendorf tube, than treatment was diluted further with serum medium, and this mixture as then used to replace the cell culture medium in 6-well-plates. Cells were incubated for the next few days (7 to 11 DIV) and then samples were obtained. Cell lysates were required for Western blot (WB) and RhoA activation assays, and cells were fixed with paraformaldehyde for immunocytochemistry (ICC).

2.4.2 siRNA transfection in primary and BHK co-culture in vitro

2.4.2.1 Principle of siRNA

siRNA are small RNA sequences that can target specific genes to knockdown or silence their expression with high selectivity (Rao *et al.*, 2009; Gavrilov and Saltzman, 2012). A mix of four different siRNA sequences for AMIGO3 (Flexi-Tube, Qiagen) have been used together in this investigation to knockdown AMIGO3 expression in both BHK cells and mixed glial cultures. This was done to help us study the role of AMIGO3 in OL cells during differentiation.

2.4.2.2 siRNA transfection procedure in primary and BHK cultures

siRNA was transfected into mixed glial culture between 5 DIV to 7 DIV, and after 70% of cell confluency with BHK cells. BHK cells were first used to optimize the effective concentration of siRNA. The AMIGO3 siRNA mix, or the control siRNA (All Starts negative control siRNA, Qiagen) were transfected at 10, 20, 30 and 50 nM in tissue culture 6-well-plate. HiPerFect vector was diluted into the siRNA reagent to deliver siRNA to the cells. The four different siRNA sequences were mixed evenly (to produce the final concentration, e.g. 10, 20 nm) and added to the HiPerFect vector in free serum medium to allow high transfection to occur, following the manufacturer's instructions. siRNA specific sequence information is protected by the supplier Qiagen. To allow the transfection complexes to form, cells were taken from cell growth condition (5% of CO_2 , humidified, at 37 °C) and incubated at room temperature (RT) for 5 to 10 mins. Then 100 ul of the medium were replaced with 100 ul of siRNA master mix (Table 2.5). siRNA was added drop-wise onto the cells and the plate was gently swirled in order to ensure the siRNA complexes are distributed in the tissue culture plate. At 7 DIV cells have been lysed for WB to test AMIGO3 expression in both the control and AMIGO3 siRNA treated cultures.

2.5 Western blot

2.5.1 Overview of Western blotting

WB or immunoblotting is an electrophoretic technique used to analyse and detect proteins. WB can also be used to study protein interactions and the presence of post-translation modifications like phosphorylation (Pillai-Kastoori, Schutz-Geschwender and Harford, 2020). In WB proteins are separated through sodium dodecyl sulphate electrophoresis polyethylene gels (SDS) (SDS-PAGE) (Figure 2.5). The negative charge of proteins leads to

flow through to the positively charged anode in the gel tank. Proteins then separate in the acrylamide gel according to their molecular size. Proteins were then transferred to a membrane via electroblotting (Trans-blot Turbo system, Bio-Rad). Proteins on the membrane are then visualized via antibody chemiluminescence detection (Booth *et al.*, 2022). Protein molecular weight marker (BLUeye; Sigma-Aldrich) was used to help identify protein sizes. Protein densitometry analysis was then used to compare protein levels between samples. Densitometry data are normalized to a loading control protein such as b-actin (Butler *et al.*, 2019). WB was used to identify and study AMIGO3 and leucine rich repeat and Ig domain containing 1 (LINGO1) expression in OL cells during the development of myelination. Also, WB was used to study AMIGO3 and LINGO1 in isolated astrocyte and microglia cells. Further, WB was used in this study to identify 2', 3'-cyclic-nucleotide 3'-phosphodiesterase (CNPase) in OL to study OL differentiation, and glial fibrillary acidic protein (GFAP) and leukocyte specific receptor (CD11b) proteins were detected by WB to confirm astrocyte and microglia cells in isolation cultures.

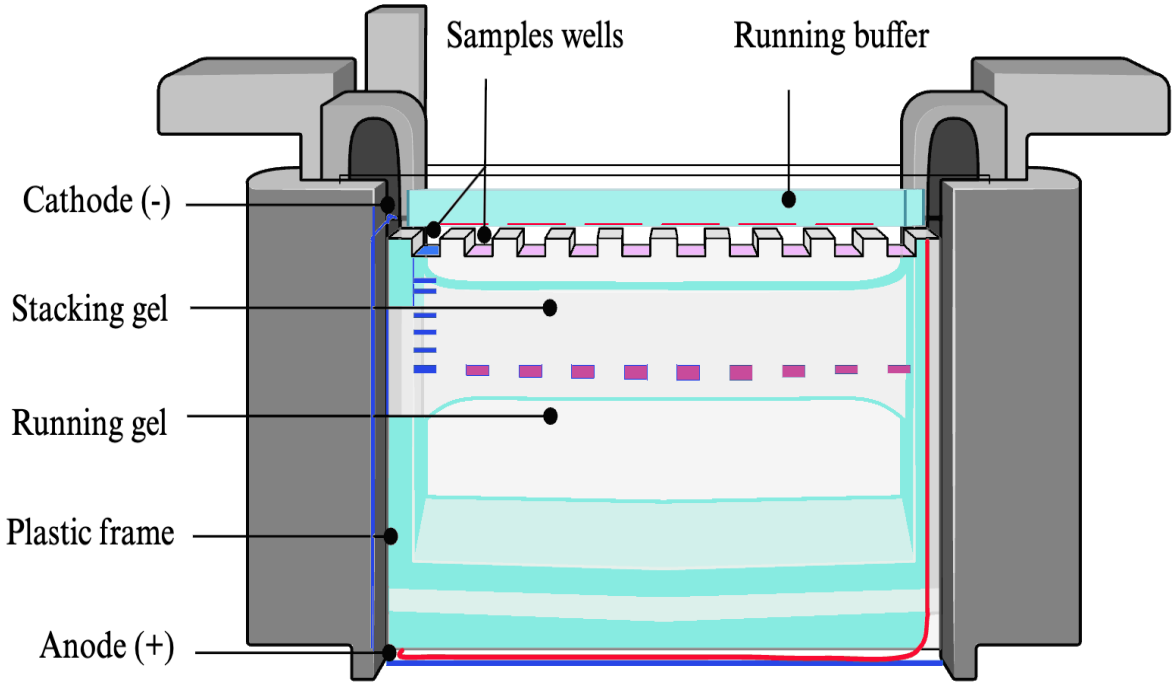


Figure 2.5: Protein electrophoresis setup. As current flows from the negative to positive terminal negatively charged protein samples are separated in the polyacrylamide gel based on size. This figure was generated by using Image Manipulation Programme and Biorender.

2.5.2 Protein extraction

Primary or cell line cultures were rinsed once with ice-cold PBS, then RIPA buffer (Sigma) was added to the cultures, before incubation for 5 minutes at 4 °C. A tablet of protease inhibitor was added to the RIPA buffer to protect protein samples (1 tablet per 10 ml of protein lysis buffer solution: Thermo Fisher Scientific). Following incubation, cells were harvested and the lysate collected. Cells lysates were then transferred into a 1.5 ml Eppendorf tube on ice. Cell lysates were centrifuged at 10000g for 5 min at 4 °C. The pellets were discarded, and protein supernatants were collected into new 1.5 ml Eppendorf tube. Protein samples were kept on ice for 30 mins to avoid protein degradation and for protein stabilization, before being stored at -20 °C until protein assays and WB analysis.

2.5.3 Protein assay

Pierce BCA protein assays kit (Thermo Fisher Scientific) was used to calculate the lysate protein concertation. Each 10 ul of lysate protein sample was loaded in triplicate into a 96 well plate, then 200 ul of BCA working solution was added into each well. Bovine serum albumin was used to make a standard curve (8 points, 0 to 2 mg/mL) to measure the different concentrations of the lysates (Figure 2.6). The plate was incubated for 30 mins at 37 °C (light protected) and protein concentrations measured as absorbance at 562 nm using a Tecan Infinite Magellan nano plate reader (Figure 2.7). Protein concentrations of lysate samples were determined from the absorbance readings using the standard line equation y= mx+b (Figure 2.7).

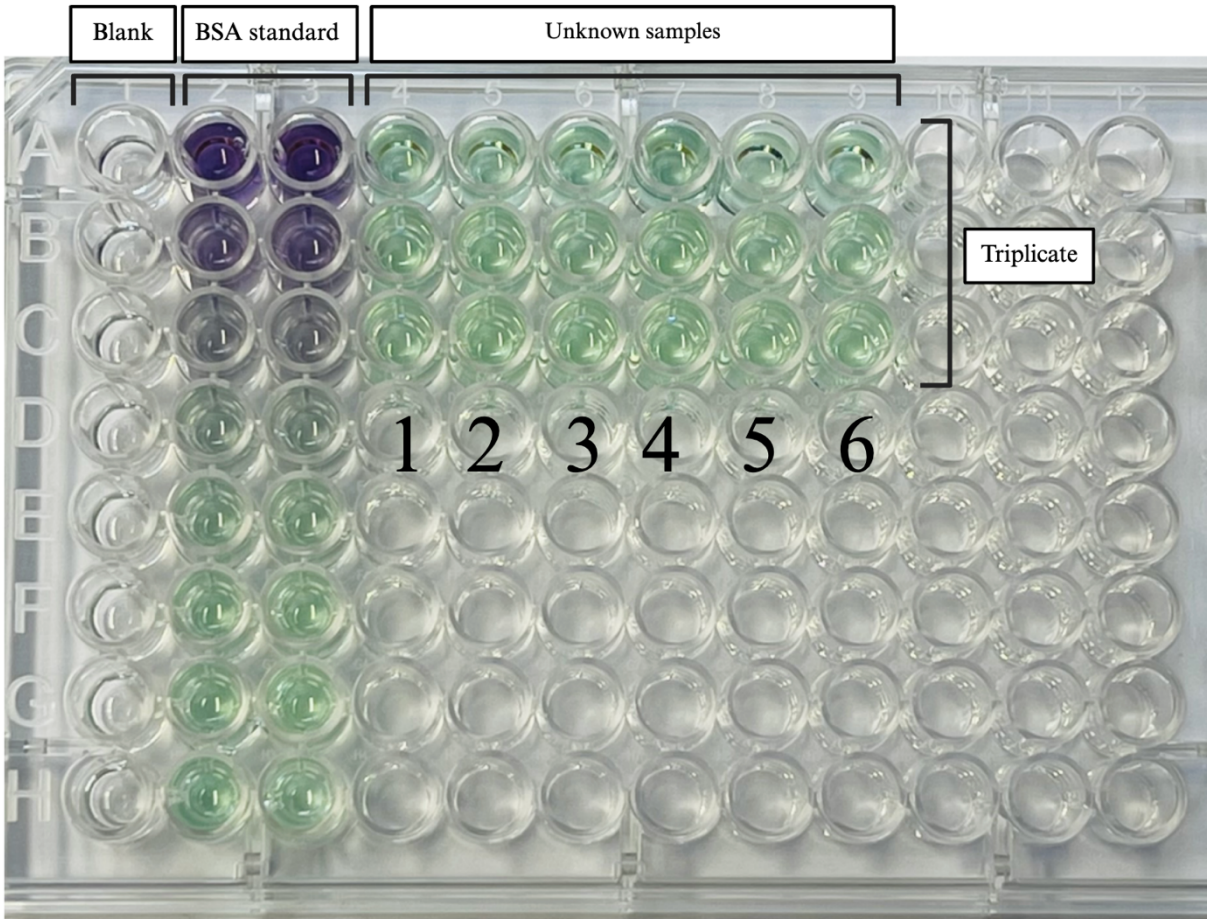


Figure 2.6: Protein assay setup. Image indicates bovine serum albumin standards and unknown samples (1-6). Blank wells were used to set up the bovine serum albumin standard. This figure was generated by using Biorender.

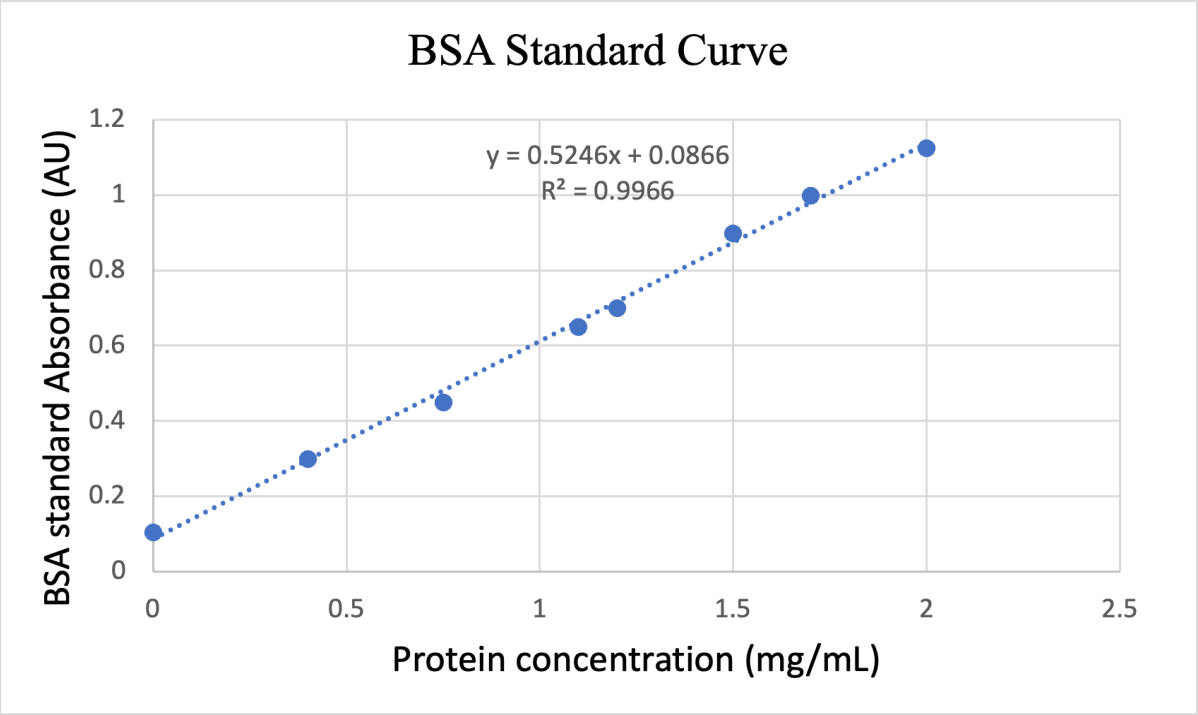


Figure 2.7: Bovine serum albumin calibration curve. Absorbance at 562 nm assayed against known protein concentrations. This figure was generated by using Microsoft excel.

2.5.4 Protein electrophoresis and transfer

Protein concentrations were adjusted with RIPA buffer, then proteins were mixed with sample reducing agent (500 mM dithiothreitol 10x DTT, Thermo Fisher Scientific) to decrease the disulfide bonds in the proteins and reduce the oxidation damage. In addition, LDS sample buffer (LDS 4X; Thermo Fisher Scientific) was added before electrophoresis. LDS was composed of Coomassie G250 and phenol red to trace the proteins through the gel. 5 ul of protein ladder (BLUeye; Sigma-Aldrich) and 20 ug/µL of protein samples were loaded onto the SDS Bio-Tris gel (20%; Thermo Fisher Scientific). The electrophoresis tank was run at 225V, 120 mins, 35mA in 50 ml of running buffer MES-SDS (20X; Thermo Fisher Scientific) diluted with 950ml of distilled H_2O. Following electrophoresis proteins were transferred to PVDF transfer membrane (Bio-Rad) by using the Trans-blot Turbo Transfer system for 7 mins.

2.5.5 Primary and secondary antibodies

Following protein electrophoresis membranes were blocked with 5% Marvel solution diluted with Tris-buffered saline (TBS) plus 1% of Tween (TBST) for one hour at RT. This step was to block nonspecific binding of antibodies (Fido, Tatham and Shewry, 1995) . TBST consisted of 100 ml of Tris-buffered saline (20x TBS-T; Sigma-Aldrich),1 ml of Tween 20 and 900 ml of distilled H_2O. After membrane blocking, membranes were incubated with primary antibody diluted in 5% of Marvel solution for one hour at RT (Table 2.3). After this membranes were washed with TBST three times, with 5 min intervals between each wash. Following TBST washes, membranes were incubated for 30 mins at RT, with 5% of Marvel solution containing the secondary antibody linked with horse radish peroxidase (HRP) to amplify the signals (Table 2.3).

Table 2-3: primary and secondary antibodies used for detecting proteins in WB:

Primary antibody

Antibody (Cat No)	Dilution Factor	Species	Supplier
b-actin	1:1000	Mouse	Sigma-Aldrich, UK
AMIGO3 (mab-2375)	1:1000	Mouse	Biotechne
AMIGO3 (SC-49881)	1:500	Goat	Santa Cruz
AMIGO3 (SC-2375)	1:1000	Mouse	Santa Cruz
LINGO1 (ab23631)	1:1000	Rabbit	Abcam
LINGO1 (Millipore)	1:1000	Rabbit	Millipore
CNPase (sigma-C5922)	1:1000	Mouse	Sigma-Aldrich
GFAP (sigma G-3893)	1:1000	Mouse	Sigma-Aldrich
Iba1 (NB-100-1028)	1:500	Goat	Novus Biologicals

CD11b (ab-133357)	1:1000	Rabbit	Abcam
NG2	1:500	Rabbit	Millipore (AB5320)
MBP	1:500	Rat	Millipore (MAB386)
MBP Proteintech	1:500	Rabbit	Proteintech, UK
CA11	1:1000	Rabbit	Abcam (Ab167362)
MOG	1:500	Mouse	Abcam (Ab109746)

Secondary antibody

Antibody	Dilution Factor	Host species	Supplier
Anti-mouse HRP	1:500	Goat	Cell signalling, UK
Anti-rat HRP	1:1000	Goat	Abcam, UK
Anti-rabbit HRP	1:2000	Goat	GE, Healthcare, UK
Anti-goat HRP	1:1000	Rabbit	Millipore, UK

2.5.6 Electrochemiluminescence detection

Enzyme Chemiluminescence WB reagent (GE Healthcare Amersham; Thermo Fisher Scientific) were used to visualize HRP linked antibodies. HRP substrate luminol and HRP peroxidase substrate were used (Alegria-Schaffer, Lodge and Vattem, 2009). Electrochemiluminescence reagents were applied equally to the membrane and incubated for 3 mins. Following electrochemiluminescence, membranes were wrapped with plastic film and place inside an imaging system (G-Box, Syngene) for image capture. After image capture membranes were stored at 4 °C for stripping and WB with different antibodies if required.

2.5.7 WB image quantification

ImageJ was used for densitometry to quantify protein bands after WB (Gallo-Oller, Ordoñez and Dotor, 2018). ImageJ was used to measure the integrated density of protein bands of interest, and integrated densities were normalized to the protein density of the housekeeper protein (actin in most cases). Beta-actin was chosen for its high and consist expression (Figure 2.8).

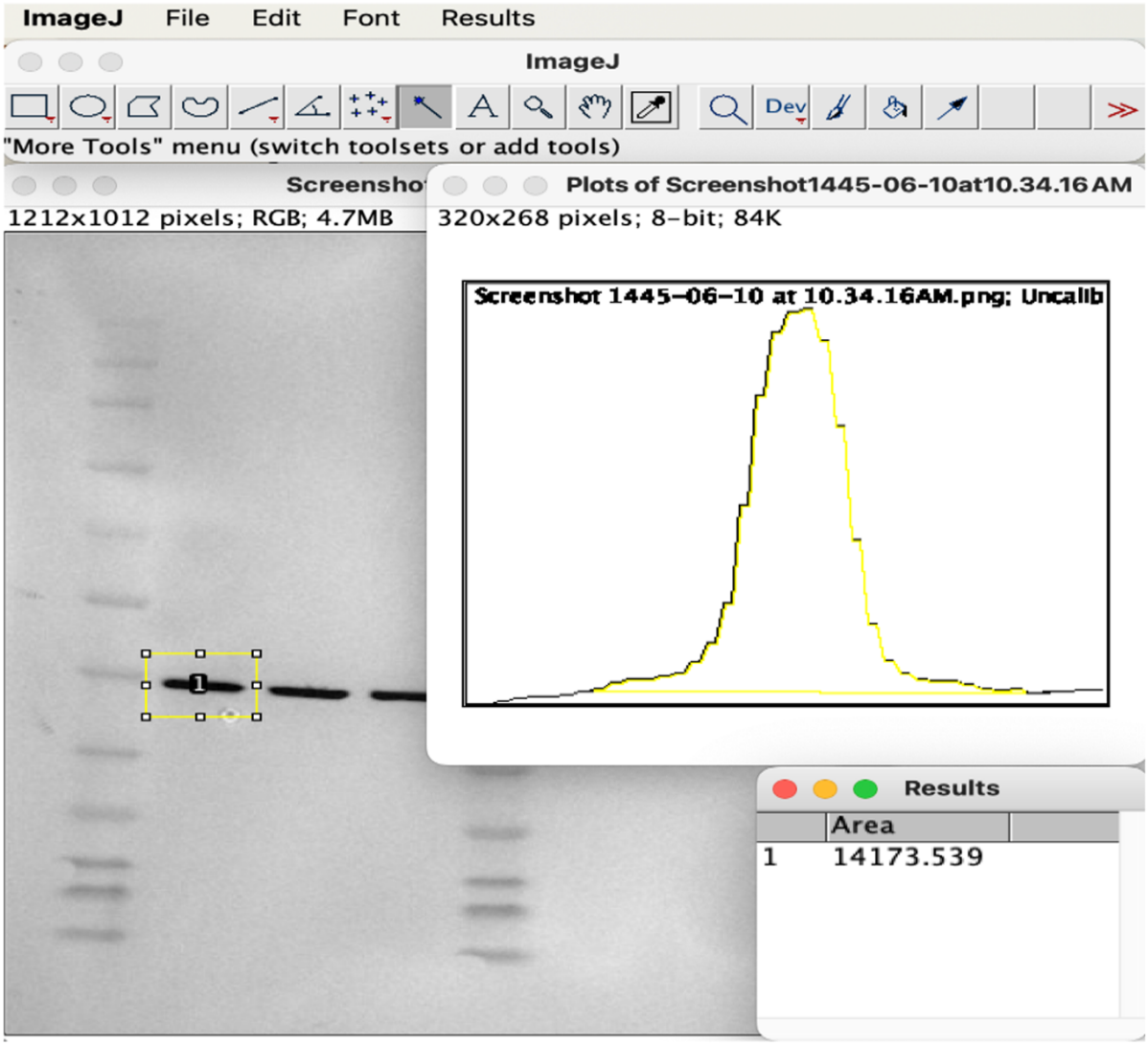


Figure 2.8: Densitometry in Image J. Left: Protein bands were selected for densitometry (yellow box). Top right: Densitometry of the bands is seen as peaks with each peak corresponding to the size of the band. Bottom right: Result box displaying the integrated density measurement. This figure was generated by using ImageJ software.

2.5.8 Blot stripping

WB stripping is a method to remove bound primary and secondary antibodies from a used membrane. This is a useful technique that allows re-probing of a stable membrane with multiples antibodies. Membranes were removed from storage at 4 °C and rinsed with TBST for 5 mins at RT. Following TBST washes, membranes were incubated with stripping buffer

(Restore Plus, Thermo Fisher Scientific) for 15 to 20 mins at RT. Membranes were then washed with TBST three times with 5 mins between each wash, and then membranes were blocked with 5% of Marvel solution for one hour at RT.

2.6 Immunocytochemistry (ICC)

2.6.1 principles of Immunocytochemistry (ICC)

ICC or immunostaining is a common laboratory method used to localize specific proteins in cells by using specific binding of primary and secondary antibodies. Primary antibodies bind to the specific antigen while secondary antibodies bind to the primary antibody. Secondary antibodies are linked with enzymes or a fluorescent tag that provide a signal at the reaction site (Figure 2.9).

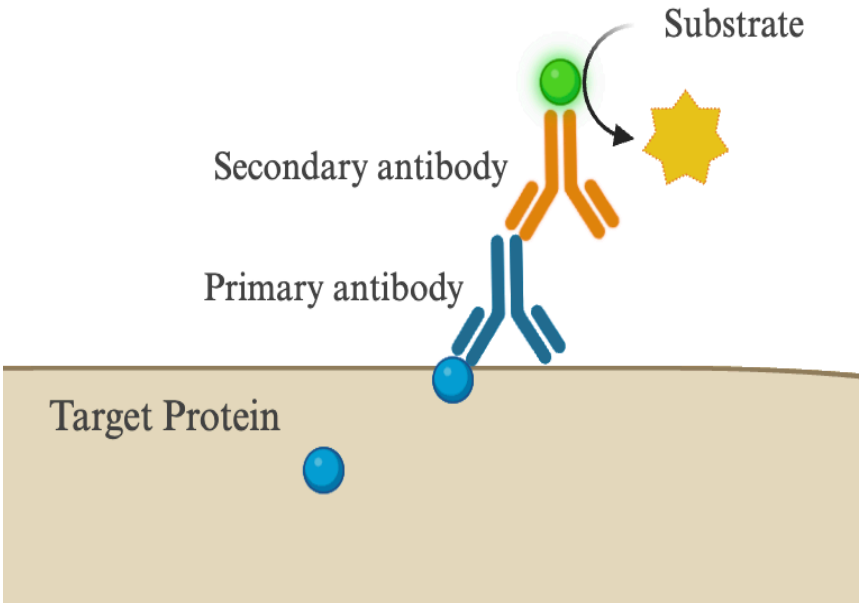


Figure 2.9: Principle of immunocytochemistry. Diagram shows primary antibodies binding to a specific antigen and a secondary antibody binds to the primary antibody. This example

shows an enzyme-based method. Work in this project used fluorescent labels. This figure was generated by BioRender.

2.6.2 Immunostaining of cell cultures

ICC was performed using 8 well chamber slides. Chamber slides with either primary cells (mixed glia, astrocytes) or BHK cells were moved from the tissue culture incubator and rinsed with PBS once and fixed with 4% of paraformaldehyde for 20 mins at RT. Then cells were washed with PBS 4 times with 5 mins between each wash. Following the PBS washes, cells were incubated for 1 hour with ice-cold blocking solution containing PBS with 10% NGS and 0.1% Triton x-100 to avoid antibodies to bind to non-specific antigens (Fujiyama, Furuta and Kaneko, 2001). Triton was included to permeabilize cells. After blocking, coverslips were washed once with ice-cold PBS then incubated with the primary antibody diluted with blocking solution (Table 2.4) overnight at 4 °C. Cells were then washed with ice-cold PBS three times, then cells were incubated with secondary antibody diluted in blocking solution (Table 2.4) for one hour at RT (light protected). Cells were then washed three times with ice-cold PBS before incubated with 4', 6-diamidino-2-phenylindole (DAPI), diluted 1:500 in PBS) for 30 mins at RT (light protected). Cells were then briefly washed with PBS and then the chamber slides detached and coverslips mounted with mounting media (Aqua-Poly Mount, Polysciences). Negative controls were used for all antibodies. Negative controls were stained only with secondary antibodies. Slides were stored at 4 °C and used for microscopy testing within 30 days.

Table 2-4: primary and secondary antibodies were used for staining and detecting proteins in immunocytochemistry:

Primary antibody

Antibody (Cat No)	Dilution Factor	Species	Supplier
AMIGO3 (Mab-2375)	1:100	Mouse	Biotechne
AMIGO3 (Sc-377209)	1:100	Mouse	Santa Cruz, USA
AMIGO3 (Sc-498881)	1:200	Goat	Santa Cruz, USA
AMIGO3 (Sc-377)	1:100	Mouse	Santa Cruz, USA
CD11b (Ab133357)	1:200	Rabbit	Abcam
Olig2 (Ab9610)	1:500	Rabbit	Millipore
CC1 (OP80)	1:500	Mouse	Merck
GFAP (sigma G-3893)	1:200	Mouse	Sigma-Aldrich, UK

Secondary antibody

Antibody (Cat No)	Dilution Factor	Host and Target Species	Supplier
Alexa Fluor 594 (A-110320)	1:500	Goat anti-Mouse	Invitrogen, UK
Alexa Fluor 488 (A27034)	1:500	Goat anti-Rabbit, goat	Invitrogen, UK

2.6.3 Imaging of ICC

A Zeiss Axioplan 2 epifluorescent microscope was used to image most ICC slides in this study. A few ICC studies were imaged with a spinning disc device (Andor DSD1, Andor Technology) connected to an inverted microscope (Zeiss Axiovert). ImageJ has been used to display all ICC images, and to perform cell counts.

2.7 RT-qPCR

2.7.1 RNA isolation

Nucleospin RNA isolation kits (Macherey-Nagel) were used to obtain the isolated RNAs for reverse transcriptase quantitative polymerase chain reaction (RT-qPCR) tests. Following the kit procedure, cultured cells were washed with ice-cold PBS once and 350 µL of lysis buffer RA1 were added to each well with 7 µL of DTT. Gently, cells were scraped and mixed with a 200 µL pipette, and then collected. Lysed contents were transferred into a 2 mL micro tube with a filter (violet ring) and centrifuged at 11,000 x g for one minute. After filtration, the filters were discarded and 350 µL of 70% of ethanol added to each sample and mixed by vortex for 3 to 5 second. Samples were removed to new columns with NucleoSpin filters and centrifuged at 11,000 x g for 30 second. This process allowed RNA to highly bind to the silica membrane. After the spin, the NucleoSpin filters were transferred to new collection tube and 350 µL of MDB (membrane Desalting Duffer) were added to each sample and centrifuged at 11,000 for one minute. MDB was used to remove soluble macromolecules (proteins) which will make the digestion with rDNase more effective. To digest DNA, 10 µL of reconstituted rDNase was mixed with 90 µL of reaction buffer for each sample. The rDNase mixture was then added onto the centre of the column membrane and incubated at RT for 15 minutes. Membranes were washed with 200 µL of RAW2 buffer and centrifuged at

11,000 x g for 30 seconds. Then 600 µL of RA3 buffer was added to the columns for a second wash and centrifuged at 11,000 x g for 30 seconds. Membranes were washed again with 250 µL of RA3 buffer and centrifuged at 11,0000 x g for 2 minutes. Finally, membranes were transferred into new tubes and 30-60 µL of RNase free water added and centrifuged at 11,000 x g for 1 minute. Eluted samples were collected and the concentration of RNA measured with a nano drop system. RNA samples were equalized to ng/mL with nuclease free H_2O, aliquoted into RNAse free micro tubes and stored at -80 °C until complementary DNA (cDNA) synthesis. cDNA synthesis was completed using Superscript III (Thermofisher) and a 1:1 mix of oligoDT and random hexamer primers.

2.7.2 RT-qPCR samples processing

The Luna Universal RT-qPCR master mix (New England Biolabs) was used to run the RT-qPCR reactions. Briefly, 1 µL of H_2O free RNase were added to each well of the non-template control (NTC) wells, and 1 µL (containing 250 ng) of cDNA samples were added to sample wells. 384 well plates were used for RT-qPCR (ThermoFisher). All samples and NTC were run in triplicate. Primers were adjusted with RNase free H_2O to 250 nM (forward and reverse). Master mix was prepared with 10 µL of 1x Luna, 0.5 µL forward primer, 0.5 µL reverse primer, and H_2O up to 19 µL per reaction. Final concentrations of primers was typically 100 nm per reaction. 19 µL of the reaction buffer was added to each well (NTC and cDNA samples), and plate covered with an adhesive cover (ThermoFisher) (Figure 2.10). Plates were centrifuged quickly at 100 rpm for 1 min at 4 °C and then applied to QuantStudio384 system (ThermoFisher) to start the RT-qPCR reaction. RT-qPCR cycles included a heat up to 95 °C for 1 min to separate the cDNA, followed by 40 cycles of 60 °C (30 seconds), 95 °C (15 seconds), and 60 °C (1 minute). Finally, samples were heated to 95 °C for 15 seconds, and then cooled at 4 °C.

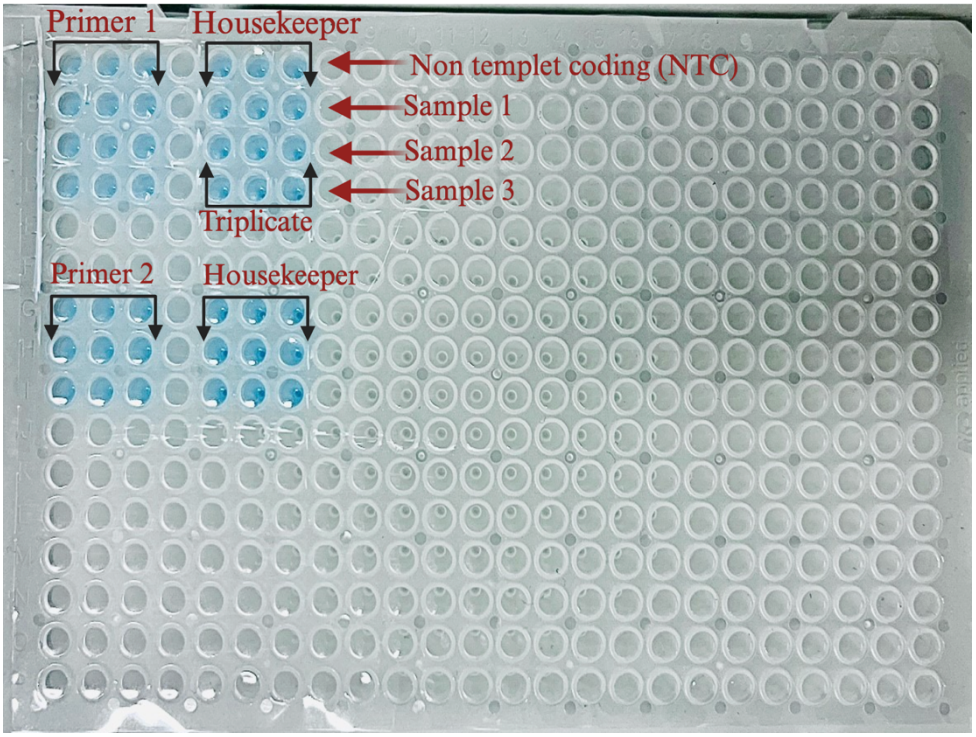


Figure 2.10: A sample RT-qPCR plate depicting NTC and cDNA samples for various primers. All combinations are run in triplicate. The housekeeper gene (β-actin or α-tubulin) is used to normalise gene expression. This figure was generated by using Biorender.

2.7.3 RT-qPCR quantification

Data were collected by the QuantStudio system and cycle time (CT) data obtained from the ThermoFisher connect cloud-based application. The ΔΔCT method was used to calculate relative gene expression values. ΔCT and ΔΔCT values were calculated using an Excel template worksheet and expression of genes normalized against the housekeeper gene (18S (supplied by Primerdesign) or α-tubulin). Finally, ΔΔCT values were converted to the fold gene expression with the Excel formula $2^{\wedge-\Delta\Delta CT}$ (Jafferali *et al.*, 2021).

Table 2-5: List of primers used in this investigation.

Primers	Forward primer	Reverse primer
AMIGO3	AGACTTGGAGGATGTTCTGCC	TGAGTGCGTTGTGGCTCAAAT
LINGO1	CAAGAGAGACATGCGATTGG	TGGTTGAGTGTCTTGATGCG
GFAP	CGTTAAGCTAGCCCTGGACATC	GGATCTGGAGGTTGGAGAAAGTC
CD11b	ACCGGAGCCATCAATCAAGA	CCTGTCCCTGGCTGTTTCTA
PDGFRα	CCATCGAGACAGGTTCCAGTAGT	GGTCCGAGGAATCTATACCAATGT
MOG	CCCTGCTGGAAGATAACACTGTT	CAGCCAGTTGTAGCAGATGATCA
α-tubulin	AAGCAGCAACCATGCGTGA	CCTCCCCCAATGGTCTTGTC
18S	Sequence protected by supplier (PrimerDesign).	Sequence protected by supplier (PrimerDesign).

2.8 RhoA activation assay (G-Lisa)

2.8.1 Principles of RhoA activation assays

RhoA activation assay or G-Lisa has been used to measure the activities of RhoA in BHK and primary mixed glial cultures. The assay works by detecting RhoA in the active guanosine triphosphate bound from. RhoA activity is a useful way to measure activity of the AMIGO3, neurite outgrowth inhibitor-66 receptor 1 (NgR1) and p75 neurotrophin receptor (p75) (AMIGO3/p75/NgR1) signalling complex (Ahmed *et al.*, 2013).

2.8.2 RhoA activation assays

A RhoA activation assay (Cytoskeleton Inc., G-Lisa kit) was used to measure RhoA activity. Briefly, cells were rinsed with ice-cold PBS and 70 µL of protein lysis buffer (Cytoskeleton,

Inc) was added to each well of the tissue cultures. Immediately, cells were harvested with a cell scraper and cell lysate was collected with a pipette and transferred into a 1.5 mL Eppendorf tube. Samples were then centrifuged at 10.000 x g at 4°C for 1 minute. Protein samples were then transferred to new tubes and immediately snap-frozen in liquid nitrogen. Samples were then placed in a Mr Frosty and transferred to a -80 °C freezer until required. The snap-freezing technique was used to prevent the formation of ice crystals which could damage sensitive proteins.

10 µL of protein samples were used to measure the protein concentration. Proteins were equalized and adjusted to between 0.4 to 2.0 mg/mL with protein lysis buffer provided from the kit. On the day of the assay, blank control samples were prepared with lysis buffer and ice-cold binding buffer, and positive controls were setup with the same plus RhoA. The number of reaction strips were placed (one for each blank, positive control and test sample) on the plate holder and kept on ice cold condition. The powder contained in strips was dissolved with 100 µL of ice-cold water and the water was removed after 2 mins from the wells by vigorously flicking the plate into a paper towel. The snap frozen proteins were thawed at RT in a water bath and immediately place on ice. Positive control and blank buffer were vortexed for 3 to 5 seconds then placed on ice. Immediately, 30 µL of both blank buffer, positive control and protein samples were loaded in duplicate in the Rho strip wells. The plate was then placed on an orbital microplate shaker set up at 300 rpm in a cold room (4 °C). Following 30 mins of incubation, solutions were removed from the wells by shaking the plate into a paper towel. Then wells were washed twice with 200 µL of ice-cold washing buffer, primary antibodies were added to the wells and the plate was placed on the orbital shaker at 300 for 45 minutes at RT. Primary antibodies were diluted with RhoA ice-cold lysis buffer 2:500 µL/mL. Following 45 mins, wells were washed three times with 200 µL of washing

buffer and secondary antibodies were diluted 8:500 µL/mL in RhoA ice-cold lysis buffer, and the plate was placed on orbital microplate shaker at 300 rpm for 45 minutes at RT. After secondary incubation, wells were then washed three times. HRP detection reagent was then used containing 50 µL of HRP detection reagent A and HRP reagent B. Cells were then incubated at 5% of CO_2 and 37 °C (light protected). Finally, 50 µL of stop solution was applied to the wells and absorbance read at 490 nm with a plate reader (Figure 2.11).

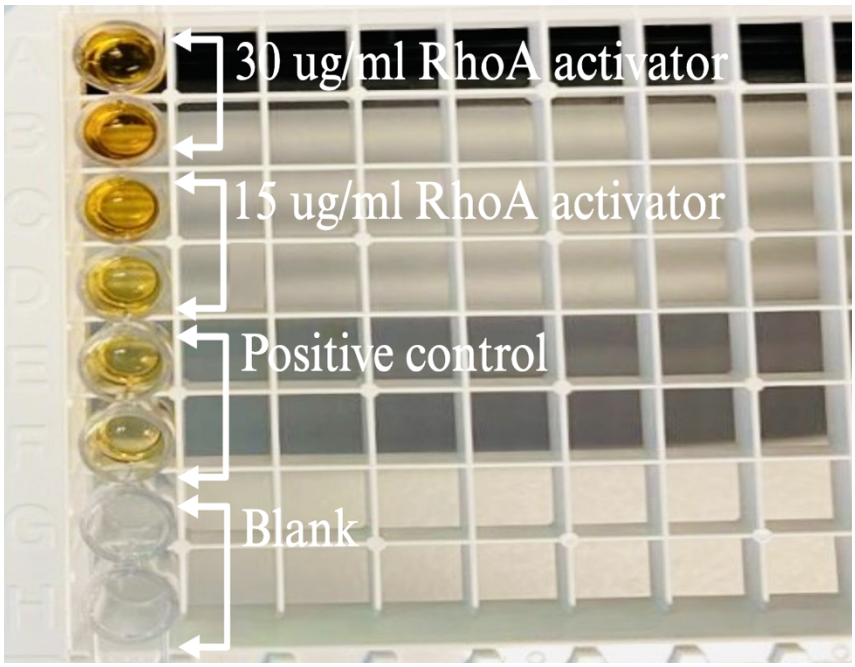


Figure 2.11:RhoA activation assay example. Examples of colour reactions when 15 and 30 ug/mL of RhoA activators were tested on BHK cells. This figure was generated by using Biorender.

2.8.3 RhoA activation assay quantification

RhoA activation assay data was transferred from the plate spectrophotometer reader to Excel software for processing. In Excel, data were normalized to relevant controls (e.g. isotype IgG). The data were then transferred to Prism to compare the levels of RhoA activation between the sample groups.

2.9 Statistical analysis

In this thesis, the biological replicates of BHK cell line are defined as different cell cultures from the same passage of cells, and for the primary cells (mixed glia, astrocytes, microglia) cultures prepared from different litters of pups represent separate biological replicates. For each individual experiment, cells were seeded from the same BHK cell line into different wells to provide the technical replicates (e.g. from the same passage of cells). Primary CNS cells were seeded from the same culture preparation into different wells to provide the technical replicates in primary cells experiments. Further, it's important to note that each primary culture was prepared by pooling 3 to 6 brains. In the following studies, 'N' denotes the biological replicates, while 'n' denotes the number of the technical replicates. Due to time limitations (see COVID statement) experiments in this thesis involved analysis of technical replicates (n=3 to n=7) from a low number of independent biological replicate (N=1 40% of experiments; N=2 10% of experiments; and N=3 50% of experiments). The figure legends of each study provided specific details of the biological and technical replicates.

In this study, given limited sample sizes involved it was not possible to reliably assess normality of the data sets. Using the small sample sizes in these experiments caused a difficulty in the choice of parametric or non-parametric tests. Further, using the parametric tests on non-normal data can cause the less reliable results, while using the non-parametric tests on normally distributed data can increase the risk of producing larger P values, hence missing significant differences. We decided to chose the parametric tests, but understanding we may not have met the test assumptions of the normal distribution. Two-group comparisons were performed with two-tailed t-tests. Multiple group (single factor) comparisons were performed by one-way analysis of variance, and inter-group differences

explored using the post-hoc Tukey test (when all groups were compared) and Dunnett's multiple comparison test (when experimental groups were compared to a control group). In this studies, the statistical calculations were performed using Prism 9.0 (Graphpad Software, El Camino Real, CA, USA). An alpha level (probability of falsely rejecting the null hypothesis) of $P < 0.05$ was used for all comparisons. All data are presented as mean ± standard devation.

Chapter 3 In vitro analysis of AMIGO3 expression and function during OL differentiation

3.1 Rationale

Previous studies show that Amphoterin-induced gene and open reading frame-3 (AMIGO3) is expressed in subcortical white matter and regulated during the development of myelination (Foale *et al.*, 2017). AMIGO3 levels in the corpus callosum peak before myelination started, and the decrease following increased myelination (Foale *et al.* 2019). This finding suggests that AMIGO3 downregulation may be important for the initiation of myelination. Leucine rich repeat and Ig domain containing 1 (LINGO1) is an leucin-rich repeat protein (LRRP) and have similar structure to AMIGO3, and LINGO1 has been shown to downregulate oligodendrocyte (OL) differentiation (Mi, Sandrock and Miller, 2008). This study validates an in vitro mixed glial model for examining OL differentiation, and then performs functional studies using short interfering ribonucleic acid (siRNA) knockdown, and stimulation of AMIGO3 signalling, to test the function of AMIGO3 on OL differentiation.

3.1.1 The NgR1 and p75 signalling pathway downregulates OL differentiation

As discussed above, the function of AMIGO3 during central nervous system (CNS) myelination has not been explored. However, AMIGO3 has been hypothesized to regulate OL differentiation in a similar fashion to LINGO1 (Foale *et al.*, 2017; Li *et al.*, 2021). Specifically, both LINGO1 and AMIGO3 bind to p75 neurotrophin receptor (p75) and neurite outgrowth inhibitor-66 receptor (NgR1) to form a signalling complex (AMIGO3/p75/NgR1) (Mi *et al.*, 2004; Ahmed *et al.*, 2013). Note, the tumor necrosis factor receptor superfamily, member 19 (TROY) can substitute for p75 in this complex (e.g. AMIGO/TROY/NgR1) (Ahmed *et al.*, 2013). These signalling complexes are coupled to the Ras homolog gene family member A (RhoA) guanosine triphosphate (RhoA GTP) system, which leads to activation of Rho-associated protein kinase (ROCK)/LIM-domain containing

protein kinases (LIMK) signalling, and finally regulation of actin cytoskeleton elements (Figure 3.1). Activation of RhoA causes growth cone collapse as it promotes depolymerization of the actin cytoskeleton. Since the initial phase of OPC differentiation relies on correct spatial and temporal polymeristion of tubulin and actin and the assembly of activated non-muscle myosin with actin fibres, RhoA GTP levels are crucial to regulating this process (Mullins, Heuser and Pollard, 1998; Wojciak-Stothard and Ridley, 2003). Therefore, RhoA GTP regulates the cell actin cytoskeleton via the downstream effector protein ROCK, which is involved in the biological processes of OL migration and differentiation (Tan *et al.*, 2011). Given that AMIGO3 interactions with p75/NgR1 or TROY/NgR1 inhibitor complexes lead to axonal growth cone collapse via RhoA activation (Ahmed *et al.*, 2013), we predict that AMIGO3 may act via the same pathway to regulate OL differentiation. Indeed, there is evidence linking the actin cytoskeleton to OL differentiation and myelination (Azevedo *et al.*, 2018). Based on the above, we studied the reaction between AMIGO3 stimulation and RhoA activation, and the effects of AMIGO3 regulation on OL differentiation.

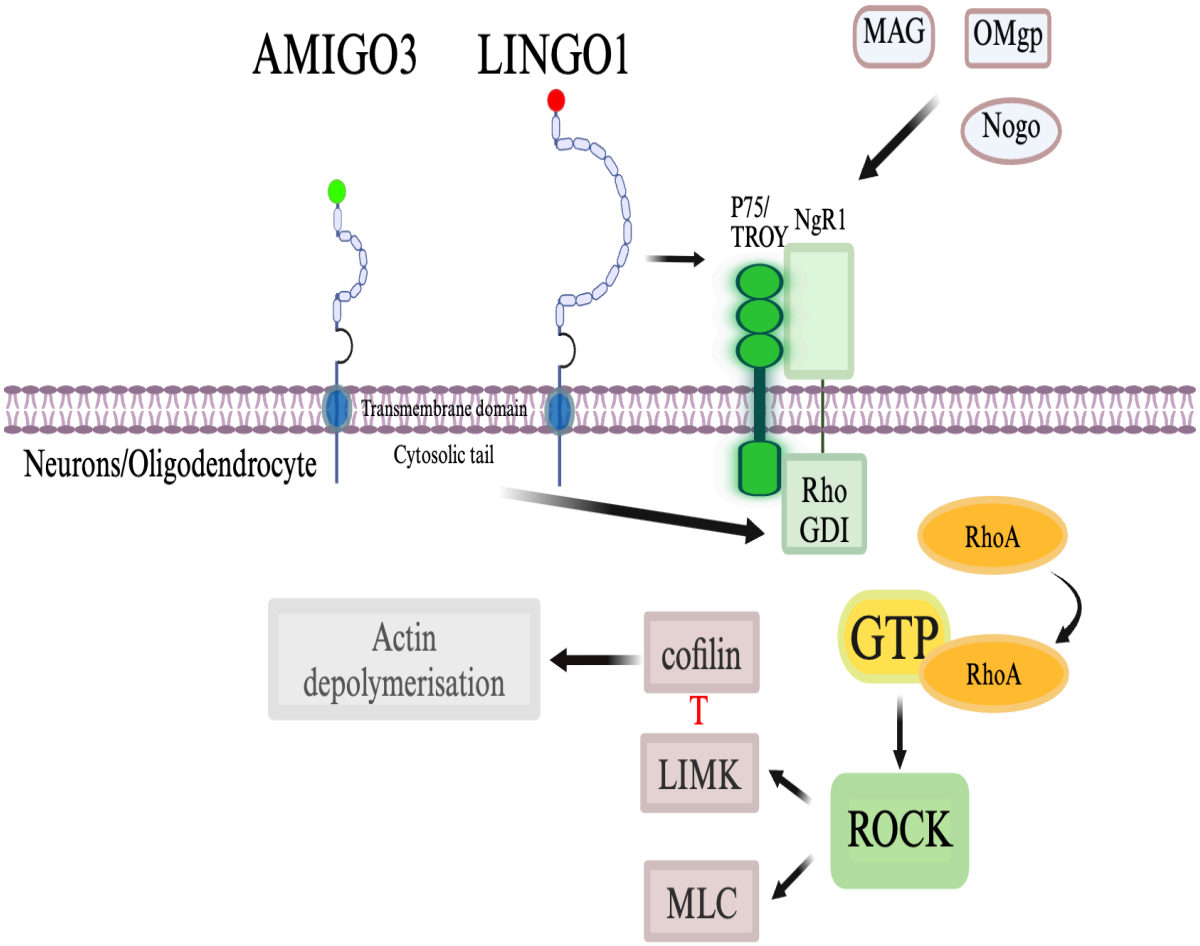


Figure 3.1: Diagram showing the AMIGO3/LINGO1/p75/TROY and NgR1 signalling pathway with links to the actin cytoskeleton. This figure was adapted from previous work (Foale *et al.*, 2017) using BioRender.

3.1.2 Potential for AMIGO3-AMIGO3 homotypic signalling to influence OL differentiation

AMIGO3 may influence OL differentiation via the RhoA signalling pathway. We therefore wished to ask which CNS ligands act to promote AMIGO3/p75 (or TROY)/NgR1 activation on oligodendrocyte precursor cell (OPC). Biochemical assays indicate that AMIGO proteins including AMIGO3 can interact through hetero and homotypic interactions (Kuja-Panula *et al.*, 2003). This suggests that AMIGO3 from different CNS cells (e.g. astrocyte, OL) could

promote AMIGO3 signalling on OPC/OL. As discussed later in chapter 4, AMIGO3 is expressed widely in the CNS, suggesting that AMIGO3-AMIGO3 homotypic signalling could be a powerful signal during OL differentiation.

3.2 Hypothesis

The hypothesis in this chapter is that stimulation of AMIGO3 expression acts to promote the RhoA GTP signalling pathway in mixed glial cultures. Furthermore, modulation of AMIGO3 signalling, either with knockdown, or treatment with recombinant AMIGO3, will influence OL differentiation. Specifically, knockdown will promote OL differentiation, while AMIGO3 stimulation will inhibit OL differentiation.

3.2.1 Aims

In this study we aim to establish the mixed glial system as a model to study OL differentiation via the development of myelination. Using this system we will examine OL differentiation during myelination by using 2', 3'-cyclic-nucleotide 3'-phosphodiesterase (CNPase) marker protein in Western blot (WB). We also aim to examine AMIGO3 function during OL differentiation in the mixed glial model by using siRNA to knockdown AMIGO3 function and to examine the ability of recombinant AMIGO3 to inhibit OL differentiation in mixed glial cultures. We will also use the Baby Hamster Kidney (BHK) cell line, which expresses naturally AMIGO3, to confirm the effect of siRNA knockdown, and to confirm that recombinant AMIGO3 activates the RhoA pathway.

3.3 Materials and method

All materials and methods used in this chapter have been described above in Materials and Method chapter (Chapter 2) (specific sections are indicated below).

3.4 Experimental design

3.4.1 Western blot

Proteins lysates were collected as previously described in chapter 2 (section 2.5). Antibody dilutions were used as previously stated (Table 2.3). Finally, proteins expression was analyzed by using ImageJ to measure the integrated densities. The data were then normalized to a reference protein (β-actin and alpha-tubulin).

3.4.2 Immunocytochemistry

Immunocytochemistry (ICC) has used to investigate and study different proteins expression in our mixed glial cultures and the BHK cell line. The basic staining protocol is described in chapter 2 (section 2.6). Anti-Olig2 and anti-adenomatous polyposis coli (APC, referred to here as CC1) were used to identify OPC and OL in mixed glial cultures. 4', 6-diamidino-2-phenylindole (DAPI), staining was used to identify cell nuclei during cell counts. Negative controls were performed using only secondary antibodies, and with no primary antibody.

3.4.3 Cell cultures

3.4.3.1 Primary mixed glial culture

Primary cultures were obtained from cortex tissues of FVB/N mice pups at 3 day postnatal (P3). The tissue was physically and enzymatically disrupted as previously described in chapter 2 (section 2.3.1). Primary mixed glial cultures were cultured for 3, 7, 14 and 21 days in vitro (DIV) to cover the peak time of developmental myelination in the mouse CNS (Jacobs *et al.*, 2005). At the end of each time-point cultures were either collected for protein lysis or fixed with paraformaldehyde for ICC (section 2.6.2).

3.4.3.2 BHK culture

BHK cells were used in this chapter to optimize AMIGO3 siRNA (section 3.4.4), recombinant AMIGO3 treatments (section 3.4.5), and to test RhoA activation assays (section 3.4.6) to study the role of AMIGO3 in mixed glial model. BHK cultures were processed for WB and ICC analysis using the same procedures as used for mixed glial cultures.

3.4.4 siRNA transfection

AMIGO3 was knocked down using Flexitube siRNA product purchased from Qiagen. Flexitube contains four siRNA sequences targeting the AMIGO3 gene. siRNA sequences were transfected into cells using the HiPerFect reagent (Qiagen). The All Stars negative control siRNA (Qiagen) was used as negative control for siRNA experiments. Both the negative control and AMIGO3 siRNA sequences were used at 30 and 50 nM. BHK cells were used to identify the efficiency of siRNA sequences, and knockdown of AMIGO3 gene was tested using WB. In primary mixed glial culture experiments, siRNA were applied from 5

DIV to 7 DIV. This time-window was chosen based on our data showing that AMIGO3 expression peaked at 3 DIV (section 3.5.2.2).

3.4.5 Recombinant AMIGO3 studies

Stimulation of AMIGO3 was achieved by treating the cultures with recombinant AMIGO3 (Biotechne). Recombinant AMIGO3 was used at either 1 or 2 µg/mL. Effective concentrations were checked in the BHK cells using the RhoA activation assay (section 3.4.6). The effect of recombinant AMIGO3 treatment on OL differentiation was tested using both WB and ICC in mixed glial cultures. For these studies, recombinant AMIGO3 has been applied between 7 DIV to 11 DIV. This time was chosen to match the highest peak of AMIGO3 expression observed in our mixed glial cultures (section 3.5.2.2).

3.4.6 RhoA activation assays

The RhoA GTP signalling pathway has been implicated in OL differentiation. We used a RhoA activation assay (Cytoskeleton Inc., G-Lisa kit) to check if recombinant AMIGO3 could activate RhoA activity in BHK cell cultures, and mixed glial cultures. The assay is based on an enzyme linked immunosorbent assay method, and the result is read out using a plate reader to measure absorbance at 490 nm. Full details of the assay are shown in chapter 2 (section 2.8.2).

3.5 Results

3.5.1 Immunocytochemical analysis of OL differentiation in mixed glial culture

Anti-Olig2, also known as OL transcription factor 2, is a used to stain all stages of OL and OPC (Liu *et al.*, 2007), while millipore anti-APC (also known as clone CC1) is the specific

antibody used to stain and label the mature OL without labelling myelin (Figure 3.2) (Bin, Harris and Kennedy, 2016). A combination of Olig2 and CC1 staining has often been used to examine OL differentiation (e.g. Fannon, Tarmier and Fulton, 2015). Therefore, we decided to stain our mixed glial cultures with Olig2/CC1 to determine OL differentiation. Anti-Olig2 was detected with Alexa fluor 594, while anti-CC1 was detected with Alexa fluor 488 green dye. Both primary and secondary antibodies dilutions were previously stated in chapter 2 (Table 2.9). All stains in this study were validated with negative controls which stained only with secondary antibodies and no primary antibodies. Also DAPI was used to highlight the nucleic in our culture cells for cell counting. The cultures were then imaged with a wide field microscope to examine the three staining channels (described previously in chapter 2, section 2.6.3).

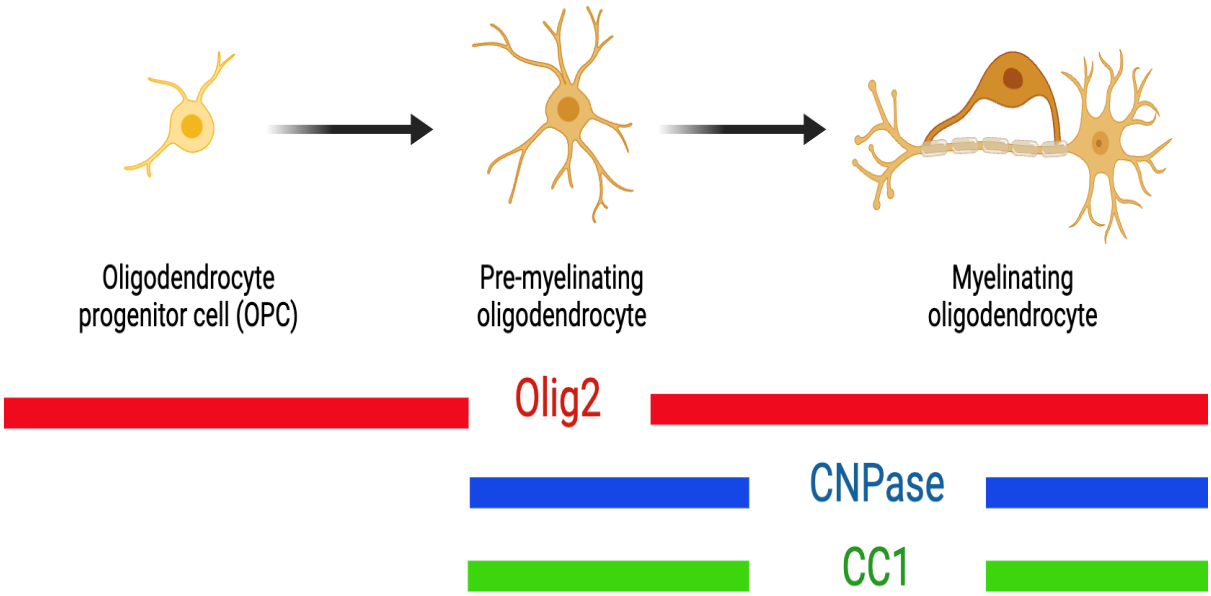


Figure 3.2: Different markers proteins for OL linage development used in this study. Anti-Olig2 marker protein is a specific stain for all OL development stages (OPC and OL). Anti-CC1 marker is specific to stain for mature OL. Anti-CNPase marker protein is a specific marker for mature OL (used in WB). In these studies, we used CC1 and Olig2 for ICC, and CNPase was used for WB experiments. This figure was generated by using BioRender.

Mixed glial culture had many cells that were positively stained by anti-Olig2 and anti-CC1. The staining was specific as shown by negative control staining. We note that olig2 staining appeared cytoplasmic. In recent studies, Olig2 has been used to stained OPC/OL nucleus (Fannon, Tarmier and Fulton, 2015). However, cytoplasmic Olig2 can indicate immature astrocytes (Figure 3.3 C) (Tatsumi *et al.*, 2018). So, the staining of these cultures cannot reliably show OPC/OL. In contrast, CC1 staining, which labeled around 40 % of all DAPI+

cells (Figure 3.4), shows the expected pattern (staining in cytoplasm) (Fannon, Tarmier and Fulton, 2015), therefore in subsequent analysis we focused on CC1 staining and ignored the olig2 signals. Olig2+ cells were more abundant than CC1+ cells, being 58.7 % (± 5.4) of DAPI cells, compared to 36.2 % (± 4.07**)** of DAPI cells for CC1+ cells (Figure 3.4). A two-tailed T-test indicated that the number of Olig2+/DAPI+ cells was significantly higher compared to the number of CC1+/DAPI+ cells ($p < 0.0001$) (Figure 3.4). This agrees with the link between that cytoplasmic Olig2 staining and immature astrocytes which are likely to be the most abundant cell in the mixed glial culture.

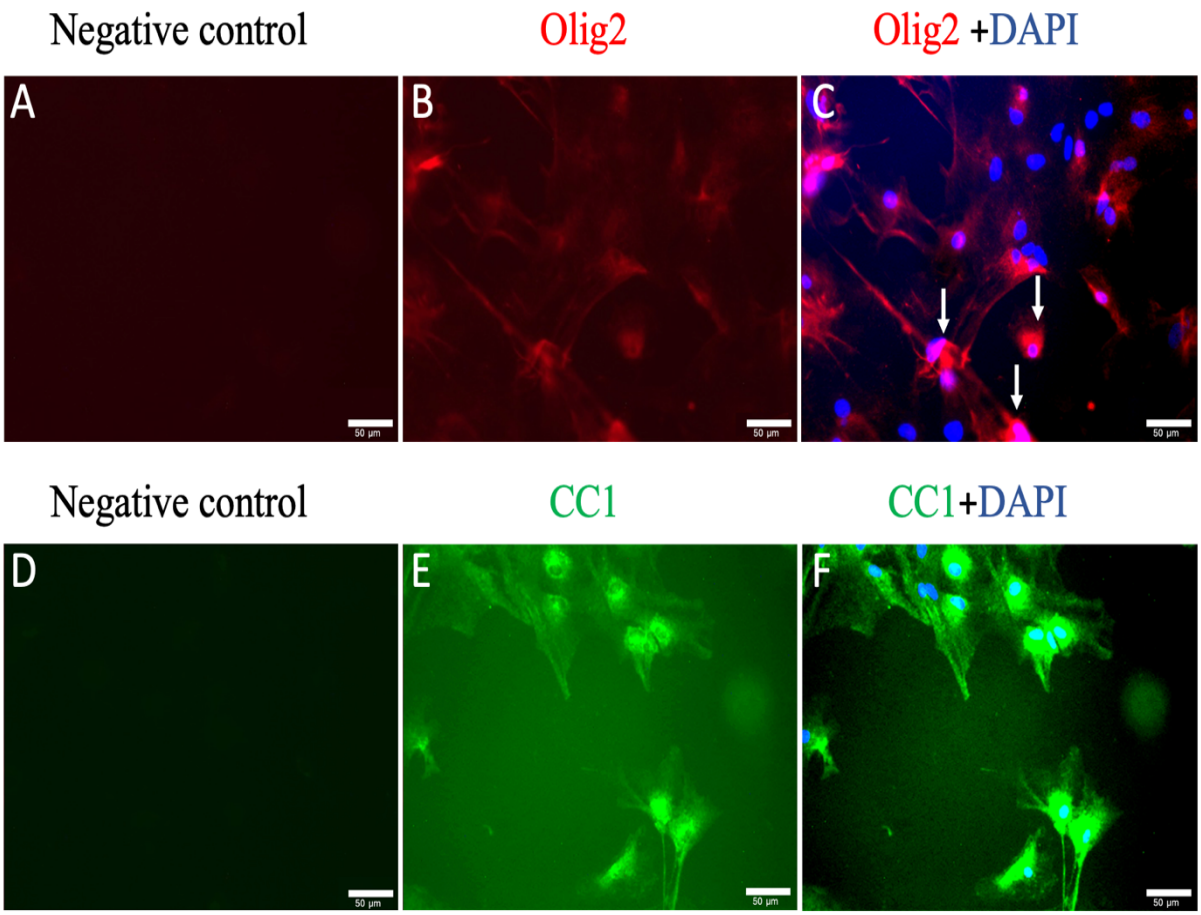


Figure 3.3: Representative positive staining for Olig2 and CC1 in primary mixed glial culture, obtained from FVB/N mice (P3). (A) Negative control for rabbit Alexa594. (B) anti-Olig2 (red). (C) Merge of anti-Olig2 (green) and DAPI (blue), (D) Negative control for mouse Alexa488. (E) anti-CC1 (green). (F) merge of anti-CC1 (green) and DAPI (blue). Arrows indicate anti-Olig2 cytoplasmic stain in mixed glial culture. Note, strong signals observed with anti-Olig2 (red) compared to anti-CC1 (green). Images are representative of one biological replicates N=1, each with seven technical replicates n=7 for each trial. Error bars represent mean ± SD.

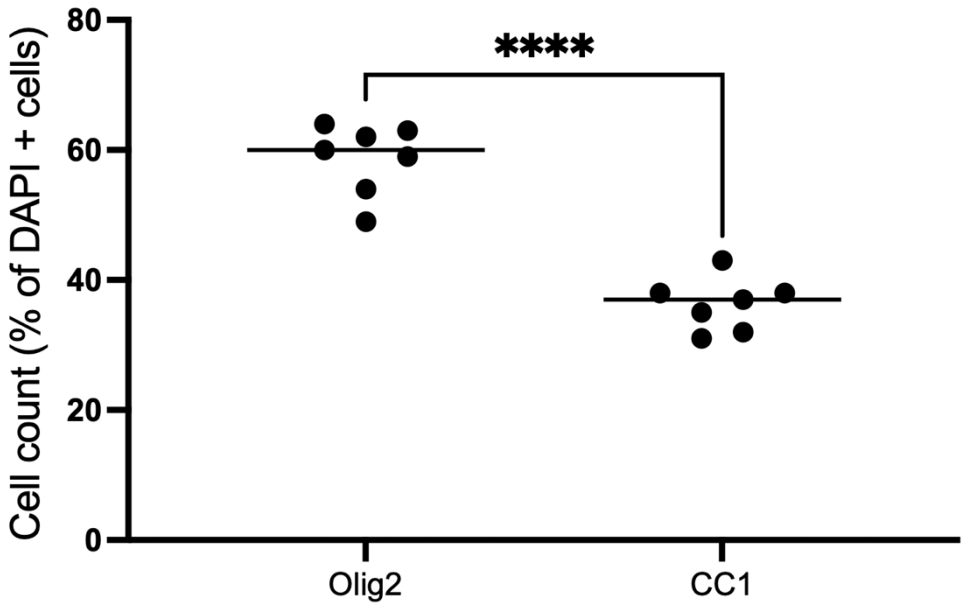


Figure 3.4: Quantification of Olig2 and CC1 staining in primary mixed glial culture. Markers (Olig2 and CC1) are expressed as % of DAPI+ cells. Data points represent the average of seven technical replicates (n=7), from a single biological replicate (N=1). **** significant at $p<0.0001$ for two-tailed T-test. Error bars represent mean ± SD.

3.5.2 Western blot analysis of AMIGO3 and LINGO1 expression during OL differentiation in mixed glial cultures.

WB experiments were preformed to test AMIGO3 and LINGO1 expression during OL differentiation in primary mixed glial cultures. To do this, we decided to investigate AMIGO3, LINGO1 and CNPase expression at four different times in cultures (3, 7, 14 and 21 DIV) as previously discussed.

3.5.2.1 Analysis of OL differentiation in mixed glial cultures.

To begin, CNPase was tested by WB as a marker for mature OL. One band was observed at 48 kDa (Figure 3.5 A), which is the expected size for CNPase (based on the antibody data sheet). CNPase integrated density (quantification method described in section 2.5.7) appears relatively low at 3 DIV before rapidly increasing through the other time-points (integrated density (arbitrary units) at: 3 DIV 1 ± 0.13; 7 DIV 5.34 ± 1.54; 14 DIV 13.90 ± 4.04; 21 DIV 17.60 ± 1.95) (Figure 3.5 B). Importantly, the highest level of CNPase was detected at 21 DIV, which is the last time-point in the series (Figure 3.5 B). One-way ANOVA identified a statistically significant source of variation for CNPase expression between the 4 time-point (ANOVA, $F(3, 8) = 30.92$ $p<0.05$) ($P= 0.0001$). Post-hoc comparison of the groups via the Tukey test showed a significant difference between 3 DIV and 14 DIV ($p<0.001$), and between 3 DIV and 21 DIV ($p<0.0002$). In addition, a significant change also occurred between 7 DIV and 14 DIV ($p<0.01$). Overall, CNPase expression increased during the time-point of mixed glial cultures, indicating OL differentiation in the development of the myelination within CNS.

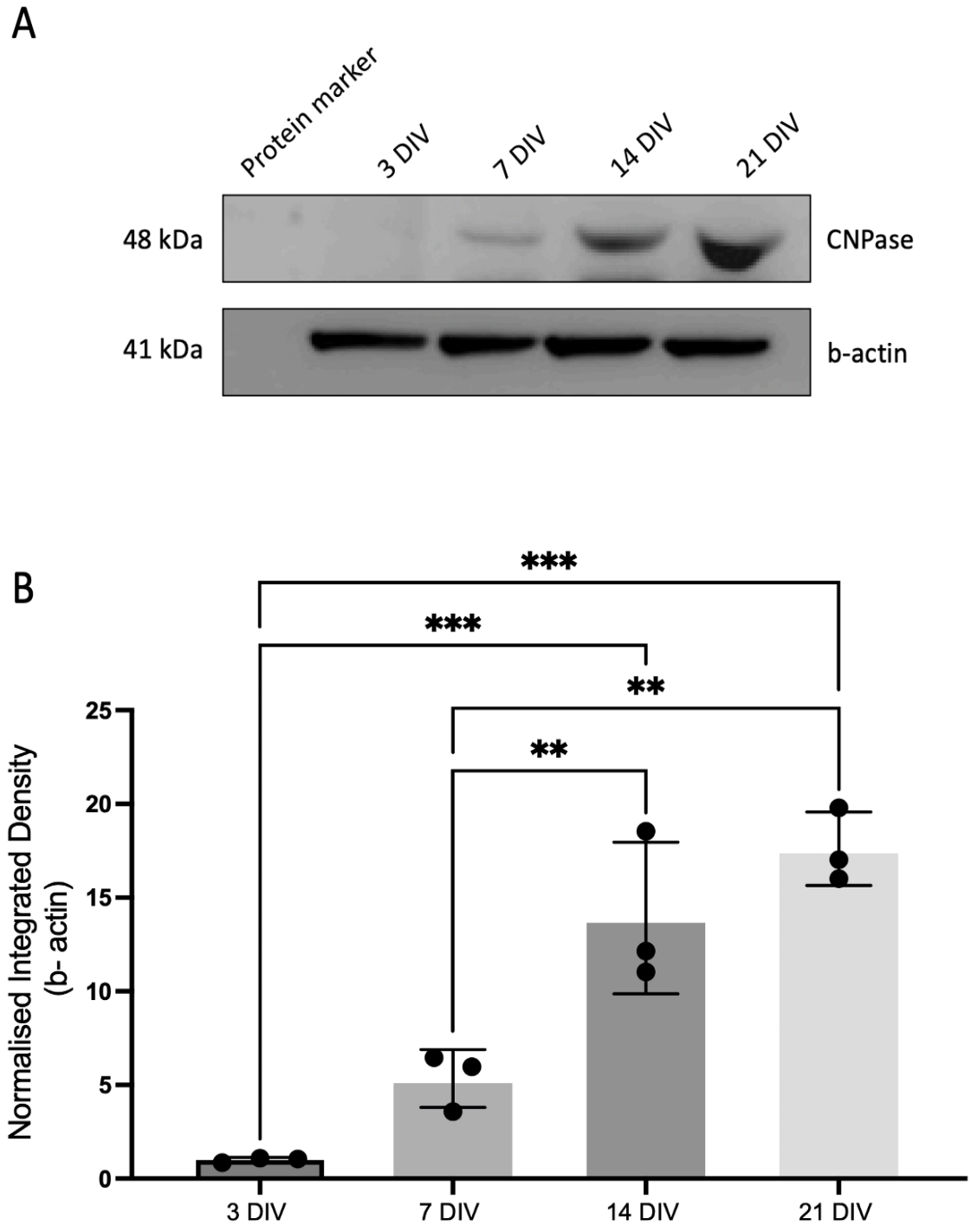


Figure 3.5: (A) Representative blots observed with anti-CNPase Ab at 48 kDa indicate oligodendrocyte differentiation increased during development in the mixed glial cultures. (B) quantification of the CNPase expression in primary mixed cells groups at 3,7,14 and 21 DIV. CNPase expression was rapidly increased throughout the development of the cultures. Protein expression was normalized to beta-actin. Data points represent the average of three technical

replicates (n= 3), from a single biological replicate (N=1). ** and *** indicate significance in the Tukey post-hoc test at $p<0.01$ and $p<0.001$ respectively. Error bars represent mean ± SD.

3.5.2.2 AMIGO3 and LINGO1 expression during OL differentiation in mixed glial cultures

AMIGO3 and LINGO1 were also examined at 3, 7, 14 and 21 DIV mixed glial cultures by WB. The Biotechne-MAB anti-AMIGO3 (MAB-2375) reliably detected a band at 70 kDa (Figure 3.6 A), but we did not see bands at the sizes previously detected in our lab (Foale *et al*., 2019) using other antibodies. The 70 kDa band is seen at 3 DIV, and then expression sharply rises to peak at 7 DIV (integrated density (arbitrary units) at: 1 DIV 1 ± 0.55; 7DIV, 6.03 ± 0.58). Expression then decreases at 14 DIV, and then remains relatively stable at 21 DIV (integrated density (arbitrary units) at: 14 DIV 2.65 ± 0.68; 21DIV 2.84 ± 1.50) (Figure 3.6 B). One-way ANOVA identified a significant change in the 70 kDa AMIGO3 band between the four time-points tested (ANOVA, $F(3,8) = 15.66$ $p<0.05$) ($P=0.001$). Post-hoc comparison of the groups via the Tukey test showed that peak expression by 7 DIV group was significantly larger than at 3 DIV ($p<0.001$), 14 DIV ($p<0.01$) and 21 DIV ($p<0.05$) (Figure 3.6 B). Overall, the highest peak of AMIGO3 expression was at 7 DIV compared to other time-points in mixed glial cultures.

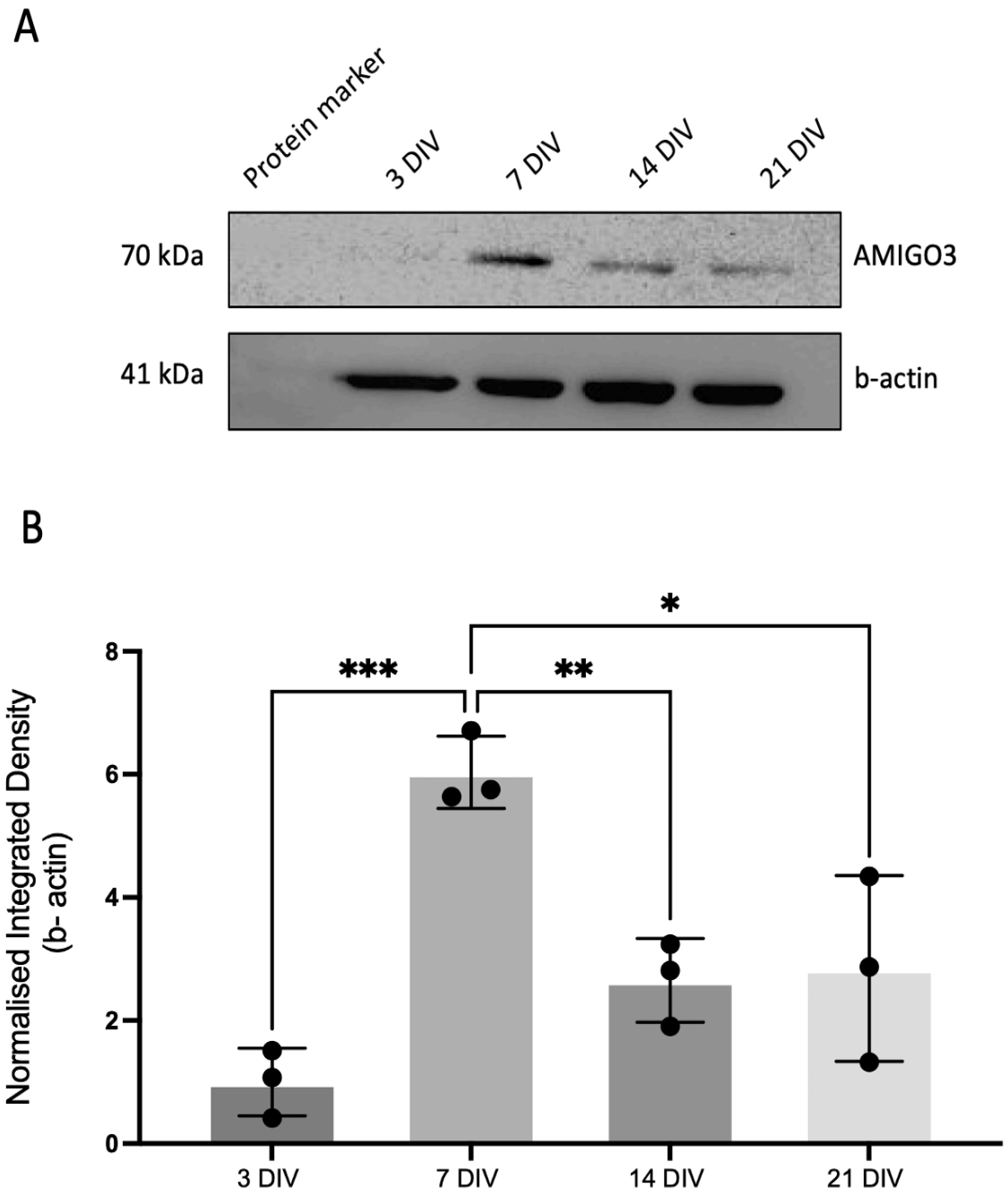


Figure 3.6: (A) Representative WB of Biotechne-MAB anti-AMIGO3 Ab AMIGO3 was observed at 70 kDa. (B) Quantification of AMIGO3 expression in primary mixed glial culture groups (3,7,14 and 21 DIV) were obtained from forebrain mice P3. AMIGO3 expressions was observed at 3 DIV before increasing at 7 DIV. AMIGO3 expressions declined at 14 DIV, and remained relatively stable between 14 DIV and 21 DIV. Integrated densities (arbitrary

units) were normalized to beta-actin. Data points represent the average of three technical replicates (n=3) from a single biological replicate (N=1). *, ** and *** indicate significance in the Tukey post-hoc test at $p<0.05$, $p<0.01$ and $p<0.001$ respectively. Error bars represent mean ± SD.

The Abcam anti-LINGO1 ab (ab-23661) was tested by WB in the primary mixed glial culture groups. One band was observed at 10 kDa (Figure 3.7 A), differing from the pattern of bands our group previously detected in mouse forebrain (17, 23, 28, 40-45 and 87 kDa) (Foale *et al*., 2019). The 10 kDa LINGO1 band was observed at 3 DIV, and was then seen to rise to peak at 7 DIV before decreasing at 14 DIV, and then becoming relatively stable at 21 DIV (integrated density (arbitrary units) at: 3 DIV 1 ± 0.6; 7 DIV 2.46 ± 0.74; 14 DIV 1.36 ± 0.7; 21 DIV 1.03 ± 0.35). (Figure 3.7B). Despite this trend, one-way ANOVA did not identify a statistically significant source of variation for the density of this 10 kDa band across the four time-points (ANOVA, $F(3, 8) = 3.63$ ($P>0.05$) ($P=0.064$). Overall, our data show that LINGO1 has a similar pattern to AMIGO3, but we could not confirm changes in LINGO1 expression in these mixed glial cultures.

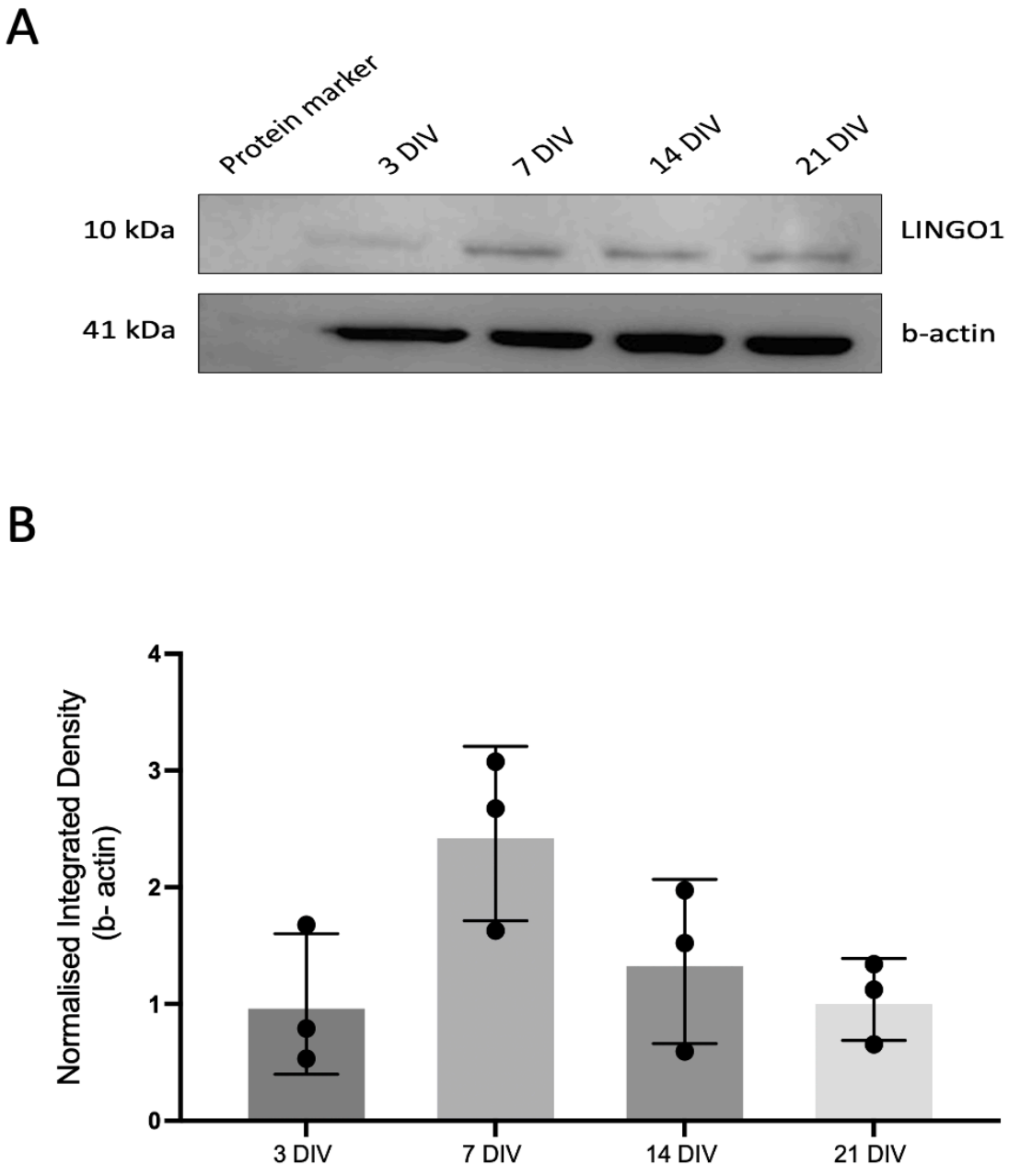


Figure 3.7: (A) Representative blots observed with Abcam anti-LINGO showing bands at 10 kDa. (B) Quantification of LINGO1 expression in primary mixed glial cultures. LINGO1 levels increased between 3 and 7 DIV before declining and remaining stable at 14 and 21 DIV. Integrated densities (arbitrary units) were normalized to beta-actin. Data points represent the average of three technical replicates (n=3) from a single biological replicate (N=1). One-way ANOVA revealed no significant difference between the time-points ($P > 0.05$). Error bars represent mean ± SD.

3.5.2.3 Summary of AMIGO3 and LINGO1 expression during OL differentiation in mixed glial cultures

The time-course of AMIGO3, LINGO1 and CNPase protein expression were re-plotted on the same graph to show changes in the level of the leucin-rich repeat protein (LRRPs) during OL differentiation in the mixed glial cultures (Figure 3.8). This graph shows AMIGO3, LINGO1 and CNPase expression during mixed glial cultures time-points. CNPase appear at 3 DIV and rapidly increases from 7 DIV through the time-points in mixed glial cultures. AMIGO3 increased at 7 DIV then declined at 14 and 21 DIV. LINGO1 expressed lower than AMIGO3 but, has similar pattern to AMIGO3 in all four different time-points.

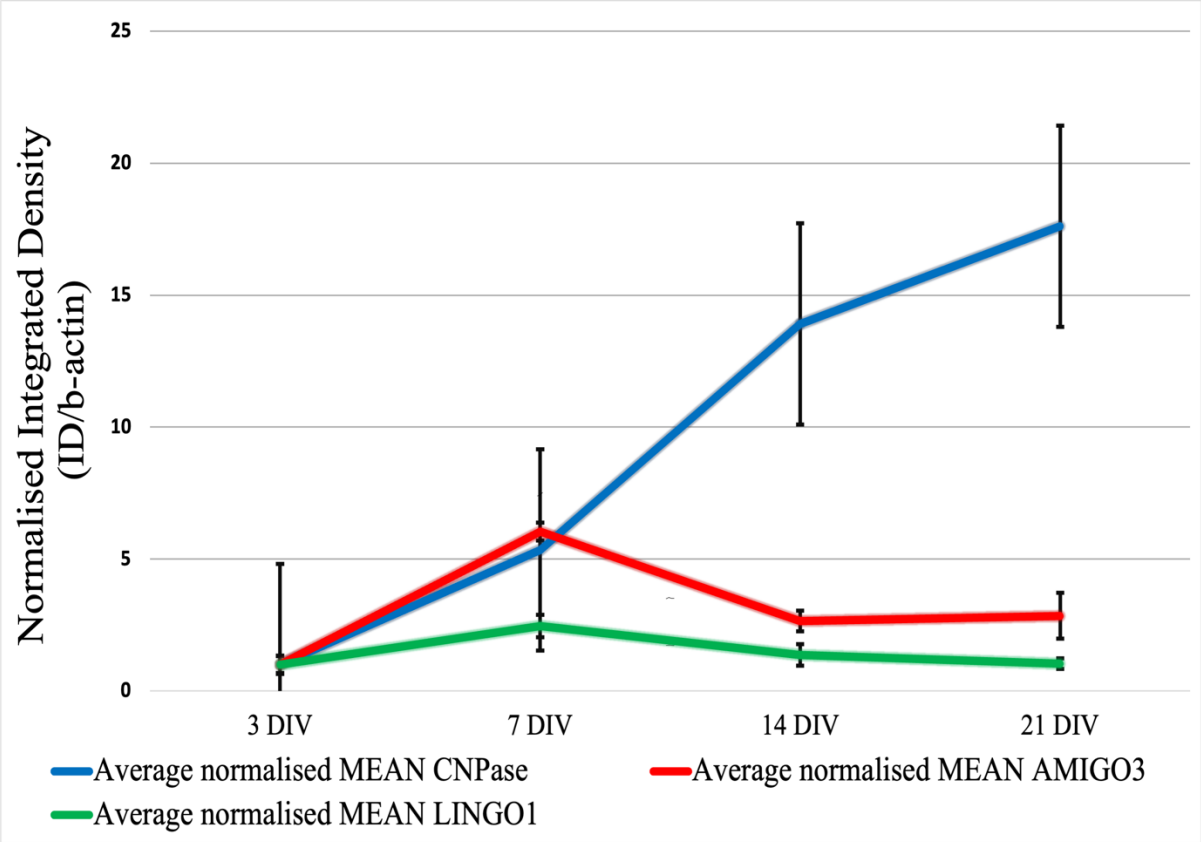


Figure 3.8: Summary of CNPase, AMIGO3 and LINGO1 protein expression data from figure 3.5, 3.6 and 3.7. CNPase increased rapidly in 3, 7, 14 and 21 DIV in mixed glial cultures. AMIGO3 increased at 7 DIV then decreased during the appearance of CNPase. LINGO1 has similar pattern to AMIGO3 but, has lower level of expression compared to AMIGO3. Data points represent the average of three technical replicates (n=3), from a single biological replicate (N=1). Error bars represent SEM.

3.5.3 Studying AMIGO3 function in OL differentiation: siRNA studies

The above data, and the results from Foale (2019), shows that AMIGO3 expression peaks at the start of OL differentiation. siRNA knockdown of AMIGO3 in mixed glial culture would be a way to study the effect of AMIGO3 expression during OL differentiation. The following

experiments test an siRNA knockdown method in BHK cells, and then use it to test the function of AMIGO3 during OL differentiation in mixed glial cultures.

3.5.3.1 Optimizing knockdown of AMIGO3 in BHK cells

We used the BHK cells line to test the Qiagen AMIGO3 siRNA kit. BHK cells were already setup in the lab from previous projects, and AMIGO3 expression has been identified in kidney tissue (Kuja-Panula *et al.*, 2003; Li *et al.*, 2021), so these cells were a logical choice for this initial study. We first confirmed that BHK cells expressed AMIGO3 using ICC. Using the Biotechne-MAB anti-AMIGO3 antibodies, a strong AMIGO3 stain was observed on the majority of the cells (Figure 3.9).

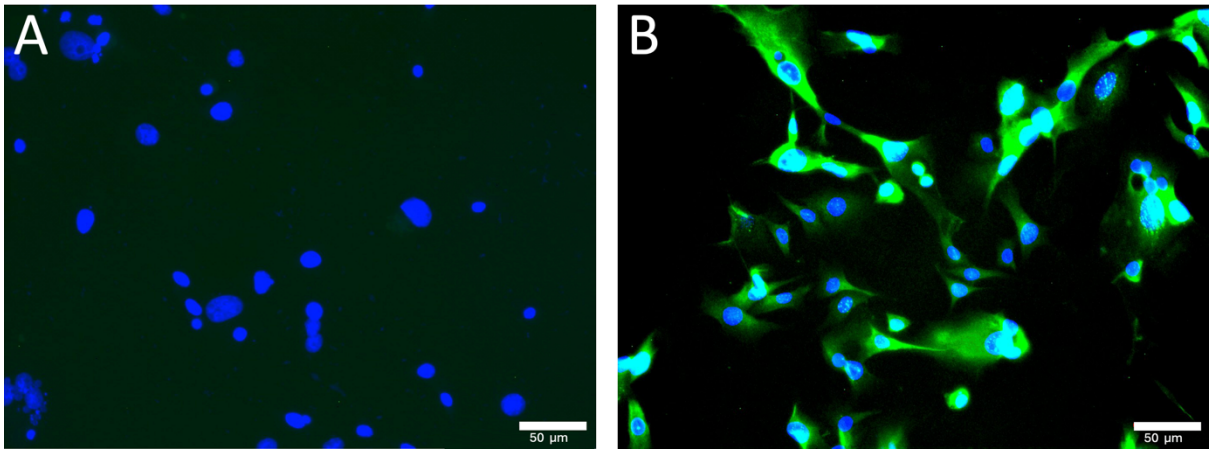


Figure 3.9: Representative AMIGO3 staining in BHK cells. (A) control (no primary antibody, incubation with mouse Alexa Fluor 488) shows no signal within BHK. Blue signal shows DAPI. (B) Strong signals of AMIGO3 within BHK cells incubated with anti-AMIGO3 and mouse Alexa Fluor 488. Images are representative of staining from three independent lines of BHK cells (cultures setup from separate tubes) (N=3), each with seven technical replicate wells (n=7).

3.5.3.2 siRNA knockdown of AMIGO3 in BHK cells

We used two different concentrations for the AMIGO3 and control siRNA: 30 nM and 50 nM. BHK cells were transfected with a mixture of four AMIGO3 siRNA sequences totaling 30 nM or 30 nM of a negative control siRNA sequences, once 70% of the confluency was achieved. 48 hours after transfection cells were lysed and samples prepared from WB. A clear band was observed at 70 kDa in BHK cells using the Biotechne MAB anti-AMIGO3 (Figure 3.10 A). This band is the same size as the band in mixed glial cultures (Figure 3.6). AMIGO3 protein expression was similar between the 30 nM control and AMIGO3 siRNA groups (normalized integrated density (arbitrary units): 30 nM AMIGO3 siRNA 0.3 ± 0.05; 30 nM negative control siRNA 0.4 ± 0.009), and a two-tailed T-test indicated no change in AMIGO3 expression ($P>0.05$) (Figure 3.10 B).

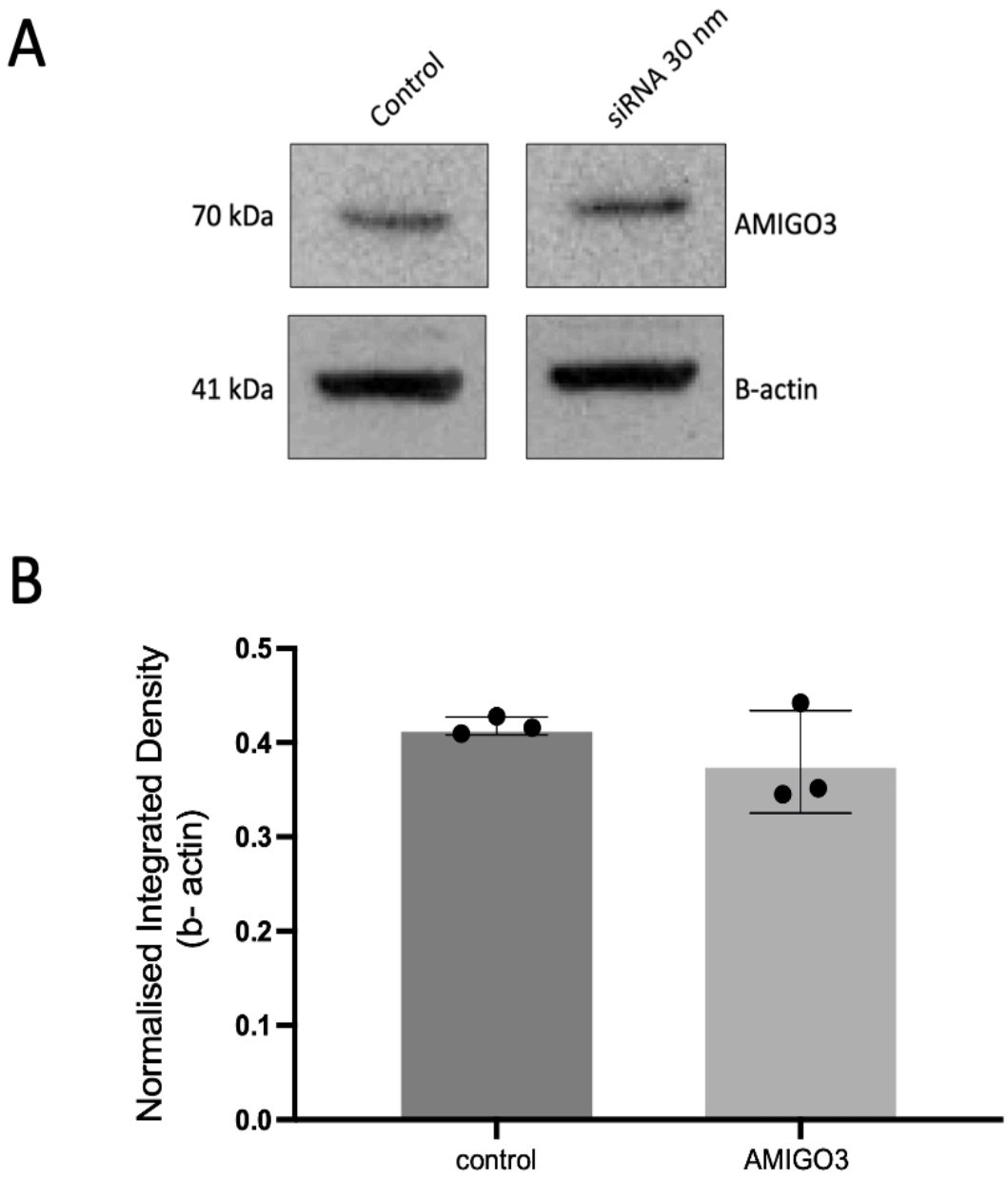


Figure 3.10: (A) Representative blot of anti-AMIGO3 bands observed at 70 kDa. (B) Quantification of AMIGO3 expression in BHK cell transfected with 30 nM of negative control and AMIGO3 siRNA. Protein expressions was normalized to beta-actin. Data points represent the average from three independent biological replicates (N=3), with each involving three technical replicates (n=3). Comparison of the data by two-tailed T-test revealed no significant difference ($P > 0.05$). Error bars represent mean ± SD.

Next, BHK cultures were transfected with 50 nM of negative control or AMIGO3 siRNA at 70 % of confluency. After 48 hours, one band of AMIGO3 was observed at 70 kDa (Figure 3.11 A). The 70 kDa AMIGO3 band was decreased by around twofold compared to the control group (normalized integrated density (arbitrary units): 50 nM AMIGO3 siRNA 0.23 ± 0.002; 50 nM negative control siRNA 0.39 ± 0.02). Finally, a two-tailed T-test showed that the reduction of AMIGO3 expression was significant ($p<0.001$) (Figure 3.11 B). This result confirms that knockdown of AMIGO3 method is working with 50 nM of siRNA, and gives further evidence that the 70 kDa band is AMIGO3.

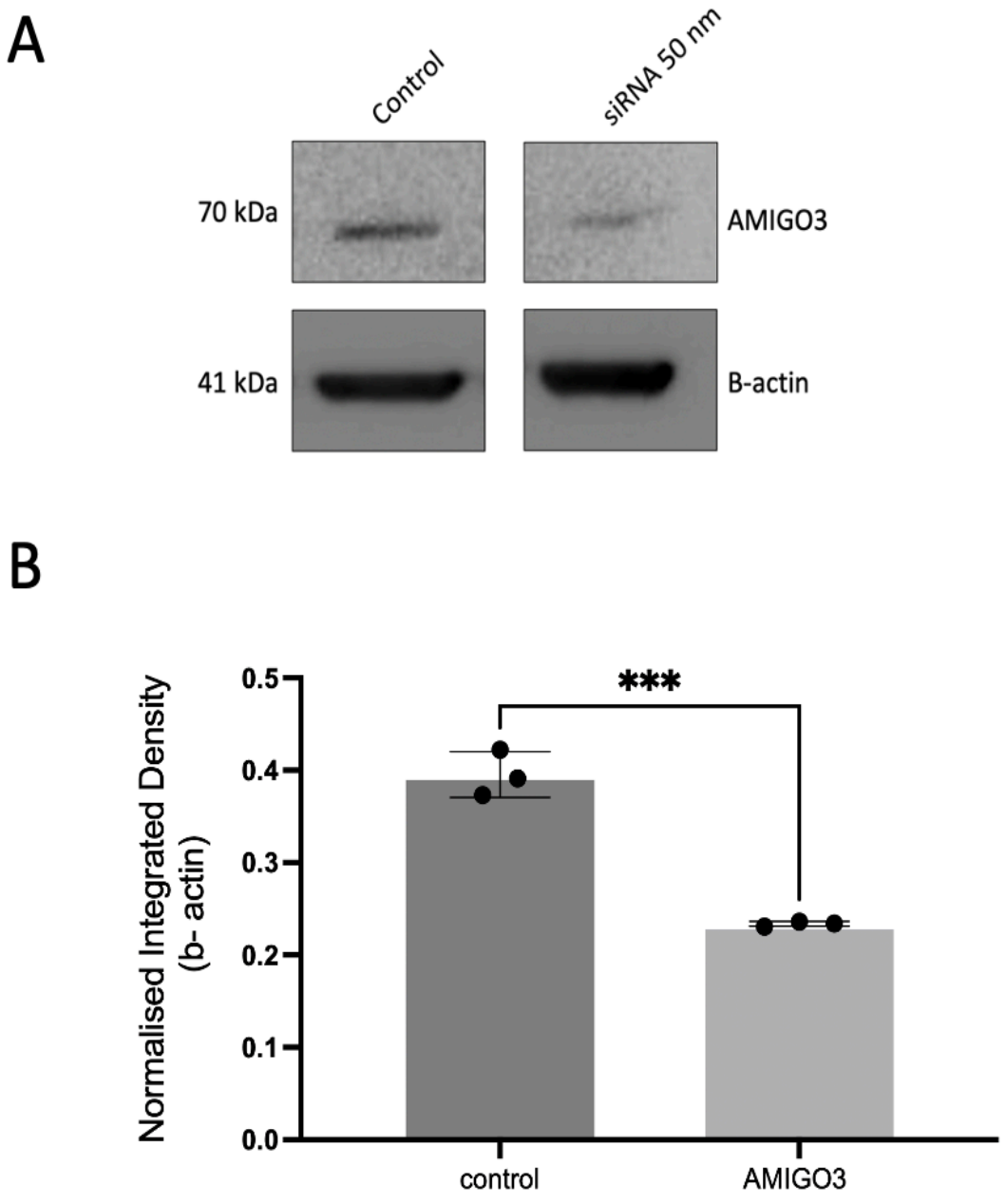


Figure 3.11: (A) Representative blot of AMIGO3 bands observed at 70 kDa. (B) Quantification of AMIGO3 expression in BHK cells, transfected with either 50 nM of negative control or AMIGO3 siRNA. Protein expression was normalized to beta-actin. Data points represent the average from three independent biological replicates (N=3), with each involving three technical replicates (n=3). *** indicates significance in the two tailed T-test at $p<0.001$. Error bars represent mean ± SD.

3.5.3.3 siRNA knockdown of AMIGO3 in mixed glial cultures

After showing successful knockdown of AMIGO3 in BHK cell line with 50 nM siRNA, we decided to knockdown AMIGO3 expression in mixed glial cultures. The results shown above indicate AMIGO3 expression was regulated, with a peak in expression observed at 7 DIV. Therefore, we decided to knockdown AMIGO3 expression between 5 DIV and 7 DIV so that the siRNA timed with the peak of AMIGO3 expression in these cultures. siRNA sequences for negative control and AMIGO3 were used at both 30 nM and 50 nM to match the BHK cell experiments.

Protein lysates were prepared at 7 DIV after 48 hours of treatment with the siRNA. After WB with anti-AMIGO3 and anti-CNPase bands were observed at 48 kDa (indicating CNPase) and another at 70 kDa indicating AMIGO3 (Figure 3.12 A). AMIGO3 expression did not differ after 30 nM AMIGO3 siRNA (normalized integrated density (arbitrary units): 30 nM AMIGO3 siRNA, 0.11±0.004; 30 nM negative control siRNA, 0.12 ± 0.02) (two-Tailed T-test $P>0.05$) (Figure 3.12 B). Similarly, CNPase expression was stable after siRNA treatment (normalized integrated density (arbitrary units): 30 nM siRNA, 0.16 ± 0.009; negative control siRNA, 0.15 ± 0.006) (two-Tailed T-test $P>0.05$) (Figure 3.12 C). Overall, the lack of change in AMIGO3 levels after 30 nM siRNA is similar to the results in BHK cell line.

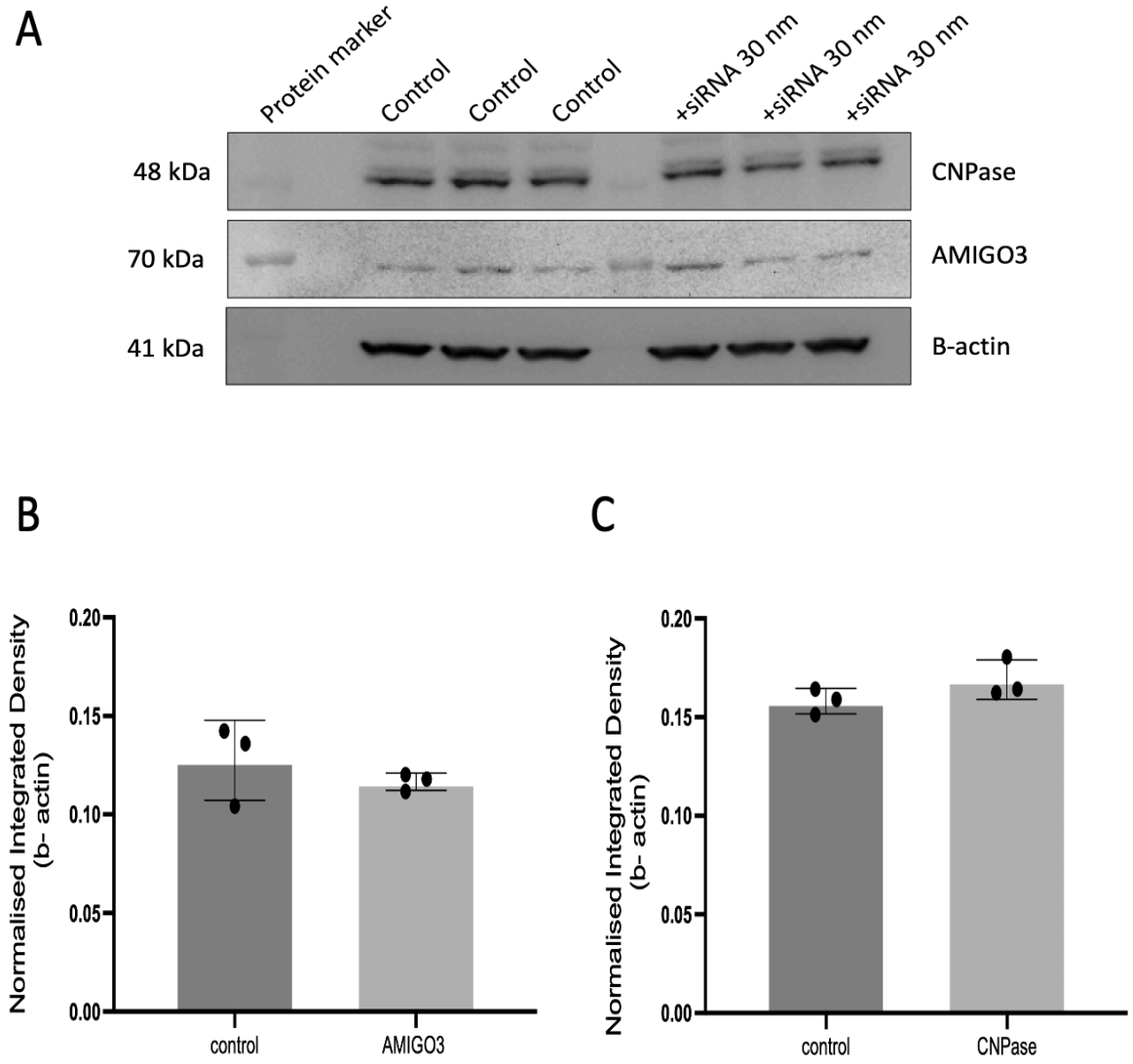


Figure 3.12: (A) Representative WB of anti-AMIGO3 and anti-CNPase expression following treatment with 30 nM AMIGO3 siRNA. AMIGO3 bands expressed at 70 kDa and CNPase at 48 kDa. (B-C) Quantification of AMIGO3 (B) and CNPase (C) expression in mixed glial cultures transfected with 30 nM negative control and AMIGO3 siRNA. Protein expression was normalized to beta-actin. Data points represent the average from three independent biological replicates (N=3), with each involving three technical replicates (n=3). Comparison of the data by two-tailed T-test revealed no significant difference ($P > 0.05$). Error bars represent mean ± SD.

Mixed glial cultures treated with 50 nM of AMIGO3 siRNA showed a clear knockdown of AMIGO3. AMIGO3 was observed at 70 kDa and 48 kDa for CNPase (Figure 3.13 A). AMIGO3 protein expression was significantly decreased in AMIGO3 siRNA treated cultures compared to the control (normalized integrated density (arbitrary units): 50 nM AMIGO3 siRNA, 0.45 ± 0.004; 50 nM negative control siRNA 0.6 ± 0.009) (two-tailed T-test, $p< 0.0001$) (Figure 3.13 B). Interestingly, CNPase protein levels (marking OL differentiation) were significantly increased in AMIGO3 siRNA treated cultures compared to the control siRNA group (normalized integrated density (arbitrary units): 50 nM AMIGO3 siRNA, 0.79 ± 0.01; 50 nM negative control siRNA, 0.60 ± 0.05) ($P < 0.01$) (Figure 3.13 C). Overall, we found that knockdown of AMIGO3 expression with 50 nM of siRNA was linked to a significant increase in CNPase expression in mixed glial cultures.

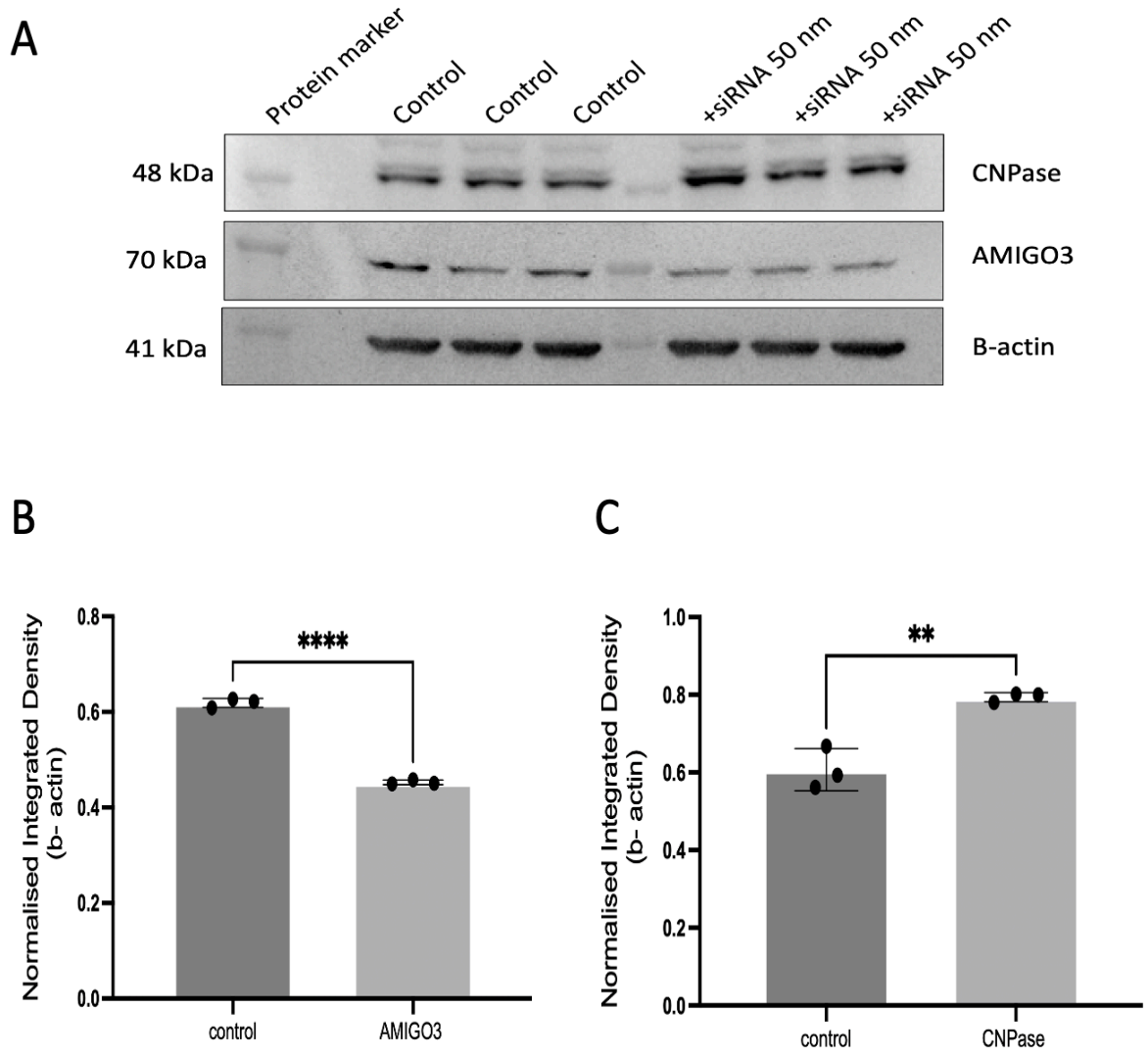


Figure 3.13: (A) Representative WB with anti-AMIGO3 and anti-CNPase in primary mixed glial culture following transfection with 50 nM of control or AMIGO3 siRNA. AMIGO3 bands were observed at 70 kDa and CNPase at 48 kDa. (B-C) Quantification of AMIGO3 (B) and CNPase (C) expression in mixed glial cultures transfected with 50 nM of AMIGO3 or control siRNA. Protein expression was normalized to beta-actin. Data points represent the average from three independent biological replicates (N=3), with each involving three technical replicates (n=3). ** and **** indicates significance in the two tailed T-test at $p<0.01$ and $p<0.0001$ respectively. Error bars represent mean ± SD.

3.5.4 studying AMIGO3 function in OL differentiation: recombinant AMIGO3 studies

AMIGO3 could be expressed at higher levels compared to LINGO1 (Ahmed *et al.*, 2013), and both AMIGO3 and LINGO1 are able to act with p75 (or TROY) and NgR1 to form a signalling complex (e.g. AMIGO3/p75/NgR1) that, in turn, can activate intercellular RhoA signalling pathways (Mi *et al.*, 2004; Ahmed *et al.*, 2013). RhoA signalling pathways can regulate the actin cytoskeleton, and actin regulation is involved in OL differentiation and myelination (Hall, 1998; Zuchero *et al.*, 2015). Based on the above, we hypothesised that AMIGO3 can act as a ligand for AMIGO3/p75/NgR1 complexes in OPC/OL. Also the interactions will stimulate RhoA signalling pathways with effects on OL differentiation (Figure 3.14).

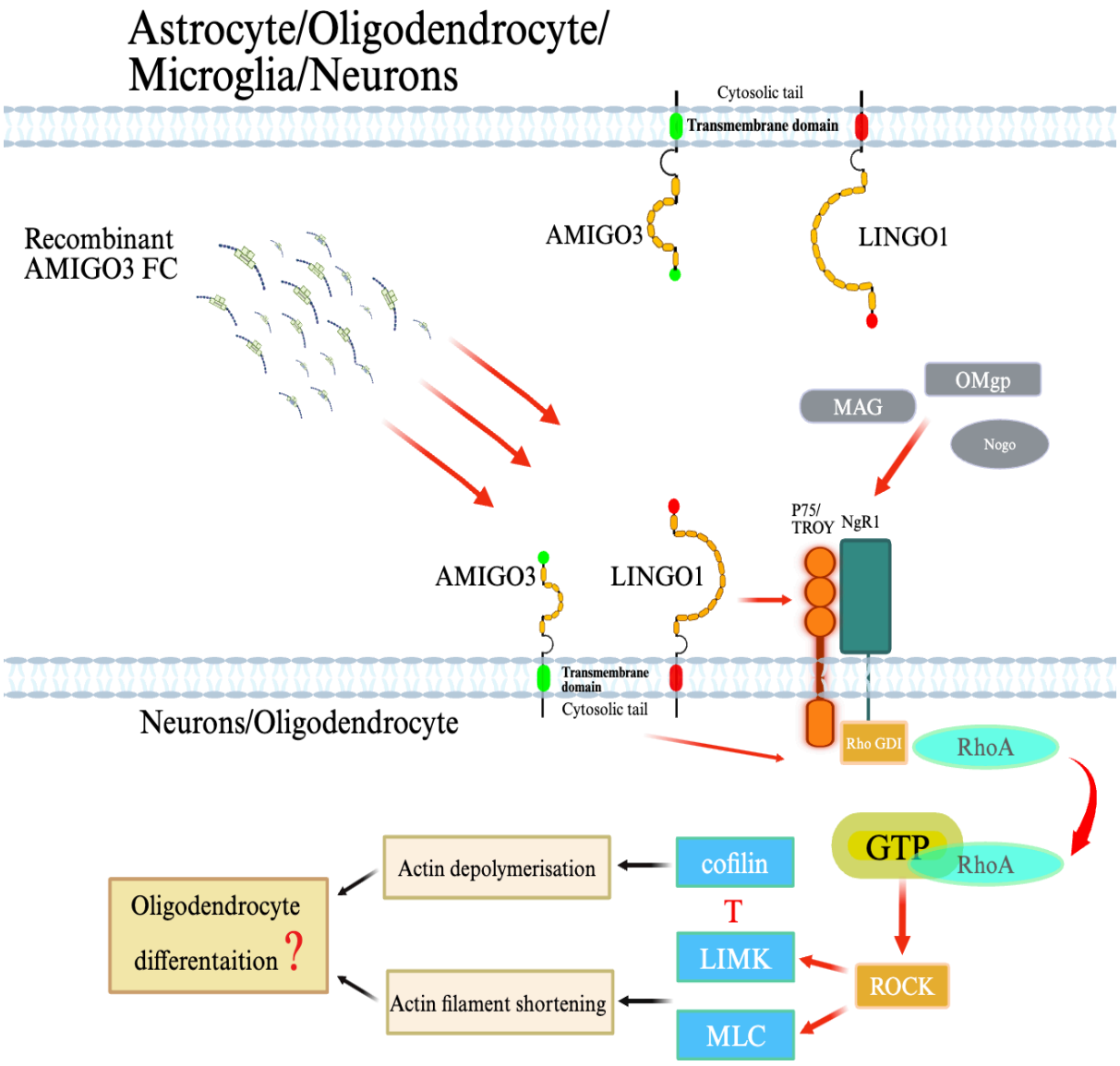


Figure 3.14: Schematic showing hypothesised action of AMIGO3 on the AMIGO3/p75/NgR1 signalling complex. Note, TROY could replace p75 in the complex. Recombinant AMIGO3 could interact with AMIGO3 leading to the activation of the AMIGO3/p75/NgR1 complex and downstream RhoA signalling pathways. RhoA activation would then influence actin filament shortening in OPC/OL leading to effects on OL differentiation.

The next experiments study the effect of recombinant AMIGO3 on RhoA activation, and OL differentiation in mixed glial cultures.

3.5.4.1 RhoA activation assay validation in BHK cells

We wished to use RhoA activation assays to examine RhoA activation after recombinant AMIGO3 treatment. Before starting work with mixed glial cultures, we first confirmed the assay worked using the BHK cell line. The BHK cell line was useful as we had previously confirmed its expression of AMIGO3 (Figure 3.9, 3.10 and 3.11).

3.5.4.1.1 RhoA activation activator study

RhoA activation assays were used to validate the recombinant AMIGO3 treatment. For the first step, a RhoA GTP activator (calpeptin; Cytoskeleton Inc) was tested in BHK cells to confirm the assay was working. BHK cells were treated with different concentrations of calpeptin (15 and 30 µg/mL), samples processed, and the signals read out using the plate reader. 30 µg/mL of RhoA activator caused a significant increase in absorbance compared to both the control group (mouse isotype IgG*)*, and to samples treated with 15 µg/mL of calpeptin (absorbance at 490 nm (arbitrary units): control 0.12 ± 0.003; calpeptin 15 µg/mL 0.13 ± 0.01; calpeptin 30 µg/mL 0.25 ± 0.01) (Figure 3.15). One-way ANOVA identified a statistically significant source of variation between the groups (ANOVA, $F(2,6) = 72.3$ $p<0.0001$) (Figure 3.15). Post-hoc comparison of the groups via Tukey's test showed a significant increase in RhoA activation in the 30 µg/mL calpeptin group compared to the control ($p<0.0001$), and the 15 µg/mL calpeptin group ($p<0.001$). This confirms that the assay is working in our lab using BHK cells.

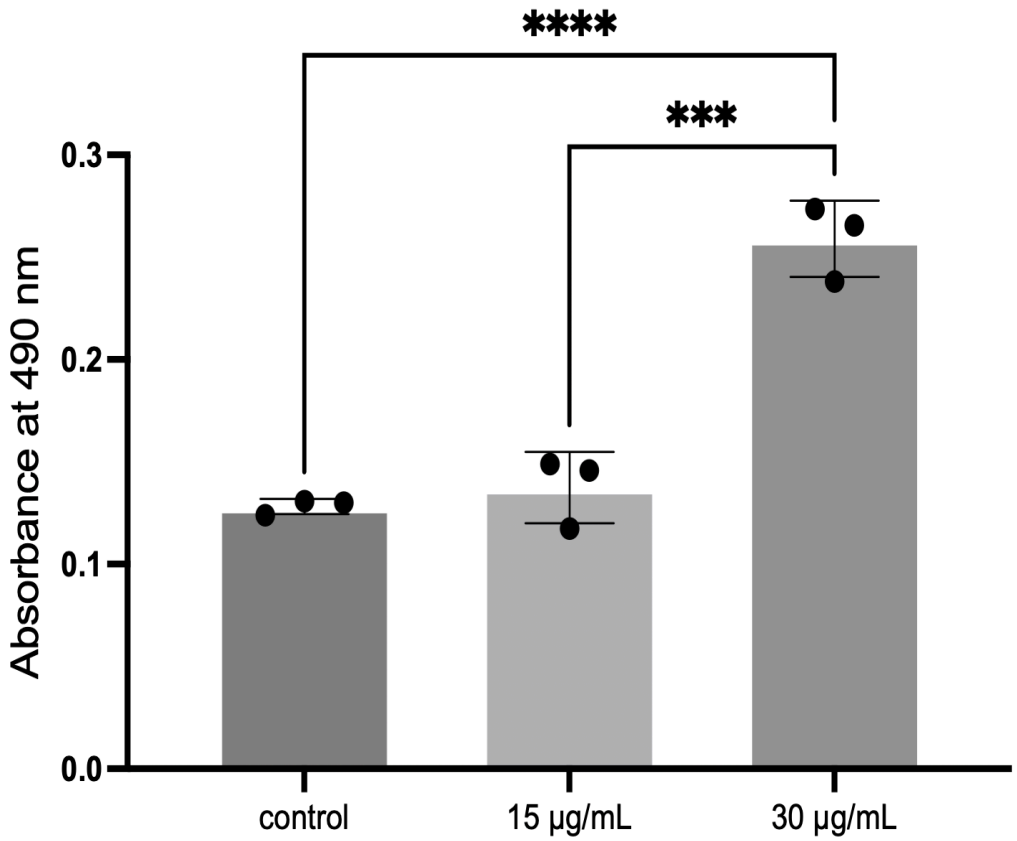


Figure 3.15: Quantification of RhoA activity in BHK samples treated with a RhoA activator (calpeptin). BHK cells were treated with 15 µg/mL and 30 µg/mL of RhoA activator calpeptin or control mouse isotype IgG. Data points represent the average of three technical replicates (n=3) from a single biological replicate (N=1). *** and **** indicate significance in Tukey's post-hoc test at $p<0.001$ and $p<0.0001$ respectively. Error bars represent mean ± SD.

3.5.4.1.2 Recombinant AMIGO3 stimulates RhoA in BHK: 1 and 2 µg/mL

In the next study, we tested if recombinant AMIGO3 could activate RhoA in BHK cells. Groups of BHK cultures were treated with 1 µg/uL and 2 µg/uL recombinant AMIGO3, or 2

µg/mL of a control protein (mouse isotype IgG). Different groups of cells were incubated with treatments for either 30 and 60 mins before RhoA assays were completed. Comparisons between groups showed that the mean level of RhoA activity appeared greater in cultures treated with recombinant AMIGO3 compared to the control group (absorbance at 490 nm (arbitrary units): control 0.19 ± 0.02; 1µg/mL 30 mins 0.21 ± 0.008; 1µg/mL 60 mins 0.22 ± 0.005; 2µg/mL 30 mins 0.24 ± 0.01; 2µg/mL 60 mins 0.25 ± 0.01) (Figure 3.16). One-way ANOVA identified a statistically significant source of variation between the groups (ANOVA. $F(4, 10) = 9.172$, ($p < 0.05$). Post-hoc comparison of the groups via Dunnett's test indicated a significant increase in RhoA activity between the control group and the groups of 2 µg/mL of recombinant AMIGO3 (30 mins $p<0.01$; 60 mins $p<0.01$). The above data demonstrates that recombinant AMIGO3 can be used to activate RhoA in BHK cells.

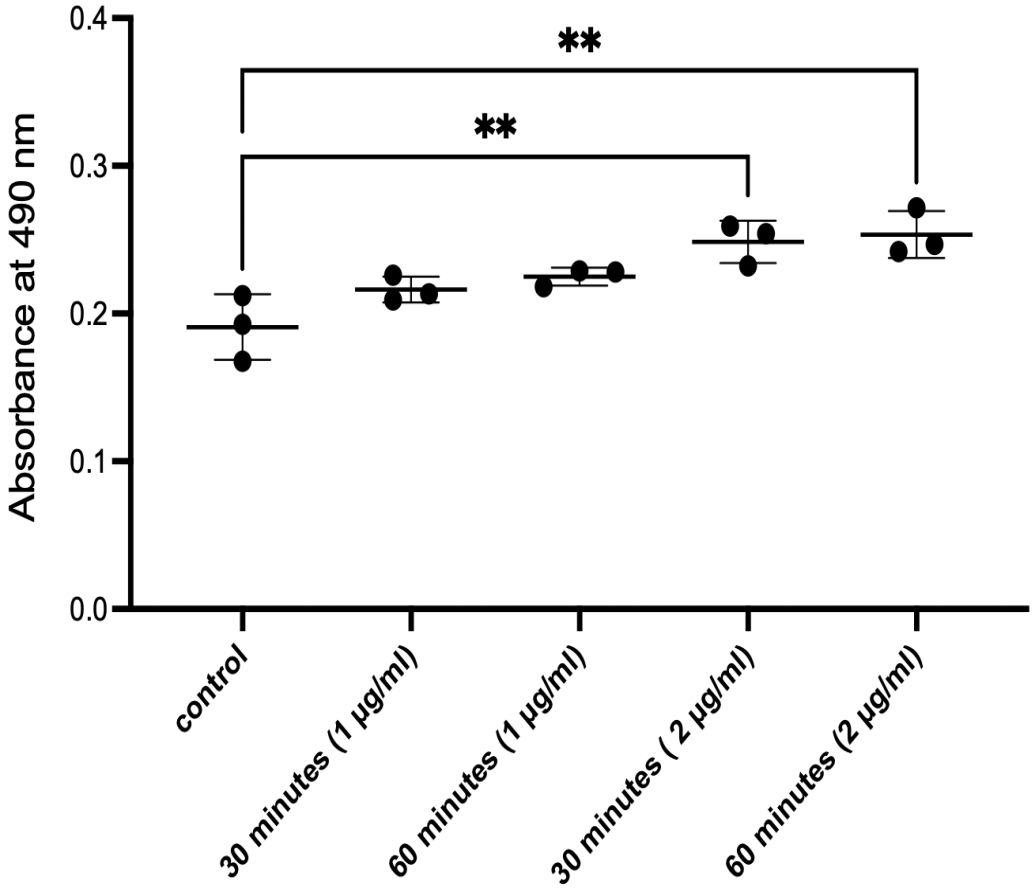


Figure 3.16: Quantification of RhoA activity in BHK cells. Cells were treated with 1 µg/mL and 2 µg/mL of recombinant AMIGO3, or control protein (mouse isotype IgG). Data points represent the average of two independent biological replicate (N=2), with each involving three technical replicates (n=3). ** represents significance in Dunnett's post-hoc test at $p<0.01$. Error bars represent mean ± SD.

3.5.4.2 Effect of 2 µg/mL of recombinant AMIGO3 on RhoA activation in mixed glial cultures

The previous RhoA GTP activation assays in BHK cells show that RhoA was activated by 2 µg/mL of recombinant AMIGO3 after a 60 mins treatment. So, we decided to treat our glial culture with this concentration. Mixed glial cultures were divided into 3 groups according to

the time of treatment, with incubations with recombinant AMIGO3 (30 mins, 60 mins and 3 hours). Control cultures were treated with 2 µg/mL of isotype IgG protein for 60 mins.

Mixed glial cultures showed a similar RhoA activity after recombinant AMIGO3 treatment to those obtained from BHK cells. Mixed glial cells treated with 2 µg/mL of recombinant AMIGO3 and incubated for 60 mins showed an increase in RhoA activity compared to the control group (mouse isotype IgG) (2 µg/mL 60 mins 0.2 ± 0.003; control 0.1 ± 0.007) (Figure 3.17). One-way ANOVA indicated a significant variance between the groups (ANOVA, $F(3, 8) = 10.75$ ($P < 0.05$). Post-hoc comparison via Dunnett's test indicated a significant increase in RhoA activity for the group treated with 2 µg/mL of recombinant AMIGO3 and incubated for 60 mins ($P < 0.01$). Overall, these results show that recombinant AMIGO3 at 2 µg/mL activates RhoA in mixed glial cultures.

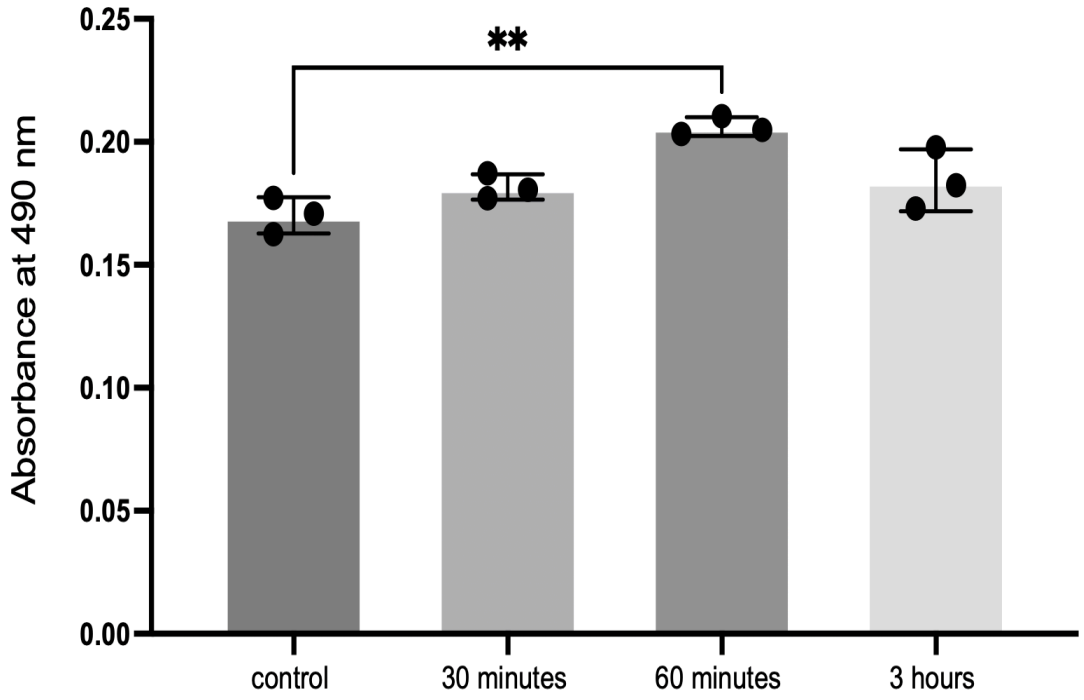


Figure 3.17: Quantification of RhoA GTP activity in primary cultures. Cultures were incubated for 30 mins, 60 mins, and 3 hours with 2 µg/mL of recombinant AMIGO3 or 2 µg/mL of a control protein for 60 mins (mouse isotype IgG). Data points represent the average from three biological replicates (N=3), with each involving three technical replicates (n=3). ** represents significance in Dunnett's post-hoc test at $p<0.01$. Error bars represent mean ± SD.

3.5.4.2.1 Western blot Analysis of OL differentiation after treatment with recombinant AMIGO3

The previous experiments confirmed that recombinant AMIGO3 treatment at 2 µg/mL produced an increase in RhoA levels in mixed glial cultures. This result depended on the dose of recombinant AMIGO3 as 1 µg/mL did not have significant effect. The next experiments examined the effect of 1 and 2 µg/mL recombinant AMIGO3 on levels of AMIGO3 and CNPase (marker of OL differentiation) in mixed glial cultures.

Using the same plan as the siRNA experiments, recombinant AMIGO3 treatment was applied to cultures from 7 DIV until 11 DIV, and then protein samples were used in WB to check AMIGO3 and CNPase expression. As before, AMIGO3 was observed at 70 kDa and CNPase at 48 kDa (fig 3.18A). Densitometry showed that AMIGO3 levels were similar between control (1µg/mL isotype control IgG) and recombinant AMIGO3 (1µg/mL) treated cultures (normalized integrated density (arbitrary units): control 0.2 ± 0.03; AMIGO3 0.3 ± 0.02) (Figure 3.18 B). A two-tailed T-test showed that these groups did not differ ($P > 0.05$) (Figure 3.18 B). In the same way, CNPase expression was not different in the control and recombinant AMIGO3 treated group (normalized integrated density (arbitrary units): control 1.65 ± 0.12; AMIGO3 1.49 ± 0.06) (two-tailed t-Test $P > 0.05$) (Figure 3.18 C). Overall, these results show that 1 µg/mL of recombinant AMIGO3 has no effects on OL differentiation in our mixed glial cultures (Figure 3.16).

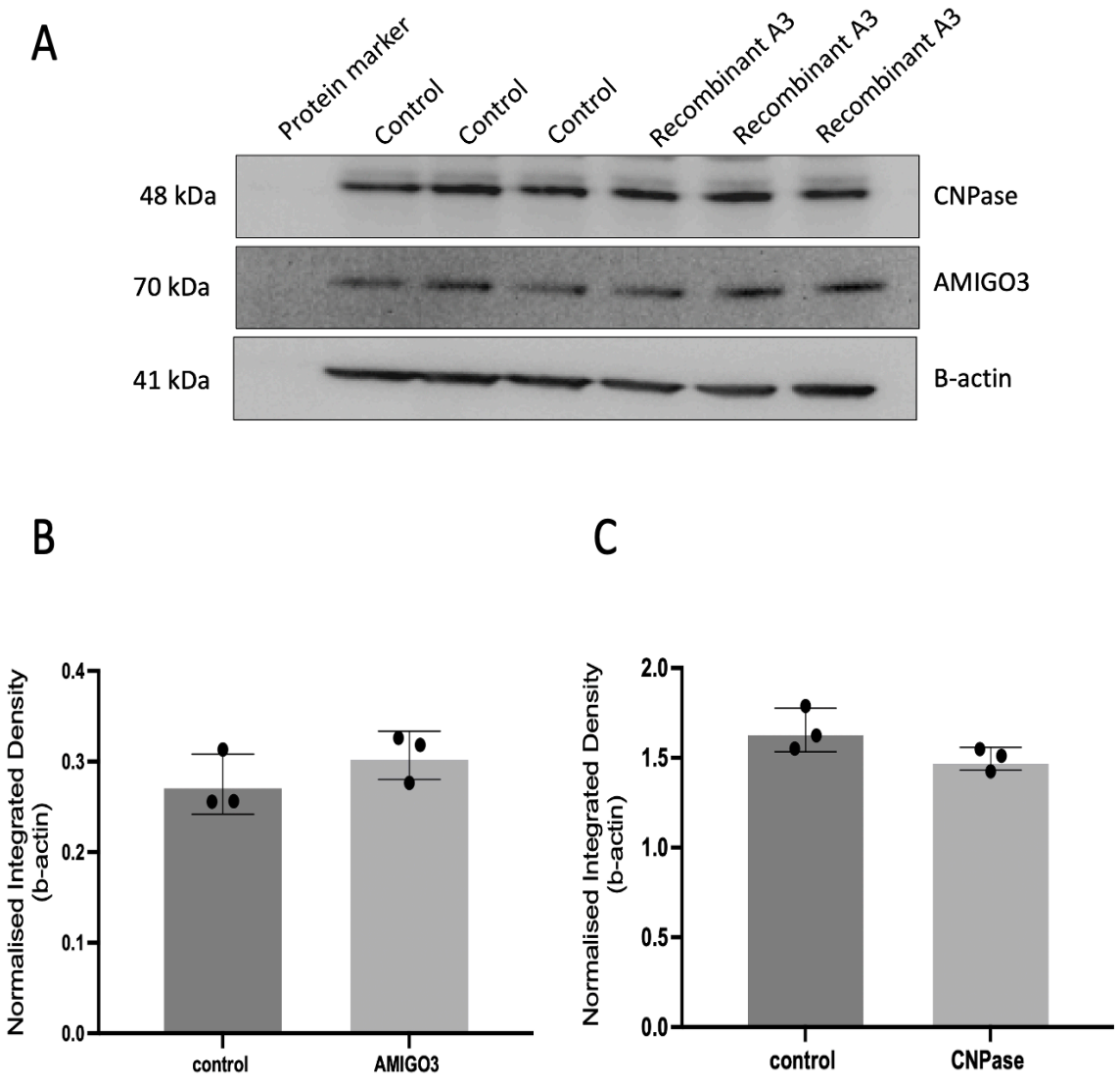


Figure 3.18: (A) Representative WB of AMIGO3 and CNPase proteins in mixed glial cultures. AMIGO3 bands were observed at 70 kDa and CNPase at 48 kDa. (B-C) Quantification of AMIGO3 (B) and CNPase (C) expression in mixed glial cultures treated with 1 µg/mL of recombinant AMIGO3 or left untreated (control). Protein expression was normalized to beta-actin. Data points represent the average of two independent biological replicates (N=2), with each invoving three technical replicates (n=3). Error bars represent mean ± SD.

A different result was found when 2 µg/mL of recombinant AMIGO3 was applied to our mixed glial cultures. As before, WB detected AMIGO3 and CNPase at 70 and 48 kDa respectively (Figure 3.19 A). Interestingly, AMIGO3 protein levels showed a significant increase in the recombinant AMIGO3 group compared with the control (normalized integrated density (arbitrary units): 2µg/mL AMIGO3 0.9 ± 0.05; control 0.7 ± 0.02; control 0.7 ± 0.02) (two-tailed T-test $p < 0.01$) (Figure 3.19 B). In addition, CNPase expression was significantly decreased after recombinant AMIGO3 treatment compared to the control (normalized integrated density (arbitrary units): 2µg/mL AMIGO3 0.7 ± 0.01; control 1.3 ± 0.03) (two-tailed T-test $p < 0.0001$) (Figure 3.19 C). Overall, these data suggest that at a dose of 2 µg/mL recombinant AMIGO3 reduces OL differentiation in our mixed cultures.

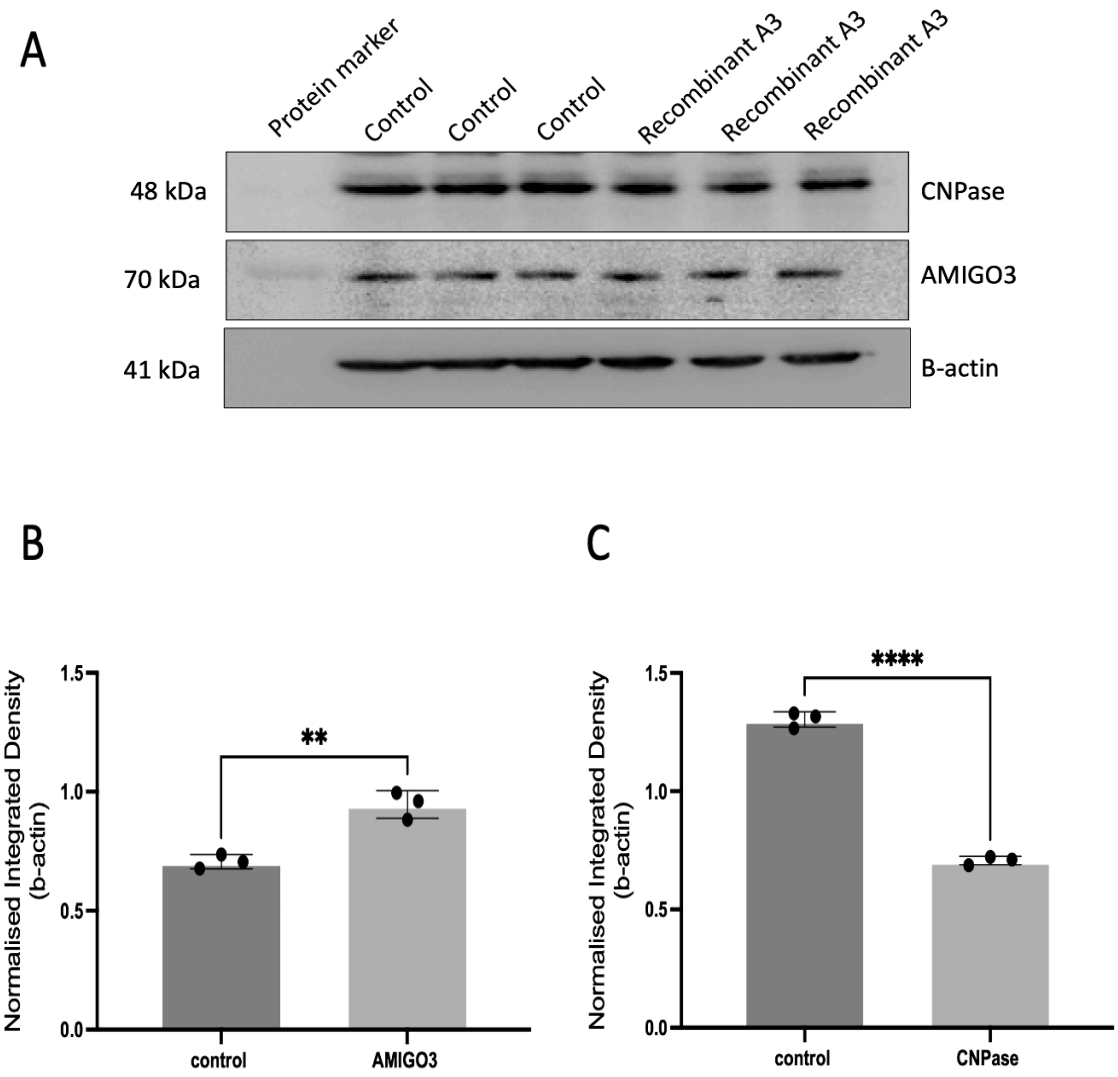


Figure 3.19: (A) Representative WB of AMIGO3 and CNPase in mixed glial cultures. AMIGO3 bands were observed at 70 kDa and CNPase at 48 kDa. (B-C) Quantification of AMIGO3 (B) and CNPase (C) expression in mixed glial cultures treated with 2 µg/mL of recombinant AMIGO3 or left untreated (control). Protein expressions was normalized to beta-actin. Data points represent the average of two independent biological replicates (N=2), with each invoving three technical replicates (n=3). ** and **** represent significant in the two-tailed T-test at $p<0.01$ and $p<0.0001$ respectively. Error bars represent mean ± SD.

3.5.4.2.2 Immunocytochemical analysis of OL differentiation after treatment with recombinant AMIGO3

We also used ICC methods to examine OL differentiation in mixed cultures treated with 2 µg/mL of recombinant AMIGO3. The treatment was applied from 7 DIV to 11 DIV in our mixed culture as previously used in the WB test. As in the previous ICC studies, anti-CC1 (optimized in this study), was used to detect mature OL, and cells were also stained with DAPI (Figure 3.20 A-F). In this experiment two groups were studied: mixed glial cultures treated with 2 µg/mL of recombinant AMIGO3, and a second group of cultures that had no treatment.

Interestingly, both the number of DAPI+ cells and the % of DAPI+ cells that were labeled with anti-CC1 appeared to be decreased by treatment with recombinant AMIGO3 (Figure 3.20). Quantification of the cell count showed that the number of DAPI+ cells in recombinant AMIGO3 treated cultures was significantly lower compared to the control (DAPI+ cells: AMIGO3 24 ± 3.5; control 56 ± 5.9) (two-tailed T-test $p<0.0001$) (Figure 3.20 G). Also, the % of DAPI+ cells that were labeled with anti-CC1 was statistically lower in recombinant AMIGO3 treated versus control cultures (DAPI+ cells: AMIGO3 7.71± 3.03; control 36 ± 6.46) (two-tailed T-test, $p<0.0001$) (Figure 3.20 H). Overall, these ICC data show that 2 µg/mL of recombinant AMIGO3 reduced OL differentiation in mixed glial culture.

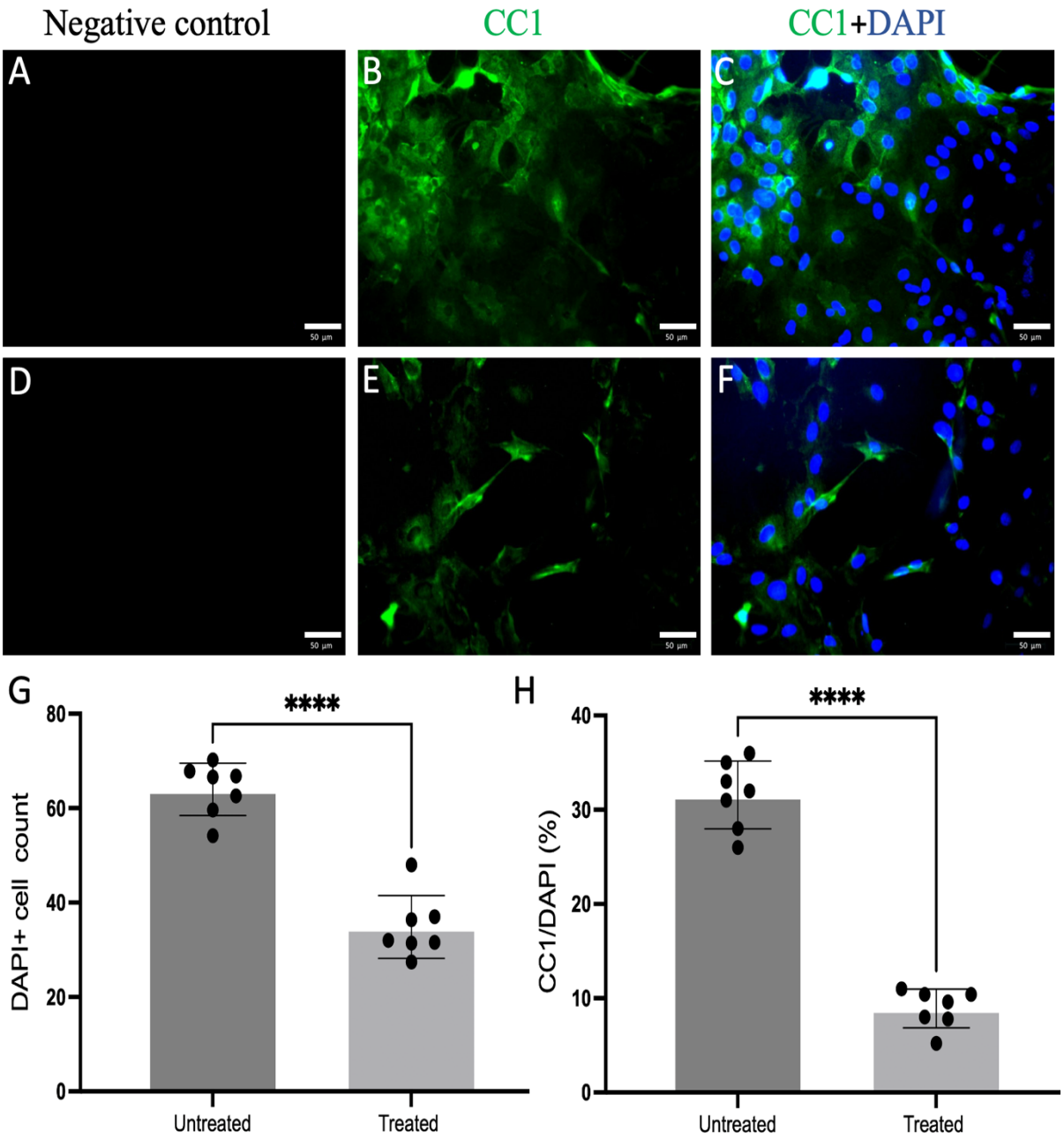


Figure 3.20: Recombinant AMIGO3 treatment in primary mixed glial culture. (A-F) Representative images of CC1 (green) and DAPI (blue) staining from mixed glial cultures either untreated (A-C) or treated with recombinant AMIGO3 (D-F). Negative control (A and D) were stained with secondary antibodies but no anti-CC1. (G). Quantification of DAPI+ cells in control (untreated) mixed glial cultures, and cultures treated with 2 µg/mL recombinant AMIGO3 (treated). (H) Quantification of CC1+/DAPI+ cells in control (untreated) mixed glial cultures, and cultures treated with 2 µg/mL recombinant AMIGO3. Data points represent the average of seven technical replicates (n=7), from a single individual

biological replicate (N=1). **** indicates significance in the twi-tailed T-test at p<0.0001. Error bars represent mean ± SD.

3.6 General discussion

3.6.1 Western blot detection of AMIGO3

Previous work in our lab detected AMIGO3 in mouse corpus callosum and cortex using an AMIGO3 antibody from Novus Biologicals (Foale *et al.*, 2019). Two bands were observed at 45 kDa and 55 kDa. During the project this antibody become unavailable from the supplier so we used a different antibody which is the R&D monoclonal MAB2375. Anti-AMIGO3 (MAB2375) identifies one clear band at 70 kDa, which is different to the previous studies (Foale *et al.*, 2019)**,** but two pieces of evidence confirm the band at 70 kDa is for AMIGO3. First the 70 kDa band is reduced by AMIGO3 siRNA, and second, levels of this band were increased following recombinant AMIGO3 treatment in mixed glial culture.

3.6.2 Mixed glial cultures demonstrate OL differentiation

Our data show that OL differentiation occurs in primary mixed glial cultures from 3 DIV to 21 DIV as the level of CNPase increase over time, indicating OPCs and OL differentiation and maturation. This finding is supported by WB of glial cells dissected from forebrain mouse and in ICC results. CNPase expression increased at 7, 14, and 21 DIV in primary mixed glial cultures, and this finding matched with a rat model of pure OL which has shown a rise in myelin basic protein (MBP) expression rise during OL differentiation (Pang *et al.*, 2012).

3.6.3 Mixed glial cultures showed a similar pattern of AMIGO3 and LINGO1 expression compared to previous studies in vivo

Our studies in mixed glial cultures showed that AMIGO3 expression peaked at 7 DIV before reducing at 14 and 21 DIV. The drop in AMIGO3 matched the point when OL differentiation began, shown by rise in CNPase levels. LINGO1 showed a similar expression pattern. All of the above evidence match with the in vivo findings from Foale (2019) who studied AMIGO3 and LINGO1 expression in mouse forebrain using WB and immunohistochemistry. These studies also indicated an effect of AMIGO3 and LINGO1 in OL differentiation. AMIGO3 increased early before the development of myelination, then declined when MBP started to appear (Foale *et al*., 2019)**.** We presented similar patterns of AMIGO3 and LINGO1 expression, which declined after CNPase increased in our mixed glial cultures. We note that AMIGO3 expression in mixed glial cultures was higher than LINGO1, but this was not true in the in vivo studies (Foale *et al.*, 2019). This previous study has been done in brain sections which contained all neurons and other CNS cells present in vivo (Foale *et al.*, 2019)**,** but our study was in mixed glial culture so only contained the major glial cells (OPC, OL, astrocyte and microglia). Interestingly, despite these differences, both studies imply similar findings of AMIGO3 and LINGO1 effects in OL differentiation.

3.6.4 Evidence that AMIGO3 plays a role in regulating OL differentiation

The data of Foale (2019) studies and our data in this chapter highlighted that AMIGO3 is down-regulated during OL differentiation. This evidence suggests that AMIGO3 may play a role in inhibiting OL differentiation during the development of the myelination. Further, LINGO1, has a similar signalling pathway to AMIGO3, which is reported to inhibit OL differentiation. In this study, we decided to study AMIGO3 function because of the similarity between AMIGO3 and LINGO1. Also, AMIGO3 has not been investigated fully before in

relation to expression by glial cells within the CNS (Kuja-Panula *et al.*, 2003). Our study using siRNA, indicated that CNPase was increased during the siRNA AMIGO3 knockdown. Also, the treatment of recombinant AMIGO3 decreased CNPase levels, and in ICC, reduced the number of DAPI+/CC1 cells. These results provide good evidence for AMIGO3 effects in OL differentiation and maturation in our mixed glial cultures.

3.6.5 Involvement of RhoA GTP pathway in AMIGO3 effects OL differentiation

Previous study indicate that AMIGO3 can interact with p75/TROY to form a complex with NgR, which allows AMIGO3 to activate RhoA signals in neurons (Ahmed *et al.* 2013). A similar mechanism works in OPC to allows LINGO1 to effect the differentiation of OL (Mi *et al.*, 2005). Previous study in our lab indicate that OPC express AMIGO3, NgR1 and p75. Here we show that evidence of AMIGO3 activation, which induce with recombinant AMIGO3 treatment and this stimulation leads to the activation of RhoA in BHK cells, and mixed glial cultures. Importantly, we found that recombinant AMIGO3 treatment reduced CNPase expression in mixed glial cultures, implying reduced OL differentiation. Also, the same treatment activated RhoA activity. Together our studies of AMIGO3 function suggest that AMIGO3 expression in OL leads to activation of RhoA signalling pathways, which can result in the down-regulation of OL differentiation. We don't have evidence that shows the RhoA pathways effect OL differentiation, but we know from other work that actin cytoskeleton regulation is important for OL differentiation (Hall, 1998; Liang, Draghi and Resh, 2004; Zuchero *et al.*, 2015).

3.6.6 Limitations

Regarding our results from WB and ICC, there are a number of limitations that need to be considered. As previously discussed, our WB and ICC results show that AMIGO3 is an inhibitor of OL differentiation and maturation within the CNS. However, knockdown of AMIGO3 with our siRNA method was only 50 %. A greater knockdown (e.g. 90 %) would have allowed better results, but we already used a high concentration of siRNA (50 nM). Higher concentrations (e.g. 100 nM) of siRNA has effects on gene expression as well as silencing of the specific gene (like off-target effects) (Semizarov *et al.*, 2003).
Further, studies in human cell lines shows high effects of siRNA concentration in silencing gene expression compared to the high concentration of siRNA (Schwarz *et al.*, 2006).
Another important issue, we don't know if the effects of AMIGO3 knockdown on OL differentiation was from increasing the OPC proliferation or increase the OPC survival. In addition, we don't know which cells AMIGO3 is influencing in our mixed cultures, or if the recombinant AMIGO3 treatment targets all cells in the culture (OPC, OL, astrocyte and microglia). So, the data does not confirm that AMIGO3 is functioning in any specific cell, or if AMIGO3 effects are involving multiple cells.

3.6.7 Future studies

A number of questions have been noted in relation to the data from the experiments in this chapter; answering these questions will provide a better understanding of AMIGO3 function, and the links between AMIGO3 and the cells responsible for myelin production, such as OPCs and OL cells. Firstly, it would be interesting to knockdown both AMIGO3 and LINGO1 protein expression in mixed glial cultures. These proteins have a similar structure, and seem to share functions in axons and OPC/OL. This mean they may be able to compensate for each other when one is knockdown. A clinical trial of an anti-LINGO1 in

multiple sclerosis did not provide significant results (Ledford *et al.*, 2015). This could be because AMIGO3 was able to replace LINGO1 function in OPC/OL. Testing a double knockdown would be a useful way to check this idea. This can also be studied in ICC using staining for CC1 to give us a better understanding of the effects of AMIGO3 and LINGO1. Furthermore, overexpression of both AMIGO3 and LINGO1 could be examined by both WB and ICC in primary mixed glial cultures. An adenovirus associated virus vector could be use in this investigation. This study will be interesting because it will provide us with more information about the role of both AMIGO3 and LINGO1 at the same time. Viral overexpression of AMIGO3 has been reported in a study examining myelin injury after seizures (Li *et al.*, 2021). In this case overexpression had no effect on MBP levels even though there was a clear increase in the level of AMIGO3. However, they did not overexpress LINGO1 so the dual effect was not tested.

Experiments involving siRNA and recombinant AMIGO3 in mixed glial cultures will effect all cells in the culture. Because of this, it is not clear if the change in OL differentiation involves AMIGO3 in OPC/OL, or in other glia such as astrocytes and microglia. Future experiments could check this by using cell-specific knockdowns for AMIGO3. A viral vector with an astrocyte or OL promoter and short hairpin RNA sequences for AMIGO3 would be a useful method.

Finally, the role of AMIGO3 in the NgR1/p75 and TROY signalling complex, and activation of RhoA pathways, were highlighted in our study. Our data demonstrated activation of RhoA during AMIGO3 stimulation in mixed glial culture. It would be interesting to knockdown AMIGO3 signalling partners, e.g. NgR1 (Zhao *et al.*, 2018) or p75 and TROY (Ahmed *et al.*, 2013; Lu *et al.*, 2013) and then look at OL differentiation in both WB and ICC experiments.

These experiments can help us understanding the relationship between AMIGO3 and this signalling complex, during OL differentiation and maturation.

3.7 Conclusion

To summarize, this study found that CNPase expression increased in primary mixed glial cultures in vitro when AMIGO3 expression decreased. This suggests that AMIGO3 levels peak at the start of OL differentiation in these cultures. Furthermore, suppressing AMIGO3 expression causes an increase in CNPase levels. This result suggests an increase in mature OL when AMIGO3 is reduced. In addition, recombinant AMIGO3 treatment reduced the amount of CNPase protein, and the number of CC1+ cells. CC1 and CNPase are markers for mature OL in primary mixed glial cultures. Recombinant AMIGO3 treatment also increased the amount of AMIGO3 protein and was found to stimulate RhoA activity. Together these results show that high AMIGO3 levels reduce the number of mature OL in the cultures, and that this effect may relate to RhoA activity.

Chapter 4 AMIGO3 and LINGO1 expression in astrocytes

1.1 Rationale

4.1.1 AMIGO3 expression in astrocytes

Astrocyte or astroglia are the major glial cells within central nervous system (CNS). Functionally, astrocytes play important roles to maintain extracellular homeostasis such as, regulating extracellular levels of neurotransmitters via NA+/K+ ATPase ion pumps (Mahmoud *et al.*, 2019). Also, astrocytes take up neurotransmitters via different transporters (Kirischuk *et al.*, 2016). In addition, astrocytes provide axonal support in health by creating brain glue structure and in inflammation by creating the scar (Nicola J. Allen and Ben A. Barres, 2009; Linnerbauer, Wheeler and Quintana, 2020). Astrocytes contribute to inflammatory diseases such as multiple sclerosis (MS) (Figure 1.6), regulating the entry of the immune cells to the CNS (Sofroniew, 2015). A study showed that amphoterin-induced gene and open reading frame-3 (AMIGO3) was expressed by astrocytes in primary astrocyte cultures isolated from mouse brain using Western blot (Chen, Hor and Tang, 2012). AMIGO3 proteins can interact with each other through AMIGO3 homotopic interactions (Kuja-Panula *et al.*, 2003), meaning AMIGO3 could carry signals between AMIGO3 expressing cells. These intercellular interactions could downregulate oligodendrocyte (OL) differentiation and maturation in neurological diseases such as MS. Given all of the above, a study of AMIGO3 expression in astrocytes would an interesting opportunity to identify a CNS source of AMIGO3 that could affect OL or neurons expressing AMIGO3. This study used mixed glial cultures to establish primary astrocyte cultures, which were then used to identify AMIGO3 expression via WB, immunocytochemistry (ICC) and RT-qPCR.

4.1.2 LINGO1 expression in astrocytes

Leucine rich repeat and Ig domain containing 1 (LINGO1) has not been reported to be expressed by astrocytes. LINGO1 protein was not expressed by astrocytes derived from neural stem cells *in vitro* (Lööv *et al.*, 2012). Also in primary astrocytes, previous studies showed that LINGO1 messenger ribonucleic acid (mRNA) was not expressed in these astrocytes (Mi *et al.*, 2004). However, this data did not provide quantification, and only a single mRNA gel was reported (Mi *et al.*, 2004). In contrast, LINGO1 mRNA was detected in primary astrocytes using RNA sequencing (Zhang *et al.*, 2014). Therefore, astrocyte expression of LINGO1 needs to be investigated and validated with different methods, for example WB and ICC. Further, clinical trials using LINGO1 monoclonal antibodies in MS have not been successful. Given the abundance of astrocytes in the CNS, and their multiple functions in the CNS, a study of LINGO1 expression in these cells could yield new insight into the effects of therapies targeting LINGO1, which may influence both OL and astrocytes.

4.1.3 AMIGO3 and LINGO1 expression in microglia

Microglia are the macrophage-like cells of the CNS. Microglial consist about 10-15 % of total brain cells, and the function of microglia is to produce an immune response within the CNS (Van Rossum and Hanisch, 2004). Microglia identify and eliminate microbes, dead cells, and protein aggregates which result from disease and injury, and can cause damage to the CNS (Colonna and Butovsky, 2017). Moreover, microglial function to regulate neuronal and synaptic development, and maintain neuronal functions, as well as to repair injury within CNS. Our previous WB finding in chapter 3, detected that AMIGO3 was expressed in mixed glial cultures and that these cultures contained microglia. Further, ICC cells counts, normalized to 4', 6-diamidino-2-phenylindole (DAPI), cells counts, indicated a small number of cells that were not CC1+/DAPI. It is possible AMIGO3 is also expressed by microglial

cell in our mixed glial culture. Importantly, AMIGO3 mRNA was detected in microglia (Zhang *et al.*, 2014), but it has not been confirmed at the protein level. Further, tumor necrosis factor receptor superfamily, member 19 (TROY) and LINGO1 immunoreactivity have been identified in microglia and macrophages, and in microglia in MS (Satoh *et al.*, 2007). The finding above, and our data from chapter 3, encouraged us to test AMIGO3 and LINGO1 expression in microglial cultures.

4.2 Hypothesis

As discussed above, astrocytes can express high levels of AMIGO3 protein, but may not express LINGO1 (Kuja-Panula *et al*., 2003; Ahmed *et al.*, 2013). The expression of AMIGO3 in microglia is not fully confirmed, but they are reported to express LINGO1 (Satoh *et al.*, 2007). AMIGO3 homotypic interactions between different glia could influence OL functions. Therefore, this chapter tests the hypothesis that AMIGO3 is expressed by primary cultures of astrocytes and microglia. LINGO1 has been a target for monoclonal antibody therapies in MS so we test the hypothesis that LINGO1 is expressed by both astrocytes and microglial cells (Xie *et al.*, 2024).

4.2.1 Aims

In this study we aim to examine AMIGO3 and LINGO1 expression in primary astrocytes and microglia isolated from primary mixed glial cultures.

4.3 Method and materials

All materials and methods used in this chapter have been described in Materials and Method (Chapter 2) (specific sections are indicated below).

4.4 Experimental design

4.4.1 Cell cultures

Primary mixed glial cultures were obtained from forebrain of FVB/N mice at postnatal day 3. Astrocyte and microglia were isolated from primary mixed glial culture at 9 days in vitro (DIV) using methods previously described in Chapter 2 (section 2.3).

4.4.1.1 Astrocyte cultures

Astrocyte cells were isolated from mixed glial cultures at 9 DIV by shaking the flask to removed loose cells (oligodendrocyte precursor cell (OPC) and microglia) from the culture. The remaining cells (astrocytes) were then detached using trypsin and applied in 6 well plates for WB, and 8 well chamber slides for ICC, as previously described in chapter 2 (section 2.3.2). High numbers of flat astrocyte-like cells were easily isolated from mixed glial culture (Figure 4.1).

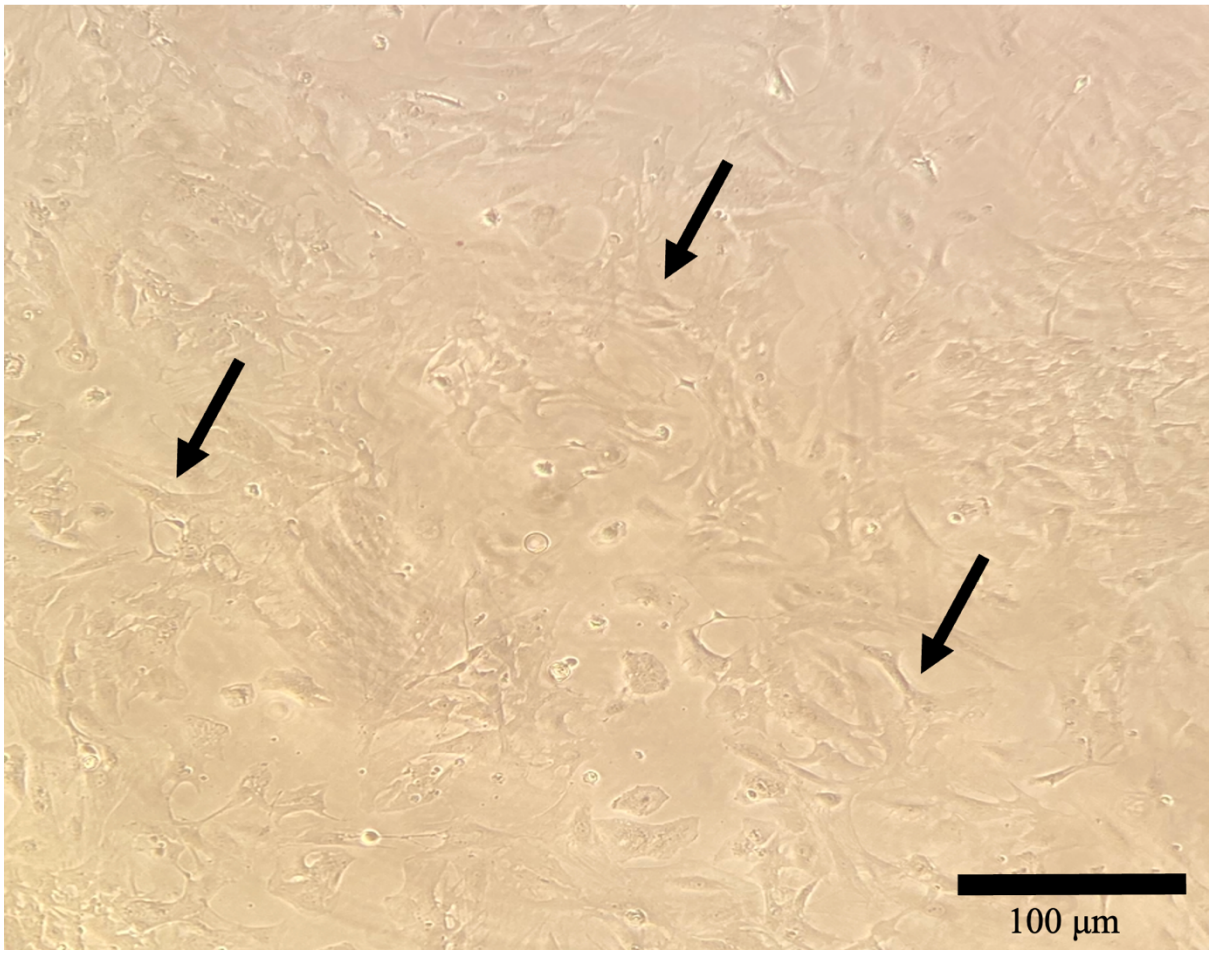


Figure 4.1: Image from a primary astrocyte culture demonstrates astrocyte cells 24 hours following the isolation. The arrows indicate the flat morphology of astrocyte cells.

4.4.1.2 Microglial cultures

Microglial cells were isolated from mixed glial cultures at 9 DIV by shaking or tapping the flask. In mixed glial culture microglia grow attached to the top of the astrocyte monolayer. Microglia are found in lower numbers of cells compared to astrocyte, so it was necessary to shake more than one flask to isolate a high number of cells (Shapiro, Wang and Ribak, 2008; Lin *et al.*, 2017). Microglial were collected from the medium once the shaking process was completed, then microglia were applied into 12 and 48 well plates for WB and 8 well chamber slides for ICC, as previously described in Chapter 2 (section 2.3.3).

4.4.2 Western blot

In this study, WB was used to test AMIGO3 and LINGO1 expression in both isolated astrocyte and Microglial cultures. The dilution of antibodies used for WB were as stated previously (Table 2.8). Glial fibrillary acidic protein (GFAP) marker protein was used to detect astrocytes. Leukocyte specific receptor (CD11b) protein was used to detect microglia. All procedures for WB are described in Chapter 2 (section 2.5).

4.4.3 RT-qPCR

RT-qPCR has been used to test AMIGO3 and LINGO1 expression in astrocyte and microglia. The methods for ribonucleic acid (RNA) isolation and the process of RT-qPCR are described in Chapter 2 (section 2.7).

4.4.4 Immunocytochemistry

ICC was used in this study to test AMIGO3 and LINGO1 protein expression in cultured astrocyte and microglia. GFAP staining was also used to identify astrocytes in cultures. Primary antibodies were detected using Alexa Fluor secondary antibodies, and DAPI was used to identify cell nuclei for cell counting. The antibody dilutions are listed in Table 2.9. ICC procedures are described in Chapter 2 (section 2.6).

4.5 Results

4.5.1 Confirming GFAP antibody in astrocyte cultures

Sigma-Aldrich mouse anti-GFAP was tested by WB as marker for astrocytes. One band was observed at 48 kDa (Figure 4.2 A). ICC using this anti-GFAP was performed using the dilution of antibodies described in Table 2.9. Anti-GFAP was detected with anti-mouse Alexa Fluor 488 secondary antibody (Figure 4.2 C). A negative control group was included that received no primary antibody (Figure 4.2 B). Overall, GFAP expression was very high, with a strong signal in most cells in the astrocyte culture indicating a high selection for astrocyte cells in the culture method (Figure 4.2).

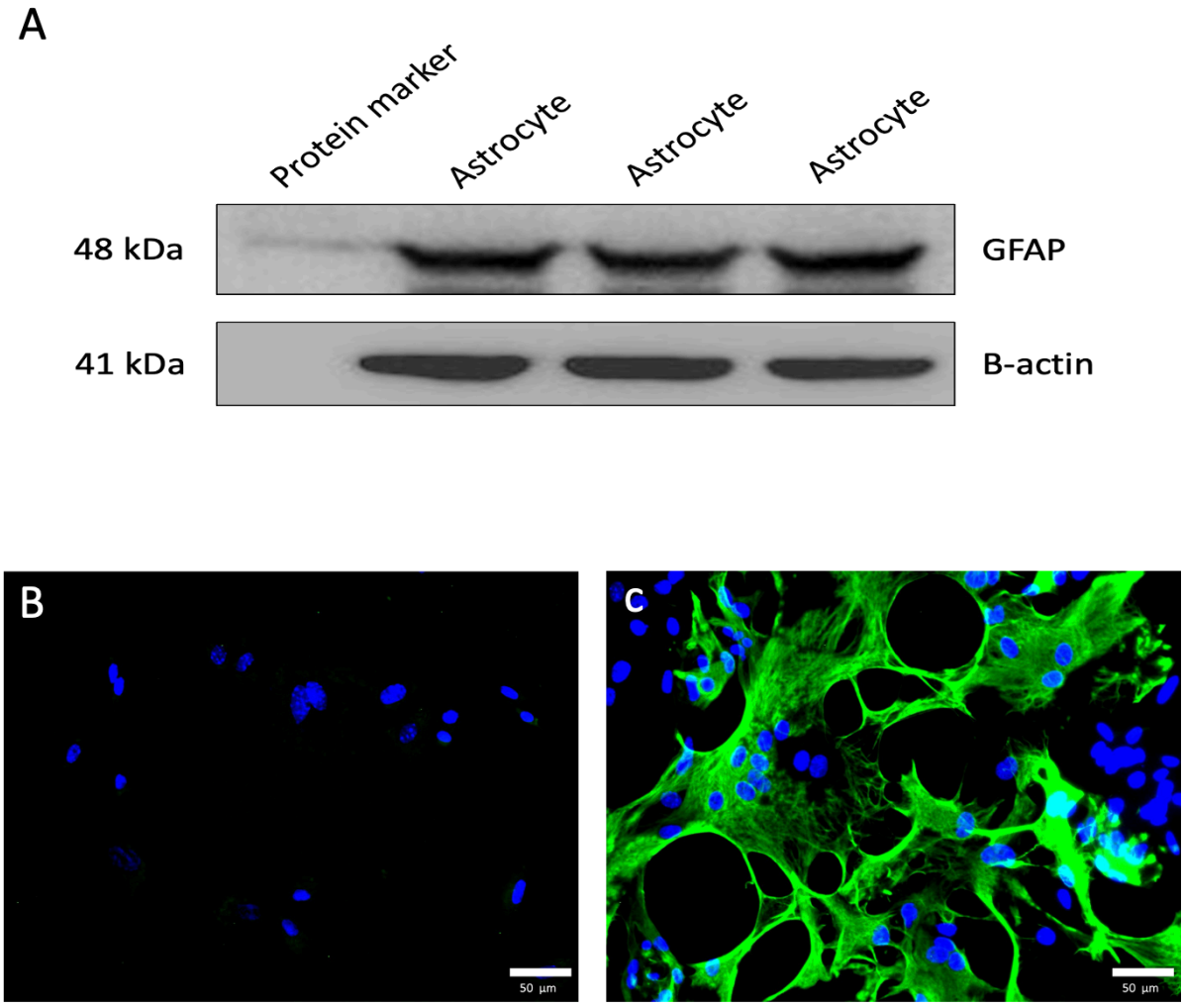


Figure 4.2: Expression of GFAP in astrocyte cultures. (A) WB of anti-GFAP band observed at 48 kDa in three astrocyte samples. (B-C) GFAP staining of isolated astrocyte cultures. (B) Representative negative control staining with only secondary antibody. (C) GFAP (green) and DAPI (blue) staining shows the astrocyte GFAP signal. Images are representative from three independent biological replicates (N=3), each with seven technical replicates (n=7).

4.5.2 AMIGO3 expression in primary astrocyte cells

Following GFAP ICC, WB was preformed to test AMIGO3 expression in the isolated astrocyte cultures. GFAP marker protein was used to confirm presence of astrocyte cells in the culture, and 7 DIV mixed glial samples were used as a control to validate the AMIGO3

and GFAP signals because mixed glial cultures contain many astrocytes and show high expression of AMIGO3 (see chapter 3, section 3.5.1). One band was observed with anti-AMIGO3 at 70 kDa, while anti-GFAP detected a band at 48 kDa, and anti-b-actin, the loading control, detected a band at 41 kDa (Figure 4.3 A). AMIGO3 protein levels in isolated astrocyte cultures were slightly lower than in mixed glial cultures (normalized integrated density (arbitrary units): mixed glial control 1.6 ± 0.005; astrocyte samples 1.4 ± 0.02). A two-tailed T-test was used to compare the means of the control and astrocyte sample groups, which proved a lower AMIGO3 expression in astrocyte cultures ($p<0.001$), perhaps because OL AMIGO3 is not found in the astrocyte cultures (Figure 4.3B). Overall, this result confirms strong AMIGO3 expression in isolated astrocyte cells.

Following WB, AMIGO3 was detected by ICC. Anti-AMIGO3 was stained with mouse Alexa Fluor 488 secondary antibody, and a negative control was stained only with secondary antibodies. Around 97.83 % of cells in these cultures expressed AMIGO3, indicating a high density of astrocytes express AMIGO3 in purified astrocyte culture (Figure 4.4). As previously described, astrocytes have a flat morphology. Importantly, the GFAP cytoplasmic stain in astrocytes provided a highly similar to the shape of AMIGO3 staining in the astrocyte cells. Overall, the above WB and ICC results of AMIGO3 expression in astrocyte, indicate high expression of AMIGO3 in our astrocyte cultures.

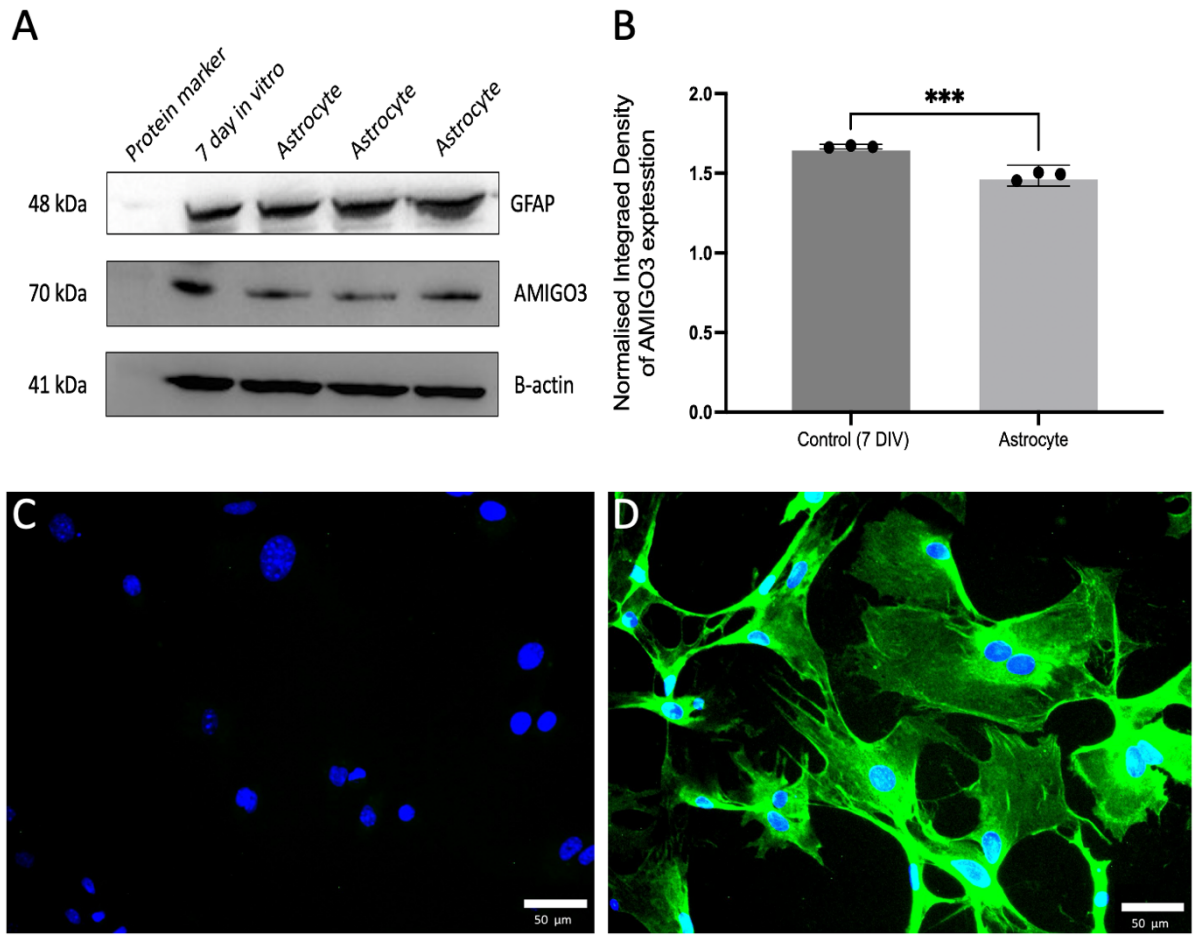


Figure 4.3: Detection of AMIGO3 in primary astrocyte culture. (A) Western blot detection of GFAP (marker protein) and AMIGO3 in astrocyte cultures. (B) Quantification of AMIGO3 expression in 7 DIV primary mixed glial cells (control) and primary astrocyte cultures. Protein expression was normalized to beta-actin. Data points represent the average from three biological replicates, each involving three technical replicates (n=3). Error bars represent mean ± SD. *** indicates significance at $p<0.001$. (C) Representative ICC negative control staining with Alexa Fluor 488 anti-mouse in astrocyte culture. (D) MAB-2375 anti-AMIGO3 staining (green) in primary astrocyte. Blue indicate DAPI stain. Images are representative of results from from three biological replicates (N=3), each involving seven technical replicates (n=7).

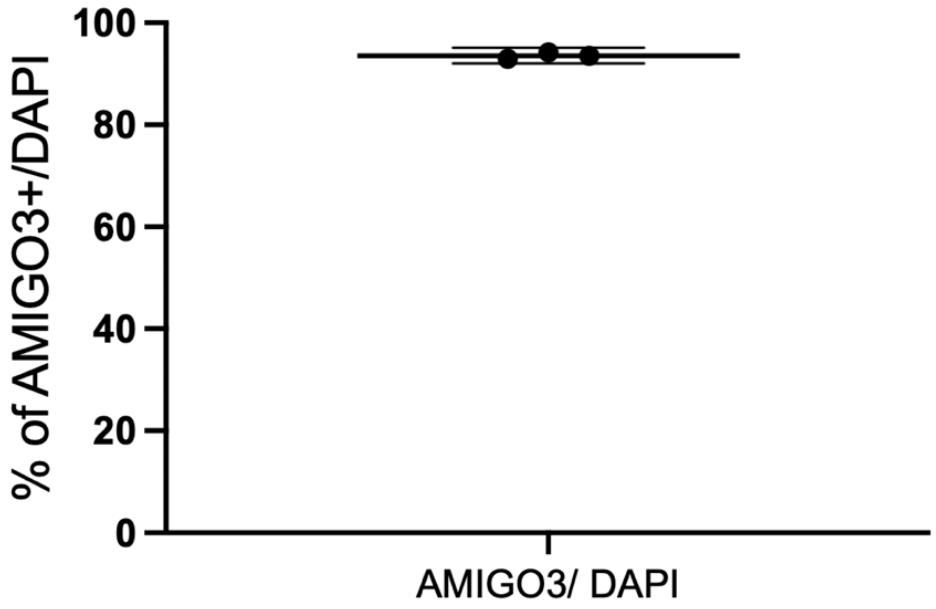


Figure 4.4: Quantification of the number of cells expressing AMIGO3 in purified astrocyte cultures (AMIGO3+/DAPI+ cells). Data points represent the average of three biological replicates (N=3), each involving three technical replicates (n=3). Error bars represent mean ± SD.

4.5.3 LINGO1 expression in primary astrocyte cultures

WB was also performed to test LINGO1 expression in astrocyte cultures. Anti-LINGO1 detected one band at 10 kDa. Again the 7 DIV mixed glial sample was used as a positive control to validate LINGO1 expression in astrocyte cultures. Surprisingly, the blots clearly showed LINGO1 protein in the astrocyte samples (Figure 4.5 A). The normalized integrated density of LINGO1 in astrocyte samples was lower compared to the control samples (normalized integrated density (arbitrary units): mixed glial control 1.44 ± 0.01; astrocyte samples 1.5 ± 0.008) ($p<0.001$) (Figure 4.5 B). These results don't match with other studies

showing that LINGO1 expression is absent from astrocytes (Mi *et al.*, 2005; Lööv *et al.*, 2012).

Following the LINGO1 WB experiment, abcam anti- LINGO1 was used to stain in astrocyte cultures. Anti- LINGO1 was detected with Rabbit Alexa Fluor 488. Negative controls were stained with secondary antibodies, but no primary antibodies. Our data showed high LINGO1 expression in astrocyte cultures (Figure 4.5 B-C) matching our previous study in WB. Cell counts showed that 97.14 % of cells in the culture were LINGO1 +/DAPI+ (Figure 4.6). LINGO1 staining in these cultures showed a similar shape to our GFAP, indicating the expression of LINGO1 in astrocytes. Overall, LINGO1 was highly expressed in our astrocyte cultures, and in both studies (AMIGO3 and LINGO1) only a few cells were found not to express these proteins. These AMIGO3/LINGO1 negative cells could be microglia, which are expected in our astrocyte cultures as these contain small number of other glial cells such as microglia.

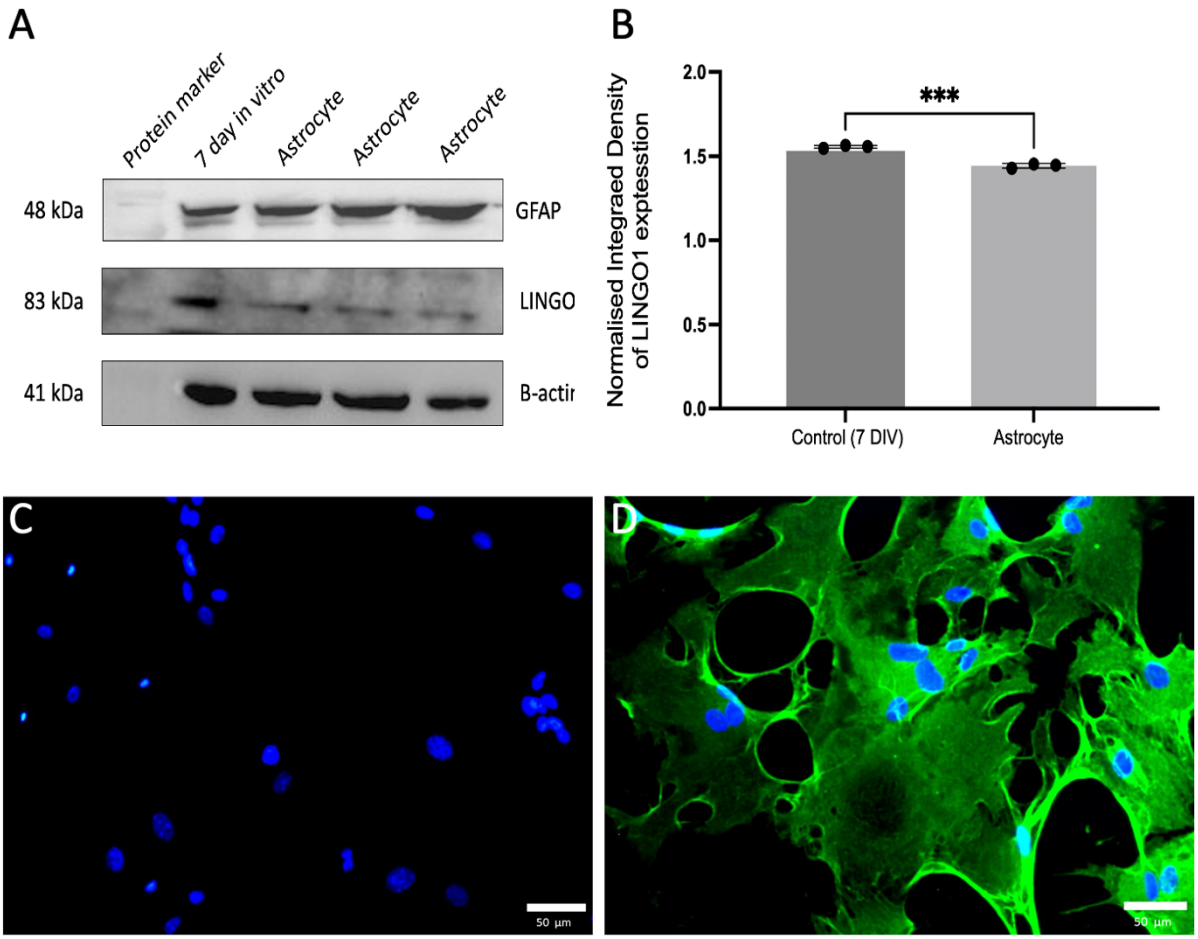


Figure 4.5: Detection of LINGO1 in primary astrocyte culture. (A) Western blot detection of GFAP (marker protein) and LINGO1 in astrocyte cultures. (B) Quantification of the LINGO1 expression in 7 DIV primary mixed glial cells (control) and purified astrocyte cultures. Protein expression normalized to beta-actin. Data points represent the average from three biological replicates (N=3), each involving three technical replicates (n=3). *** indicates significance at $p < 0.001$. Error bars represent mean ± SD. (C-D) Representative ICC staining with (C) 488 anti-mouse alone (negative control) and (D) Abcam 23631 anti-LINGO1 (green). Blue indicates DAPI stain. Images are representative of three biological replicates (N=3), each involving seven technical replicates (n=7).

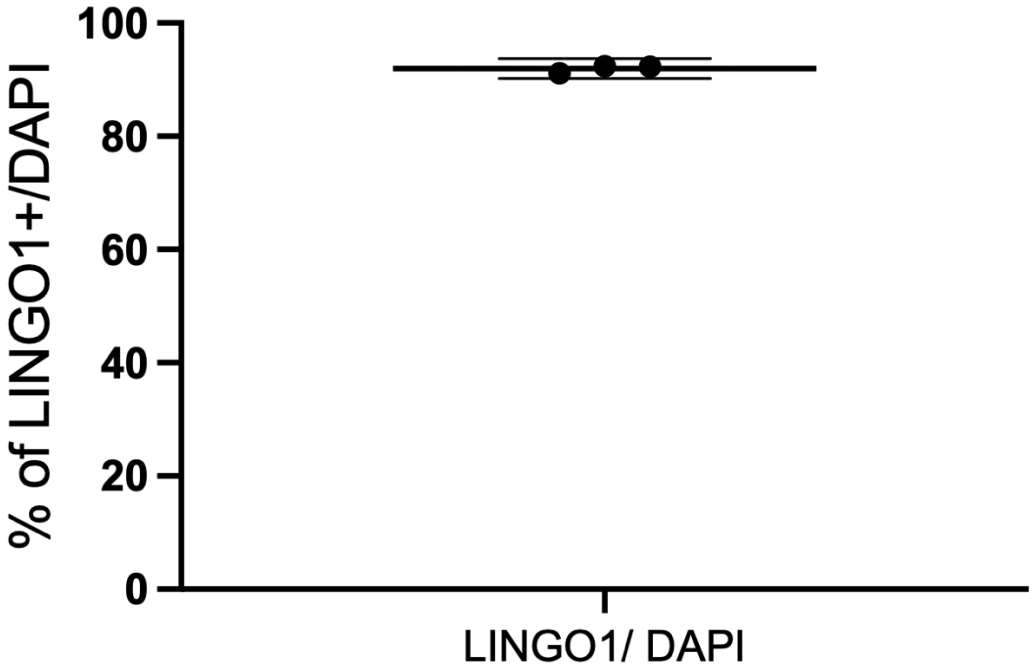


Figure 4.6: Quantification of the number of cells expressing LNGO1 in purified astrocyte cultures (LINGO1+/DAPI+ cells). Data points represent the average of three biological replicates (N=3), each involving three technical replicates (n=3). Error bars represent mean ± SD.

4.5.4 RT-qPCR of AMIGO3 and LINGO1 mRNA.

RT-qPCR was performed to quantify mRNA for the glial markers GFAP, Cd11b and platelet-derived growth factor α receptor (PDGFRα), and to confirm expression of AMIGO3 and LINGO1 mRNA in astrocyte samples. GFAP mRNA was identified in astrocyte samples at a higher level than the microglial marker Cd11b, or the OPC marker PDGFRα (relative expression normalised to α-tubulin: GFAP 1.02 ± 0.2; Cd11b 0.0004 ± 0.0004; PDGFRα 0.1 ± 0.04). One-way ANOVA identified a statistically significant source of variation for relative

expression between the three marker genes (ANOVA, F (2, 6) = 35.52 $p<0.05$). Post-hoc comparison of the groups via the Tukey test showed a significant difference in expression between GFAP and Cd11b ($p<0.001$), and between GFAP and PDGFRα ($p<0.01$) (Figure 4.7). Overall, GFAP mRNA levels were high, CD11b mRNA was not detected, and PDGFRα mRNA was low, indicating the high number of astrocyte cells in the culture, the absence of Cd11b+ microglia, and a small contamination with PDGFRα+ OPC (Figure 4.7). Both AMIGO3 and LINGO1 mRNA were highly expressed in astrocytes and at similar levels (relative expression normalised to α-tubulin: AMIGO3 1.003 ± 0.1; LINGO1 1.3 ± 0.4) (Figure 4.8).

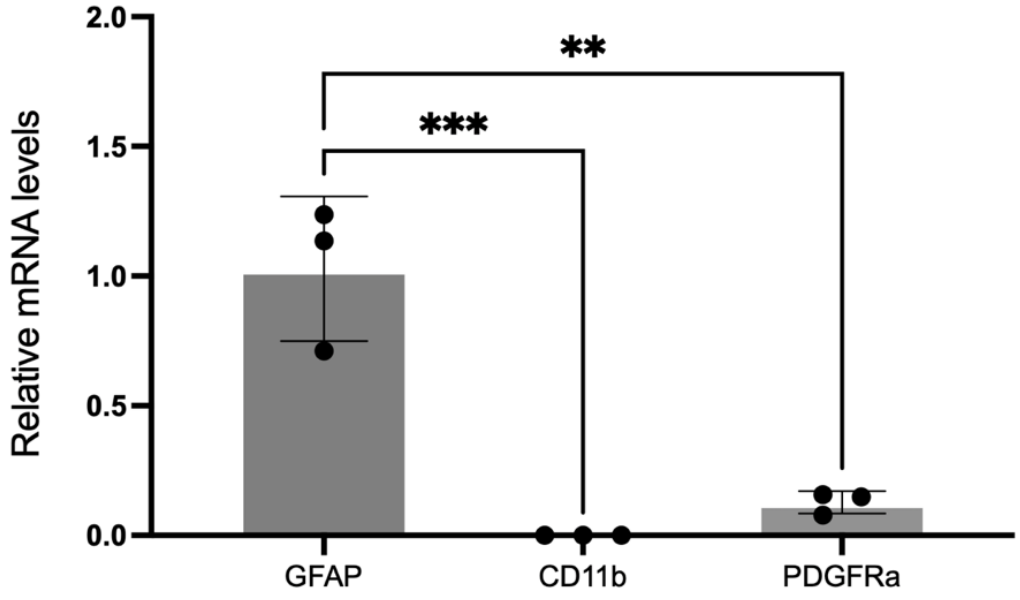


Figure 4.7: RT-qPCR analysis of GFAP, CD11b and PDFRa expression in primary astrocyte cultures. Cells were isolated at 9 DIV from mixed glial culture. mRNA of GFAP was highly expressed while CD11b was not expressed, and the mRNA for PDGFRα was expressed at a low level in astrocyte cultures. Data points represent the average of three technical replicates

(n=3), from a single biological replicate (N=1). ** and *** indicate significance for the Tukey test at $p<0.01$ and $p<0.001$ respectively. Error bars represent mean ± SD.

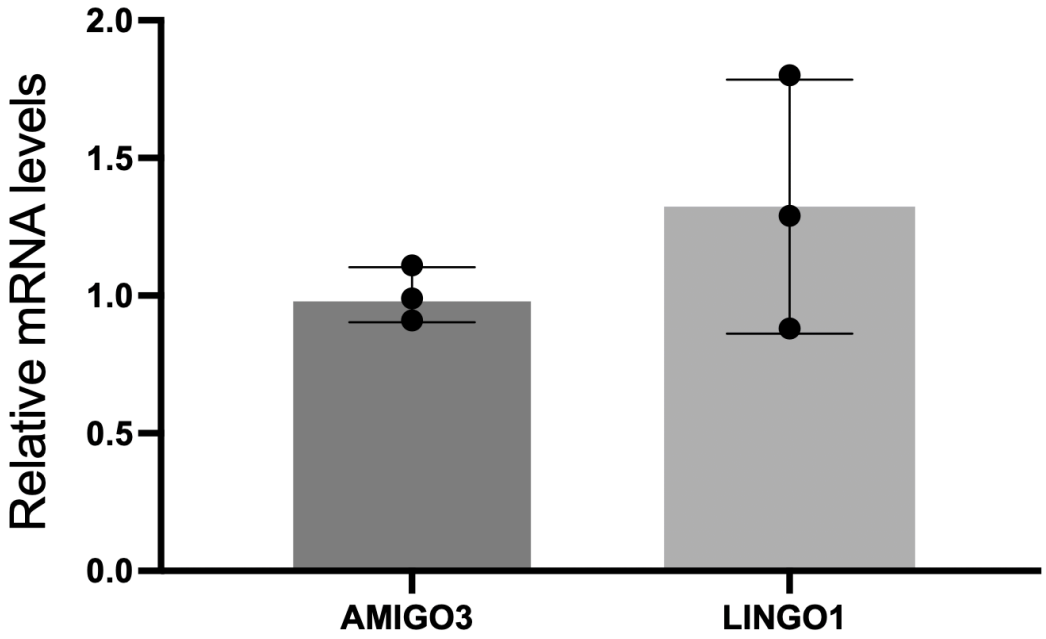


Figure 4.8: RT-qPCR analysis of AMIGO3 and LINGO1 expression in primary astrocyte culture. Cells were isolated at 9 DIV from mixed glial culture. mRNA for AMIGO3 and LINGO1 were observed in astrocyte culture at similar levels. Data points represent the average of three technical replicates (n=3), from a single biological replicate (N=1). Error bars represent mean ± SD.

4.5.5 AMIGO3 and LINGO1 expression in primary microglial cultures

Following the astrocyte studies, anti-AMIGO3 (mab-2375) and anti-LINGO1(abcam-23631) were used to probe protein samples from microglia cultures isolated from mixed glia at 9 DIV. Anti-CD11b was used as a specific marker protein for microglia cells. CD11b is one of the integrin family receptors that is widely expressed in innate immune cells such as microglia and macrophages. CD11b protein was detected at 127 kDa (the expected size) in our microglia cultures. However, our WB data from anti-AMIGO3 and anti-LINGO1 indicated that AMIGO3 and LINGO1 have no expression within the microglia cultures (Figure 4.9)

We tried to study AMIGO3 and LINGO1 expression in our microglial cultures using ICC. This experiment failed as our ICC primary microglia cultures were contaminated with other cells such as astrocyte and OPC cells. Taking the WB data, microglia had no expression of AMIGO3 and LINGO1 (Figure 4.12) but, this study needs to be repeated using ICC with purer microglia cultures.

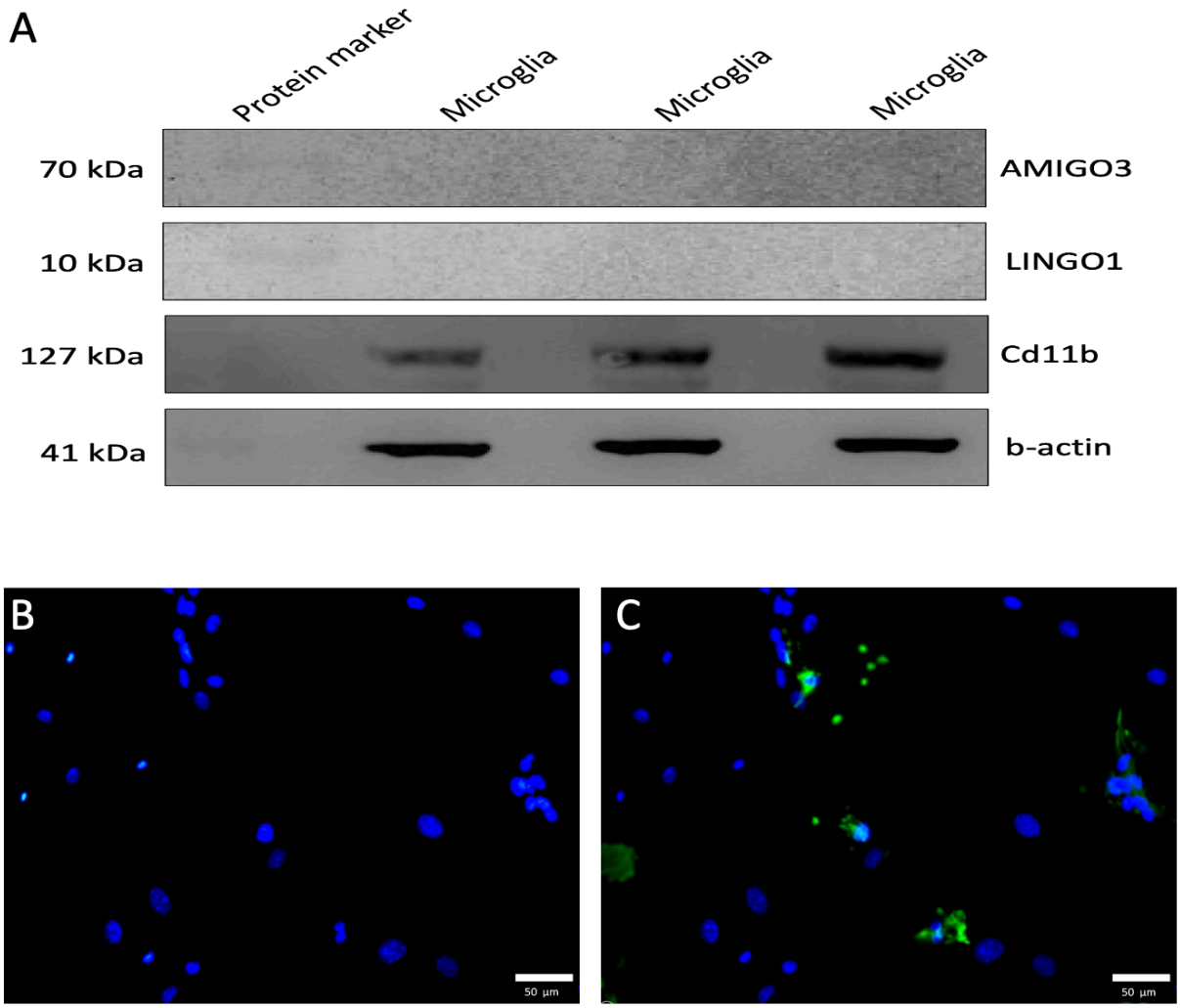


Figure 4.9: Detection of mab-2375 anti-AMIGO3, ab-23631 anti-LINGO1 and abcam-133357 anti-CD11b expression in primary microglia culture. (A) Western blot observed the marker protein for microglia Cd11b at 127 kDa. AMIGO3 and LINGO1 expression was not observed in microglia culture. Protein loading was confirmed by WB for beta-actin. (B) Representative negative control staining with Rabbit Alexa Fluor488 in microglia culture. (C) anti-CD11b staining (green) in primary microglia. Blue indicates DAPI stain. Images are representative of three biological replicates (N=3), with each involving seven technical replicates (n=7).

4.6 General discussion

4.6.1 Western blot and ICC detection of AMIGO3 and LINGO1 in astrocytes

In this chapter we tested AMIGO3 and LINGO1 in primary astrocyte cultures, which are the majority of cells in mixed glial cultures. AMIGO3 expression has previously been identified in OPC (Foale, 2019) and we have demonstrated that AMIGO3 is expressed in mixed glial cultures containing astrocytes, OPC, OL and microglia (Chapter 3). Previous studies, demonstrated that AMIGO3 is expressed widely in OL, astrocyte and neurons (Kuja-Panula *et al.*, 2003; Ahmed *et al.*, 2013), which match with our finding of AMIGO3 expression in astrocyte cells and mixed glial cultures. Interestingly, in this chapter we showed that AMIGO3 was highly expressed in astrocytes and this was confirmed by WB, ICC and RT-qPCR. Furthermore, our data indicated high LINGO1 expression in our astrocyte cells by WB, ICC and with RT-qPCR. Surprisingly, LINGO1 mRNA has been reported to be absent in astrocyte cultures (Mi *et al.*, 2004), also LINGO1 was not expressed in neural stem/progenitor cells culture by ICC (Lööv *et al.*, 2012), but was detected in a RNA sequencing study (Zhang *et al.*, 2014). We note that both AMIGO3 and LINGO1 are leucine rich repeat proteins (LRRP), and both have similar patterns of staining by ICC in astrocyte.

4.6.2 Western blot and ICC detection AMIGO3 and LINGO1 in microglia

Microglia have been shown to express Neurite outgrowth inhibitor-66 receptor 1 (NgR1), Tumor necrosis factor receptor superfamily, member 19 (TROY) and LINGO1 proteins in both MS and non-MS samples collected from the brain (Satoh *et al.*, 2007). In contrast, our WB data showed that AMIGO3 and LINGO1 are not expressed by microglia cells. We also tried to examine AMIGO3 and LINGO1 expression in microglia using RT-qPCR, but low expression of house keeper genes caused by the low number of microglia in our culture

caused issues with the experiment. It would be interesting to test AMIGO3 and LINGO1 expression in microglia cells further by repeating the RT-qPCR and ICC work in an optimized culture with higher purity and density of microglia, and also through immunostaining in brain slices. It would be valuable to use double staining in the brain slices with anti-AMIGO3 and markers such as Iba1 for microglia.

4.6.3 Limitations

The data in this chapter shows that AMIGO3 and LINGO1 are expressed in astrocytes. They also suggest that these LRRP are not expressed by microglia. There are a number of limitations linked with this study that need to be solved to improve our findings on this topic. First, during the shaking process to isolate astrocyte cells, a few microglia cells were retained in the astrocyte culture. We know this from the ICC studies that shows DAPI+ cells with no expression of GFAP. Using different method to isolate astrocyte and microglia such as magnetic cell sorting would provide a higher purity of cells to culture. Similarly, during the tapping to isolate microglia, contamination occurred with astrocyte shaped cells, and low number of cells obtained caused problems for the ICC and RT-qPCR analysis (low expression of house keeper gene alpha-tubulin). This issue could also be solved using magnetic cell sorting methods.

4.6.4 Future study

To further the investigation of AMIGO3 function, there are several studies that could provide information related to the functions of AMIGO3 in CNS glia cells such as astrocyte and microglia. This is because the availability of antibodies we used in this study was limited, and the number of microglia cells was too low compared to the other cultures of mixed glia and astrocytes. Also, contamination from astrocytes was detected within the microglia cultures. It

would be useful to validate our finding with multiple marker proteins in ICC studies. It would be helpful and valuable to stain our astrocyte and microglia cultures with two markers such as AMIGO3 and GFAP, LINGO1 and GFAP, and AMIGO3/ LINGO1 and Iba1. In addition, mixed glial culture dissected and obtained from mice forebrains contained smaller numbers of microglia compared to astrocytes, which are the major cells in this culture. Therefore, our microglia culture have small number of microglia cells. It would be useful to use a different method to isolate microglia from our mixed culture such as magnetic cell sorting to have a purer microglia culture (Gordon *et al.*, 2011). Moreover, it's possible to use brain slice immunohistochemistry to study AMIGO3 expression in GFAP+ astrocytes and Iba1+ microglia. Astrocyte and microglia both have two different biological morphology, which can be known from the shape of their cell body and the process which change under different health and inflammation conditions (Lee, Wheeler and Quintana, 2022; Yong, 2022). It would be useful to model cells in different conditions, such as during inflammation, in mixed glia, isolated glial cultures (astrocyte / microglia), and in brain slice cultures, by using inflammation factors such as IL 1-beta or tumour necrosis factor alpha. This study would help to indicate the functions of AMIGO3 and LINGO1 in astrocyte and microglia in inflammatory neurological diseases such as MS. Overall, AMIGO3 and LINGO1 are expressed in oligodendroglia, where they are indicated to be an inhibitory factor for OL differentiation, myelination and remyelination (Mi *et al.*, 2005). Also, LINGO1 and AMIGO3 have been shown to cause a negative regulation on axonal growth after injury (Mi *et al.*, 2004; Ahmed *et al.*, 2013). AMIGO3 and LINGO1 expression in astrocyte cells could potentially inhibit OL differentiation and maturation via AMIGO3 homotypic interactions, which could allow intercellular signalling between astrocytes and oligodendrocytes (Kuja-Panula *et al.*, 2003). Astrocyte AMIGO3 could interact with oligodendrocytes expressing the NgR1 signalling complexes containing AMIGO3 and either p75 neurotrophin receptor, or

TROY and (Ahmed *et al.*, 2013). Testing these ideas would be useful for understanding the relationship of AMIGO3 with oligodendrocyte functions and myelin repair in demyelinating diseases and CNS axon injury.

4.7 Conclusion

In conclusion, in this study we highlight the possible role of AMIGO3 and LINGO1 roles in astrocytes. We do not find expression of AMIGO3 or LINGO1 in microglia cells, but additional work is needed. AMIGO3 can interact with other AMIGO3 proteins expressed on other cells as previously described (chapter 1 and 3) (Kuja-Panula *et al.*, 2003), and one of our ideas is that AMIGO3 expressed by astrocytes will interact with AMIGO3 expressed by OPC/OL, neurons, or other astrocytes. This interaction could lead to activation of the NgR1 and p75/TROY signalling complex, resulting in activation of the intercellular Ras homolog gene family member A pathway, and downregulation OL differentiation (Foale *et al.*, 2017) or axon growth (Mi *et al.*, 2004; Ahmed *et al.*, 2013). On the other hand, astrocytes have been shown to have positive influences in MS by promoting OPC migration, proliferation and differentiation (Moore *et al.*, 2011). Whether AMIGO3 or LINGO1 regulate these astrocyte functions, or others, remains to be tested.

Chapter 5 General Discussion

5.1 AMIGO3 in mixed glial cultures

5.1.1 AMIGO3 in mixed glial culture

In this study we used mixed glial culture cultures to study the expression of amphoterin-induced gene and open reading frame-3 (AMIGO3) in cortical central nervous system (CNS) cells during postnatal development (Chapter 3). Furthermore, mixed glial cultures were used to isolate glial cells to study AMIGO3 expression in cells such as astrocytes and microglia (Chapter 4). Also, we used knockdown of AMIGO3 expression by short interfering RNA (siRNA) to test the function of AMIGO3 within the CNS. We also treated mixed glial cultures during the development of oligodendrocytes (OL) with recombinant human AMIGO3 to stimulate AMIGO3 signalling on oligodendrocyte precursor cell (OPC)/OL and other glial cells. AMIGO3 treatment increased ras homolog gene family member A (RhoA) guanosine triphosphate (RhoA GTP) activity in the cultures suggesting that AMIGO3 treatments activated receptor complexes involving p75 neurotrophin receptor (p75)/tumor necrosis factor receptor superfamily, member 19 (TROY) and NgR1 (Ahmed et al., 2013; Mi *et al*., 2004).

Our data suggests that AMIGO3 protein is downregulated in the CNS when OL differentiation increases. This data match in vivo findings from our group (Foale *et al*., 2019), which together suggest AMIGO3 may inhibit OPC maturation and myelination. Also our data match in vitro and in vivo data from (Mi *et al.*, 2005), showing similar effects of LINGO1 protein inhibiting oligodendrocyte differentiation and axonal myelination. In agreement, knockdown of AMIGO3 increased 2', 3'-cyclic-nucleotide 3'-phosphodiesterase (CNPase) levels, and recombinant AMIGO3 reduced them.

Importantly, the data provided by our mixed glial cultures was not able to determine which specific cells mediated the effects of AMIGO3 on OL differentiation. The knockdown and recombinant AMIGO3 treatments effects could involve astrocytic AMIGO3 as well as AMIGO3 in OPC/OL.

5.1.2 siRNA (suppression)

As described above, we highlighted that AMIGO3 levels decreased during the development of OL differentiation in primary mixed glial culture. Therefore, the expression of AMIGO3 was knocked down in mixed glial cultures to detect the effects of reduced levels of AMIGO3 expression on OL differentiation. Our knockdown data show significantly decreased levels of AMIGO3 at 7 DIV (the high peak of AMIGO3 expression in the culture model). Importantly, CNPase expression was significantly increased by AMIGO3 knockdown. This data show that AMIGO3 plays an important role in OL differentiation and myelination. This finding also shows that the increase of CNPase (a marker for OL differentiation) detected by Western blot (WB) in mixed glial cultures (Chapter 3), like the changes in myelin basic protein (MBP) detected in vivo (Foale *et al*., 2019), has a strong correlation with levels of AMIGO3 expression. In agreement with this, studies using adenovirus to knockdown AMIGO3 in the status convulsion model in vivo showed increased MBP levels after 1 and 5 days after the injury (Li *et al.*, 2021).

5.1.3 Recombinant human AMIGO3

As previously stated, AMIGO3 is downregulated during OPC/OL differentiation during postnatal development. Also, suppression of AMIGO3 expression by siRNA promoted OL differentiation, so this could be a potential method to encourage the remyelination process and treat demyelinating diseases such as multiple sclerosis (MS). These observations of

AMIGO3 expression suggested that a stimulation of AMIGO3 levels in mixed glial cultures can be a valuable method to provide stronger links between AMIGO3 and reduced OL differentiation. Therefore, in this study recombinant human AMIGO3 was used in mixed glial cultures and levels of CNPase expression were examined after this treatment. CNPase levels were reduced, as was the number of CC1+ cells. This data suggests that AMIGO3 is involved in inhibiting OL differentiation and maturation. Interestingly, the total cell population (DAPI+ cells) was reduced suggesting that AMIGO3 has effects on the growth of other glia. This finding fits with a previous study linking AMIGO2 ERK signalling to a regulation of fibroblast growth (Benedetti *et al.*, 2016).

As we stated previously, AMIGO3 and leucine rich repeat and Ig domain containing 1 (LINGO1) are able to interact with receptor complexes containing NgR1, p75/TROY and either AMIGO3 or LINGO1, leading to activation of RhoA signalling pathways (Ahmed *et al*., 2013; Mi *et al*., 2004). All of the key proteins in this pathway are expressed by OPC (Foale *et al*., 2019). Also in this study, we used the RhoA activation assay to determine the effects of AMIGO3 on RhoA levels in mixed glial cultures. We observed that recombinant AMIGO3 treatment stimulated RhoA activity in the glial cultures, and in Baby Hamster Kidney (BHK) cells. Both OPC and OL expressed AMIGO3 (Foale *et al*., 2019), also we showed that astrocyte can expresse AMIGO3 (Chapter 4). We don't know which glia responded, but it is possible that high levels of AMIGO3 lead to downregulated OPC/OL differentiation via Rho-associated protein kinase (ROCK)/RhoA signalling pathway (Mi *et al.*, 2004; Ahmed *et al.*, 2013).

5.1.4 The roles of leucin-rich repeat protein in mixed glial cell cultures

As previously mentioned the leucine rich repeat (LRR) is a protein structural motif of 20 to 30 amino acids in length that forms an α/β horseshoe fold (Bella *et al.*, 2008). In addition, LRR transmembrane proteins are essential in the development, function, and disorders of neural circuits (de Wit and Ghosh, 2014). Specifically, LRR proteins (LRRP) contribute to regulate axons guidance, synapse formation, target selection and stabilization of neuronal connections. Recently, studies shows that the LRRP function not only to organizing the neural connections in nervous system, but also, LRRP are implicated in various nervous system disorder (De Wit *et al.*, 2011). LINGO1 is a transmembrane protein containing LRR that has been therapeutically downregulated in clinical trials for MS and optic neuritis (Foale *et al.*, 2017; Ahmed, Fulton and Douglas, 2020; Kalafatakis *et al.*, 2023). Previous studies have shown the inhibitory effects of LRRP such as LINGO1 in OPC/OL differentiation (Mi et al., 2005). Inhibiting the action of LINGO1 protein in primary rodent and OPC cultures increased the production of myelin sheaths (MBP) (Mi et al., 2005), and overexpression of LINGO1 in primary OPC culture caused decreases in MBP level (Petrinovic *et al.*, 2010). In other neural cells, neurite growth was promoted rapidly in primary dorsal root ganglia and retinal cultures after knockdown of AMIGO3 (Ahmed *et al.*, 2013), LINGO1 had similar effects on neurite growth (Mi *et al.*, 2004). Further, inhibiting AMIGO3 expression in vivo reduced myelin sheath and synaptic damage caused by experimental convulsions, and increased the myelin production (Li *et al*., 2021). Also, in vivo overexpression of AMIGO3 suppressed OL cells and increased myelin damage (Li *et al.*, 2021).

Our data support the negative correlation between AMIGO3 expression and the early stage of myelination (OL differentiation) in the mixed glial model. Further, our data highlighted the link between AMIGO3 and RhoA signalling pathways. Interestingly, knockdown of

AMIGO3 promoted CNPase expression, and recombinant AMIGO3 decreased CNPase expression in mixed glial cultures. So, the negative correlation could represent actions involving RhoA/ROCK signalling leading to effects on actin dynamics required for the morphological differentiation of OL. Whether this mechanism involves NgR1 and p75/TROY (Ahmed *et al.*, 2013) is not known but could be explored by experiments involving recombinant AMIGO3 stimulation and siRNA knockdown of NgR1 and or p75/TROY (Li *et al.*, 2021).

5.1.5 AMIGO3 mechanism of action in OL

As we discussed previously, AMIGO3 can interact with AMIGO3/p75/TROY and NgR1 complex leading to activation of RhoA signalling pathways (Mi *et al.*, 2004; Ahmed *et al.*, 2013). Further, AMIGO3 is able to interact with the p75/TROY/ NgR1 complex in cell lines, which activates RhoA signalling pathway then leading to apoptosis of the cell (Ahmed *et al.*, 2013). In this study, we showed that AMIGO3 protein levels were increased following the recombinant AMIGO3 treatment in mixed glial cultures. It was also interesting to highlight that treatment with AMIGO3 actived RhoA signalling pathways. This finding matches with previous reports where overexpression of AMIGO3 leads to an increase in ROCK/RhoA expression (Li *et al.*, 2021). Moreover, COS7 cells transfected with full-length NgR1/p75 and AMIGO3 genes led to increased RhoA activity when the cells were stimulated with myelin fragments (Ahmed *et al.*, 2013). LINGO1 inhibited OL differentiation (Mi *et al.*, 2005), and this inhibition can be via the NgR1 signalling complex (Mi *et al.*, 2005) and in our studies we demonstrate that stimulation AMIGO3 expression leads to effects on OL differentiation via RhoA GTP signalling pathways. So, we suggest this could be further explored by designing an experiment using drugs to inhibit RhoA GTP pathway activity in mixed glial cultures.

5.1.6 AMIGO3 role in multiple sclerosis

LRRPs have been identified as a potential therapy for MS. LINGO1 inhibition has been used to promote and encourage the myelination process in MS but, the results of the clinical trials targeting LINGO1 have been failure (Foale *et al.*, 2017; Li *et al.*, 2021). Our data explain this failure of LINGO1 blocking therapy could be caused by the action of AMIGO3 leading to downregulation of the remyelination process. Especially because AMIGO3 is expressed, and can increase rapidly after injury (Ahmed *et al*., 2013). So, AMIGO3 is an alternative therapeutic target, and to target both AMIGO3 (extracellularly) and LINGO1 (intracellularly) could be more effective in promoting myelination in MS (Meabon *et al.*, 2015). In our study, we highlighted that AMIGO3 is highly expressed at the early stage of myelination in mixed glial cell cultures. However, in this study we haven't analysed AMIGO3 expression in samples from MS patients. Doing so would provide valuable data on AMIGO3 expression during different stage of MS that could help guide AMIGO3 therapeutic studies.

5.2 Limitation and future studies

5.2.1 Models of myelination

According to our knockdown results, AMIGO3 knockdown in primary mixed glial cultures indicate the negative effect of AMIGO3 during the early stage of the myelination. It would be interesting to knockdown both AMIGO3 and LINGO1 in primary mixed glial cultures and examine the level of CNPase. It would also be interesting to look at OL differentiation and myelination in vivo in an AMIGO3 knockout mouse, and to knockdown LINGO1 in this mouse.

Recombinant AMIGO3 was used in primary mixed glial cultures and the results indicate the effects of increased AMIGO3 levels during myelination with deceased CNPase expression. However, recombinant AMIGO3 has been tested in mixed glial culture with only two biological replicates, so it would be important to repeat the experiments with additional biological replicates. Also, it will be interesting to use AMIGO3 gene overexpression (e.g. via adenovirus associated virus vectors) rather than recombinant AMIGO3 (Li *et al.*, 2021). This method could be used in vivo to improve understanding of AMIGO3 functions.

5.2.2 Astrocytes and AMIGO3 expression

One of the interesting results in this study was the observation of AMIGO3 in astrocytes. AMIGO3 expression was detected by WB and immunocytochemistry (ICC). This finding shows that AMIGO3 is expressed by various cells within CNS. It would be interesting to study and investigate AMIGO3 expression by astrocyte using immunohistochemistry (IHC) in brain tissues. This study will provide a strong formational link between AMIGO3 and astrocyte cells within CNS. Also, in this study astrocyte cells were isolated by the shaking protocol, but we saw some contamination from other glia. It would be interesting to use magnetic cell sorting protocols to get a high selection of the astrocyte cells and ensure that AMIGO3 is expressed by astrocyte. Also, it would be interesting to stain astrocytes with multiple marker proteins (other than glial fibrillary acidic protein GFAP) to validate our findings. Further, in our study, we showed no expression of AMIGO3 and LINGO1 in microglia by WB. Our microglia ICC study was contaminated with other cells and we had low cell yields. It would be valuable to use different protocols to isolate microglia (e.g. magnetic cell sorting) from mixed glial cells and use multiple staining markers to confirm our data.

5.3 Final conclusions

AMIGO3 is expressed in glial cells within the CNS including astrocytes. We have found that AMIGO3 can downregulate OL differentiation in developing CNS cell cultures. AMIGO3 protein levels were increased during the early stage of OL development and decreased after differentiation appeared. Interestingly, in this study we observed that AMIGO3 increased before CNPase in the mixed glial model. This is similar to the pattern in vivo (Foale *et al*., 2019). Both AMIGO3 and LINGO1 patterns are similar, and both interact with p75/TROY and NgR1 complex presented by OPC cells. This interaction leads to higher activity of the RhoA signalling pathway (Ahmed *et al*., 2013; Mi *et al*., 2004), and this complex likely mediates downregulation of remyelination in the CNS (Foale *et al.*, 2017). Our knockdown and recombinant AMIGO3 data highlight AMIGO3 as a promising potential therapeutic target to promote the remyelination processes in demyelinating diseases. Future work to confirm this idea requires the use of methods such as knockout mice and the knockdown of multiple genes (e.g. AMIGO3 and LINGO1) in mixed glial cultures and in vivo.

References

Ahmed, Z. *et al.* (2013) 'AMIGO3 Is an NgR1/p75 Co-Receptor Signalling Axon Growth Inhibition in the Acute Phase of Adult Central Nervous System Injury', *PLOS ONE*, 8(4), p. e61878. doi:10.1371/JOURNAL.PONE.0061878.

Ahmed, Z., Fulton, D. and Douglas, M.R. (2020) 'Opicinumab: is it a potential treatment for multiple sclerosis?', *Annals of Translational Medicine*, 8(14), pp. 892–892. doi:10.21037/ATM.2020.03.131.

Alegria-Schaffer, A., Lodge, A. and Vattem, K. (2009) 'Chapter 33 Performing and Optimizing Western Blots with an Emphasis on Chemiluminescent Detection', *Methods in Enzymology*, 463(C), pp. 573–599. doi:10.1016/S0076-6879(09)63033-0.

Alizadeh, A., Dyck, S.M. and Karimi-Abdolrezaee, S. (2015) 'Myelin damage and repair in pathologic CNS: challenges and prospects', *Frontiers in Molecular Neuroscience*, 8(JULY). doi:10.3389/FNMOL.2015.00035.

Amini Harandi, A. *et al.* (2018) 'Balo's concentric sclerosis: An update and comprehensive literature review', *Reviews in the Neurosciences*, 29(8), pp. 873–882. doi:10.1515/REVNEURO-2017-0096/ASSET/GRAPHIC/J_REVNEURO-2017-0096_FIG_001.JPG.

Arnett, H.A. *et al.* (2004) 'bHLH transcription factor Olig1 is required to repair demyelinated lesions in the CNS', *Science*, 306(5704), pp. 2111–2115. doi:10.1126/SCIENCE.1103709/SUPPL_FILE/ARNETT.SOM.PDF.

Attwell, D. *et al.* (2016) 'What is a pericyte?', *Journal of Cerebral Blood Flow and Metabolism*, 36(2), pp. 451–455. doi:10.1177/0271678X15610340.

Avila, S. *et al.* (2019) 'A differential sex-specific pattern of IgG2 and IgG4 subclasses of anti-drug antibodies (ADAs) induced by glatiramer acetate in relapsing-remitting multiple

sclerosis patients', *Multiple Sclerosis and Related Disorders*, 34, pp. 92–99. doi:10.1016/J.MSARD.2019.06.021.

Azevedo, M.M. *et al.* (2018) 'Jmy regulates oligodendrocyte differentiation via modulation of actin cytoskeleton dynamics', *Glia*, 66(9), pp. 1826–1844. doi:10.1002/GLIA.23342.

Bella, J. *et al.* (2008) 'The leucine-rich repeat structure', *Cellular and Molecular Life Sciences*, 65(15), pp. 2307–2333. doi:10.1007/s00018-008-8019-0.

Benedetti, G. *et al.* (2016) 'IL-17A and TNF-α increase the expression of the antiapoptotic adhesion molecule Amigo-2 in arthritis synoviocytes', *Frontiers in Immunology*, 7(JUN), p. 196070. doi:10.3389/FIMMU.2016.00254/BIBTEX.

Bergles, D.E. and Richardson, W.D. (2016) 'Oligodendrocyte Development and Plasticity', *Cold Spring Harbor Perspectives in Biology*, 8(2). doi:10.1101/CSHPERSPECT.A020453.

Bin, J.M., Harris, S.N. and Kennedy, T.E. (2016) 'The oligodendrocyte-specific antibody "CC1" binds Quaking 7', *Journal of Neurochemistry*, 139(2), pp. 181–186. doi:10.1111/JNC.13745.

Block, M.L. and Hong, J.S. (2005) 'Microglia and inflammation-mediated neurodegeneration: Multiple triggers with a common mechanism', *Progress in Neurobiology*, 76(2), pp. 77–98. doi:10.1016/J.PNEUROBIO.2005.06.004.

Boggs, J.M. (2006) 'Myelin basic protein: a multifunctional protein', *Cellular and molecular life sciences : CMLS*, 63(17), pp. 1945–1961. doi:10.1007/S00018-006-6094-7.

Bonetto, G., Belin, D. and Káradóttir, R.T. (2021) 'Myelin: A gatekeeper of activity-dependent circuit plasticity?', *Science*, 374(6569). doi:10.1126/SCIENCE.ABA6905/ASSET/B1868569-EB16-4793-9AE6-92BB76BBA035/ASSETS/IMAGES/LARGE/SCIENCE.ABA6905-F3.JPG.

Booth, P.P.M. *et al.* (2022) 'Capillary electrophoresis Western blot using inkjet transfer to membrane', *Journal of Chromatography A*, 1679, p. 463389.

doi:10.1016/J.CHROMA.2022.463389.

Boullerne, A.I. (2016) ‘The history of myelin’, *Experimental Neurology*, 283, pp. 431–445. doi:10.1016/J.EXPNEUROL.2016.06.005.

Bradl, M. and Lassmann, H. (2010) ‘Oligodendrocytes: Biology and pathology’, *Acta Neuropathologica*, 119(1), pp. 37–53. doi:10.1007/S00401-009-0601-5/FIGURES/2.

Brodal, P. (2010) ‘The central nervous system : structure and function’, p. 591.

Bui, T. and Das, J.M. (2022) ‘Neuroanatomy, Cerebral Hemisphere’, *StatPearls* [Preprint]. Available at: https://www.ncbi.nlm.nih.gov/books/NBK549789/ (Accessed: 2 January 2023).

Butler, T.A.J. *et al.* (2019) ‘Misleading Westerns: Common Quantification Mistakes in Western Blot Densitometry and Proposed Corrective Measures’. doi:10.1155/2019/5214821.

Calvo-Garrido, J. *et al.* (2021) ‘Protocol for the derivation, culturing, and differentiation of human iPS-cell-derived neuroepithelial stem cells to study neural differentiation in vitro’, *STAR Protocols*, 2(2), p. 100528. doi:10.1016/J.XPRO.2021.100528.

Cantile, C. and Youssef, S. (2016) ‘Nervous System’, *Jubb, Kennedy & Palmer’s Pathology of Domestic Animals: Volume 1*, 1, p. 250. doi:10.1016/B978-0-7020-5317-7.00004-7.

Catala, M. and Kubis, N. (2013) ‘Gross anatomy and development of the peripheral nervous system’, *Handbook of Clinical Neurology*, 115, pp. 29–41. doi:10.1016/B978-0-444-52902-2.00003-5.

Ceprian, M. and Fulton, D. (2019) ‘Glial Cell AMPA Receptors in Nervous System Health, Injury and Disease’, *International Journal of Molecular Sciences 2019, Vol. 20, Page 2450*, 20(10), p. 2450. doi:10.3390/IJMS20102450.

Chauhan, P. *et al.* (2021) ‘The Anatomy of the Cerebral Cortex’, *Cerebral Ischemia* [Preprint]. Available at: http://europepmc.org/books/NBK575742 (Accessed: 2 January 2023).

Chen, Y., Hor, H.H. and Tang, B.L. (2012) ‘AMIGO is expressed in multiple brain cell types

and may regulate dendritic growth and neuronal survival', *Journal of Cellular Physiology*, 227(5), pp. 2217–2229. doi:10.1002/JCP.22958.

Colombo, J.A. (2018) 'Interlaminar Glia and Other Glial Themes Revisited: Pending Answers Following Three Decades of Glial Research', *Neuroglia 2018, Vol. 1, Pages 7-20*, 1(1), pp. 7–20. doi:10.3390/NEUROGLIA1010003.

Colonna, M. and Butovsky, O. (2017) 'Microglia Function in the Central Nervous System During Health and Neurodegeneration', *Annual review of immunology*, 35, p. 441. doi:10.1146/ANNUREV-IMMUNOL-051116-052358.

Cramer, G.D. and Darby, S.A. (2013) 'Clinical Anatomy of the Spine, Spinal Cord, and ANS', *Clinical Anatomy of the Spine, Spinal Cord, and ANS*, pp. 1–672. doi:10.1016/C2009-0-42801-0.

Cross, S.A. (2005) 'The Central Nervous System: Structure and Function, 3rd Edition', *Journal of Neuro-Ophthalmology*, 25(4), p. 335. doi:10.1097/01.WNO.0000190071.06611.B0.

Daneman, R. and Prat, A. (2015) 'The Blood–Brain Barrier', *Cold Spring Harbor Perspectives in Biology*, 7(1), p. a020412. doi:10.1101/CSHPERSPECT.A020412.

Diaz, E. and Morales, H. (2016) 'Spinal Cord Anatomy and Clinical Syndromes', *Seminars in Ultrasound, CT and MRI*, 37(5), pp. 360–371. doi:10.1053/J.SULT.2016.05.002.

Dobson, R. and Giovannoni, G. (2019) 'Multiple sclerosis – a review', *European Journal of Neurology*, 26(1), pp. 27–40. doi:10.1111/ENE.13819.

Dotiwala, A.K., McCausland, C. and Samra, N.S. (2023) 'Anatomy, Head and Neck: Blood Brain Barrier', *StatPearls* [Preprint]. Available at: https://www.ncbi.nlm.nih.gov/books/NBK519556/ (Accessed: 30 December 2023).

Dyment, D.A., Ebers, G.C. and Sadovnick, A.D. (2004) 'Genetics of multiple sclerosis', *The Lancet Neurology*, 3(2), pp. 104–110. doi:10.1016/S1474-4422(03)00663-X.

Eckstein, C., Saidha, S. and Levy, M. (2011) 'A differential diagnosis of central nervous system demyelination: beyond multiple sclerosis', *Journal of Neurology 2011 259:5*, 259(5), pp. 801–816. doi:10.1007/S00415-011-6240-5.

Falcone, C. *et al.* (2021) 'Cortical Interlaminar Astrocytes Are Generated Prenatally, Mature Postnatally, and Express Unique Markers in Human and Nonhuman Primates', *Cerebral Cortex*, 31(1), pp. 379–395. doi:10.1093/CERCOR/BHAA231.

Fannon, J., Tarmier, W. and Fulton, D. (2015) 'Neuronal activity and AMPA-type glutamate receptor activation regulates the morphological development of oligodendrocyte precursor cells', *Glia*, 63(6), pp. 1021–1035. doi:10.1002/GLIA.22799.

Farhy-Tselnicker, I. and Allen, N.J. (2018) 'Astrocytes, neurons, synapses: a tripartite view on cortical circuit development', *Neural Development 2018 13:1*, 13(1), pp. 1–12. doi:10.1186/S13064-018-0104-Y.

Fido, R.J., Tatham, A.S. and Shewry, P.R. (1995) 'Western blotting analysis.', *Methods in molecular biology (Clifton, N.J.)*, 49, pp. 423–437. doi:10.1385/0-89603-321-X:423/FIGURES/3.

Filipi, M. and Jack, S. (2020) 'Interferons in the Treatment of Multiple Sclerosis: A Clinical Efficacy, Safety, and Tolerability Update', *International Journal of MS Care*, 22(4), p. 165. doi:10.7224/1537-2073.2018-063.

Foale, S. *et al.* (2017) 'LINGO-1 and AMIGO3, potential therapeutic targets for neurological and dysmyelinating disorders?', *Neural Regeneration Research*, 12(8), p. 1247. doi:10.4103/1673-5374.213538.

Foale, S. (2019) 'Characterising the role of AMIGO3 in oligodendrocytes and demyelinating diseases', (August).

Franklin, R.J.M. and Ffrench-Constant, C. (2008) 'Remyelination in the CNS: from biology to therapy', *Nature Reviews Neuroscience 2008 9:11*, 9(11), pp. 839–855.

doi:10.1038/nrn2480.

Franklin, R.J.M. and Kotter, M.R. (2008) 'The biology of CNS remyelination', *Journal of Neurology 2008 255:1*, 255(1), pp. 19–25. doi:10.1007/S00415-008-1004-6.

Fujiyama, F., Furuta, T. and Kaneko, T. (2001) 'Immunocytochemical localization of candidates for vesicular glutamate transporters in the rat cerebral cortex', *Journal of Comparative Neurology*, 435(3), pp. 379–387. doi:10.1002/CNE.1037.

Fulton, D., Paez, P.M. and Campagnoni, A.T. (2010) 'The multiple roles of myelin protein genes during the development of the oligodendrocyte', *ASN neuro*, 2(1), pp. 25–37. doi:10.1042/AN20090051.

Gallo-Oller, G., Ordoñez, R. and Dotor, J. (2018) 'A new background subtraction method for Western blot densitometry band quantification through image analysis software', *Journal of Immunological Methods*, 457, pp. 1–5. doi:10.1016/J.JIM.2018.03.004.

Gavrilov, K. and Saltzman, W.M. (2012) 'Therapeutic siRNA: Principles, Challenges, and Strategies', *The Yale Journal of Biology and Medicine*, 85(2), p. 187. Available at: /pmc/articles/PMC3375670/ (Accessed: 11 June 2023).

Ghasemi, N., Razavi, S. and Nikzad, E. (2017) 'Multiple Sclerosis: Pathogenesis, Symptoms, Diagnoses andCell-Based Therapy', *Cell Journal (Yakhteh)*, 19(1), p. 1. doi:10.22074/CELLJ.2016.4867.

Gibson, E.M. *et al.* (2014) 'Neuronal activity promotes oligodendrogenesis and adaptive myelination in the mammalian brain', *Science*, 344(6183). doi:10.1126/SCIENCE.1252304/SUPPL_FILE/PAPV2.PDF.

Ginhoux, F. *et al.* (2013) 'Origin and differentiation of microglia', *Frontiers in Cellular Neuroscience*, 0(MAR), p. 45. doi:10.3389/FNCEL.2013.00045/BIBTEX.

Gordon, R. *et al.* (2011) 'A simple magnetic separation method for high-yield isolation of pure primary microglia', *Journal of Neuroscience Methods*, 194(2), pp. 287–296.

doi:10.1016/J.JNEUMETH.2010.11.001.

Gudz, T.I. *et al.* (2002) 'Myelin Proteolipid Protein Forms a Complex with Integrins and May Participate in Integrin Receptor Signaling in Oligodendrocytes', *The Journal of Neuroscience*, 22(17), p. 7398. doi:10.1523/JNEUROSCI.22-17-07398.2002.

Hall, A. (1998) 'Rho GTpases and the actin cytoskeleton', *Science*, 279(5350), pp. 509–514. doi:10.1126/SCIENCE.279.5350.509/ASSET/BA3BA44B-6EFA-45C0-9E4D-6F324E5F7690/ASSETS/GRAPHIC/SE0386202005.JPEG.

Haq, E. *et al.* (2003) 'Molecular mechanism of psychosine-induced cell death in human oligodendrocyte cell line', *Journal of Neurochemistry*, 86(6), pp. 1428–1440. doi:10.1046/J.1471-4159.2003.01941.X.

Hauser, S.L. and Cree, B.A.C. (2020) 'Treatment of Multiple Sclerosis: A Review', *The American Journal of Medicine*, 133(12), pp. 1380-1390.e2. doi:10.1016/J.AMJMED.2020.05.049.

Hjorth, M., Dandu, N. and Mellergård, J. (2020) 'Treatment effects of fingolimod in multiple sclerosis: Selective changes in peripheral blood lymphocyte subsets', *PLOS ONE*, 15(2), p. e0228380. doi:10.1371/JOURNAL.PONE.0228380.

Howell, O.W. *et al.* (2006) 'Disruption of neurofascin localization reveals early changes preceding demyelination and remyelination in multiple sclerosis', *Brain*, 129(12), pp. 3173–3185. doi:10.1093/BRAIN/AWL290.

Hu, W. and Lucchinetti, C.F. (2009) 'The pathological spectrum of CNS inflammatory demyelinating diseases', *Seminars in Immunopathology*, 31(4), pp. 439–453. doi:10.1007/S00281-009-0178-Z/FIGURES/8.

Jacobs, E.C. *et al.* (2005) 'Region-Specific Myelin Pathology in Mice Lacking the Golli Products of the Myelin Basic Protein Gene', *The Journal of Neuroscience*, 25(30), p. 7004. doi:10.1523/JNEUROSCI.0288-05.2005.

Jafferali, M.H. *et al.* (2021) 'Benchmarking virus concentration methods for quantification of SARS-CoV-2 in raw wastewater', *Science of The Total Environment*, 755, p. 142939. doi:10.1016/J.SCITOTENV.2020.142939.

Jessen, K.R. (2004) 'Glial cells', *The International Journal of Biochemistry & Cell Biology*, 36(10), pp. 1861–1867. doi:10.1016/J.BIOCEL.2004.02.023.

Ji, B. *et al.* (2006) 'LINGO-1 antagonist promotes functional recovery and axonal sprouting after spinal cord injury', *Molecular and Cellular Neuroscience*, 33(3), pp. 311–320. doi:10.1016/J.MCN.2006.08.003.

Kajava, A. V. (1998) 'Structural diversity of leucine-rich repeat proteins', *Journal of Molecular Biology*, 277(3), pp. 519–527. doi:10.1006/JMBI.1998.1643.

Kalafatakis, I. *et al.* (2023) 'Nogo-A and LINGO-1: Two Important Targets for Remyelination and Regeneration', *International Journal of Molecular Sciences 2023, Vol. 24, Page 4479*, 24(5), p. 4479. doi:10.3390/IJMS24054479.

Kasindi, A. *et al.* (2022) 'Glatiramer Acetate Immunomodulation: Evidence of Neuroprotection and Cognitive Preservation', *Cells 2022, Vol. 11, Page 1578*, 11(9), p. 1578. doi:10.3390/CELLS11091578.

Kaskow, B.J. and Baecher-Allan, C. (2018) 'Effector T Cells in Multiple Sclerosis', *Cold Spring Harbor Perspectives in Medicine*, 8(4), p. a029025. doi:10.1101/CSHPERSPECT.A029025.

Khaledian, S. *et al.* (2022) 'Efficiency of lipid-based nano drug delivery systems in crossing the blood–brain barrier: A review', *Journal of Molecular Liquids*, 346, p. 118278. doi:10.1016/J.MOLLIQ.2021.118278.

Kierdorf, K. and Prinz, M. (2013) 'Factors regulating microglia activation', *Frontiers in Cellular Neuroscience*, 7(MAR), p. 44. doi:10.3389/FNCEL.2013.00044/BIBTEX.

Kim, Y., Park, J. and Choi, Y.K. (2019) 'cused on BK Channel and Heme OxygenaThe Role

of Astrocytes in the Central Nervous System Fose Metabolites: A Review', *Antioxidants 2019, Vol. 8, Page 121*, 8(5), p. 121. doi:10.3390/ANTIOX8050121.

Kira, J.I. (2011) 'Astrocytopathy in Baló's disease', *Multiple Sclerosis Journal*, 17(7), pp. 771–779. doi:10.1177/1352458511400475.

Kirischuk, S. *et al.* (2016) 'Astrocyte sodium signaling and the regulation of neurotransmission', *Glia*, 64(10), pp. 1655–1666. doi:10.1002/glia.22943.

Kister, A. and Kister, I. (2022) 'Overview of myelin, major myelin lipids, and myelin-associated proteins', *Frontiers in Chemistry*, 10, p. 1041961. doi:10.3389/FCHEM.2022.1041961/BIBTEX.

Kouhi, A. *et al.* (2021) 'Brain Disposition of Antibody-Based Therapeutics: Dogma, Approaches and Perspectives', *International Journal of Molecular Sciences 2021, Vol. 22, Page 6442*, 22(12), p. 6442. doi:10.3390/IJMS22126442.

Kuehn, M.H., Fingert, J.H. and Kwon, Y.H. (2005) 'Retinal Ganglion Cell Death in Glaucoma: Mechanisms and Neuroprotective Strategies'. doi:10.1016/j.ohc.2005.04.002.

Kuja-Panula, J. *et al.* (2003) 'AMIGO, a transmembrane protein implicated in axon tract development, defines a novel protein family with leucine-rich repeats', *Journal of Cell Biology*, 160(6), pp. 963–973. doi:10.1083/JCB.200209074.

Lalive, P.H. *et al.* (2011) 'Glatiramer acetate in the treatment of multiple sclerosis: Emerging concepts regarding its mechanism of action', *CNS Drugs*, 25(5), pp. 401–414. doi:10.2165/11588120-000000000-00000/FIGURES/1.

Ledford, H. (2015) 'Drug that boosts nerve signals offers hope for multiple sclerosis', *Nature*, 520(7548), p. 417. doi:10.1038/520417A.

Lee, H.G., Wheeler, M.A. and Quintana, F.J. (2022) 'Function and therapeutic value of astrocytes in neurological diseases', *Nature Reviews Drug Discovery 2022 21:5*, 21(5), pp. 339–358. doi:10.1038/s41573-022-00390-x.

Levine, J.M., Reynolds, R. and Fawcett, J.W. (2001) 'The oligodendrocyte precursor cell in health and disease', *Trends in Neurosciences*, 24(1), pp. 39–47. doi:10.1016/S0166-2236(00)01691-X.

Li, N. and Leung, G.K.K. (2015) 'Oligodendrocyte Precursor Cells in Spinal Cord Injury: A Review and Update', *BioMed Research International*, 2015. doi:10.1155/2015/235195.

Li, X. *et al.* (2021) 'The Role and Mechanism of AMIGO3 in the Formation of Aberrant Neural Circuits After Status Convulsion in Immature Mice', *Frontiers in Molecular Neuroscience*, 14. doi:10.3389/FNMOL.2021.748115.

Liang, X., Draghi, N.A. and Resh, M.D. (2004) 'Signaling from integrins to Fyn to Rho family GTPases regulates morphologic differentiation of oligodendrocytes', *Journal of Neuroscience*, 24(32), pp. 7140–7149. doi:10.1523/JNEUROSCI.5319-03.2004.

Lim, B.C. and Rasband, M.N. (2020) 'Saltatory Conduction: Jumping to New Conclusions', *Current Biology*, 30(7), pp. R326–R328. doi:10.1016/J.CUB.2020.02.037.

Lin, L. *et al.* (2017) 'Characteristics of primary rat microglia isolated from mixed cultures using two different methods', *Journal of Neuroinflammation*, 14(1), pp. 1–10. doi:10.1186/s12974-017-0877-7.

Linnerbauer, M., Wheeler, M.A. and Quintana, F.J. (2020) 'Astrocyte Crosstalk in CNS Inflammation', *Neuron*, 108(4), pp. 608–622. doi:10.1016/J.NEURON.2020.08.012.

Liu, Z. *et al.* (2007) 'Induction of oligodendrocyte differentiation by Olig2 and Sox10: Evidence for reciprocal interactions and dosage-dependent mechanisms', *Developmental Biology*, 302(2), pp. 683–693. doi:10.1016/J.YDBIO.2006.10.007.

Lööv, C. *et al.* (2012) 'Neutralization of LINGO-1 during In Vitro Differentiation of Neural Stem Cells Results in Proliferation of Immature Neurons', *PLOS ONE*, 7(1), p. e29771. doi:10.1371/JOURNAL.PONE.0029771.

Lu, Y. *et al.* (2013) 'TROY interacts with Rho guanine nucleotide dissociation inhibitor α

(RhoGDIα) to mediate nogo-induced inhibition of neurite outgrowth', *Journal of Biological Chemistry*, 288(47), pp. 34276–34286. doi:10.1074/jbc.M113.519744.

Lubetzki, C. *et al.* (2020) 'Remyelination in multiple sclerosis: from basic science to clinical translation', *The Lancet Neurology*, 19(8), pp. 678–688. doi:10.1016/S1474-4422(20)30140-X.

Mahmoud, S. *et al.* (2019) 'Astrocytes Maintain Glutamate Homeostasis in the CNS by Controlling the Balance between Glutamate Uptake and Release', *Cells 2019, Vol. 8, Page 184*, 8(2), p. 184. doi:10.3390/CELLS8020184.

Mancardi, G. and Saccardi, R. (2008) 'Autologous haematopoietic stem-cell transplantation in multiple sclerosis', *The Lancet Neurology*, 7(7), pp. 626–636. doi:10.1016/S1474-4422(08)70138-8.

Mason, S. (2017) 'Lactate shuttles in neuroenergetics-homeostasis, allostasis and beyond', *Frontiers in Neuroscience*, 11(FEB), p. 239964. doi:10.3389/FNINS.2017.00043/BIBTEX.

Mayo, L., Quintana, F.J. and Weiner, H.L. (2012) 'The Innate Immune System in Demyelinating Disease', *Immunological Reviews*, 248(1), p. 170. doi:10.1111/J.1600-065X.2012.01135.X.

McCorry, L.K. (2007) 'Physiology of the Autonomic Nervous System', *American Journal of Pharmaceutical Education*, 71(4). doi:10.5688/AJ710478.

McGinley, M.P., Goldschmidt, C.H. and Rae-Grant, A.D. (2021) 'Diagnosis and Treatment of Multiple Sclerosis: A Review', *JAMA*, 325(8), pp. 765–779. doi:10.1001/JAMA.2020.26858.

Meabon, J.S. *et al.* (2015) 'LINGO-1 protein interacts with the p75 neurotrophin receptor in intracellular membrane compartments', *Journal of Biological Chemistry*, 290(15), pp. 9511–9520. doi:10.1074/jbc.M114.608018.

Mi, S. *et al.* (2004) 'LINGO-1 is a component of the Nogo-66 receptor/p75 signaling

complex', *Nature Neuroscience 2004 7:3*, 7(3), pp. 221–228. doi:10.1038/nn1188.

Mi, S. *et al.* (2005) 'LINGO-1 negatively regulates myelination by oligodendrocytes', *Nature Neuroscience 2005 8:6*, 8(6), pp. 745–751. doi:10.1038/nn1460.

Mi, S., Blake Pepinsky, R. and Cadavid, D. (2013) 'Blocking LINGO-1 as a therapy to promote CNS repair: From concept to the clinic', *CNS Drugs*, 27(7), pp. 493–503. doi:10.1007/S40263-013-0068-8/TABLES/1.

Mi, S., Sandrock, A. and Miller, R.H. (2008) 'LINGO-1 and its role in CNS repair', *The International Journal of Biochemistry & Cell Biology*, 40(10), pp. 1971–1978. doi:10.1016/J.BIOCEL.2008.03.018.

Migliaccio, F. *et al.* (2022) 'Microglia Depletion from Primary Glial Cultures Enables to Accurately Address the Immune Response of Astrocytes', *Biomolecules 2022, Vol. 12, Page 666*, 12(5), p. 666. doi:10.3390/BIOM12050666.

Min, Y. *et al.* (2009) 'Interaction forces and adhesion of supported myelin lipid bilayers modulated by myelin basic protein', *Proceedings of the National Academy of Sciences of the United States of America*, 106(9), pp. 3154–3159. doi:10.1073/PNAS.0813110106/ASSET/F52BE036-BAAA-4E3C-94E3-54C418DBB9DC/ASSETS/GRAPHIC/ZPQ9990967380005.JPEG.

Mirsky, R. *et al.* (2002) 'Schwann cells as regulators of nerve development', *Journal of Physiology-Paris*, 96(1–2), pp. 17–24. doi:10.1016/S0928-4257(01)00076-6.

Molina-Gonzalez, I. and Miron, V.E. (2019) 'Astrocytes in myelination and remyelination', *Neuroscience Letters*, 713, p. 134532. doi:10.1016/J.NEULET.2019.134532.

Monk, K.R., Feltri, M.L. and Taveggia, C. (2015) 'New insights on schwann cell development', *Glia*, 63(8), pp. 1376–1393. doi:10.1002/GLIA.22852.

Moore, C.S. *et al.* (2011) 'How factors secreted from astrocytes impact myelin repair', *Journal of Neuroscience Research*, 89(1), pp. 13–21. doi:10.1002/JNR.22482.

Morell, P. (2013) ‘Myelin’, p. 545.

Mullins, R.D., Heuser, J.A. and Pollard, T.D. (1998) ‘The interaction of Arp2/3 complex with actin: Nucleation, high affinity pointed end capping, and formation of branching networks of filaments’, *Proceedings of the National Academy of Sciences*, 95(11), pp. 6181–6186. doi:10.1073/PNAS.95.11.6181.

Ndubaku, U. and de Bellard, M.E. (2008) ‘Glial cells: Old cells with new twists’, *Acta Histochemica*, 110(3), pp. 182–195. doi:10.1016/J.ACTHIS.2007.10.003.

Newell, K.L. and Tessa Hedley-Whyte, E. (2003) ‘Glia’, *Encyclopedia of the Neurological Sciences*, pp. 452–455. doi:10.1016/B0-12-226870-9/01523-9.

Nicola J. Allen and Ben A. Barres (2009) ‘Glia-more than just brain glue’, *Nature*, 457(February), pp. 675–677.

Nógrádi, A. and Vrbová, G. (2006) ‘Anatomy and Physiology of the Spinal Cord’, *Transplantation of Neural Tissue into the Spinal Cord*, pp. 1–23. doi:10.1007/0-387-32633-2_1.

Nouh, R.A. *et al.* (2024) ‘Unveiling the Potential of Cannabinoids in Multiple Sclerosis and the Dawn of Nano-Cannabinoid Medicine’, *Pharmaceutics 2024, Vol. 16, Page 241*, 16(2), p. 241. doi:10.3390/PHARMACEUTICS16020241.

Pang, Y. *et al.* (2012) ‘Neuron-oligodendrocyte myelination co-culture derived from embryonic rat spinal cord and cerebral cortex’, *Brain and Behavior*, 2(1), pp. 53–67. doi:10.1002/BRB3.33.

Patel, M.M. *et al.* (2009) ‘Getting into the brain: Approaches to enhance brain drug delivery’, *CNS Drugs*, 23(1), pp. 35–58. doi:10.2165/0023210-200923010-00003/FIGURES/6.

Petrinovic, M.M. *et al.* (2010) ‘Neuronal Nogo-A regulates neurite fasciculation, branching and extension in the developing nervous system’, *Development*, 137(15), pp. 2539–2550. doi:10.1242/DEV.048371.

Petrović, A. *et al.* (2021) 'Establishment of Long-Term Primary Cortical Neuronal Cultures From Neonatal Opossum Monodelphis domestica', *Frontiers in Cellular Neuroscience*, 15, p. 75. doi:10.3389/FNCEL.2021.661492/BIBTEX.

Pillai-Kastoori, L., Schutz-Geschwender, A.R. and Harford, J.A. (2020) 'A systematic approach to quantitative Western blot analysis', *Analytical Biochemistry*, 593, p. 113608. doi:10.1016/J.AB.2020.113608.

Popescu, B.F.G., Pirko, I. and Lucchinetti, C.F. (2013) 'Pathology of Multiple Sclerosis: Where Do We Stand?', *Continuum : Lifelong Learning in Neurology*, 19(4 Multiple Sclerosis), p. 901. doi:10.1212/01.CON.0000433291.23091.65.

Quan, Y. *et al.* (2020) 'Inhibition of the leucine-rich repeat protein lingo-1 enhances RGC survival in optic nerve injury', *Experimental and Therapeutic Medicine*, 19(1), pp. 619–629. doi:10.3892/ETM.2019.8250.

Ramos González, E.J. *et al.* (2021) 'A comparative study of melatonin and immunomodulatory therapy with interferon beta and glatiramer acetate in a mouse model of multiple sclerosis', *Neurología (English Edition)*, 36(4), pp. 262–270. doi:10.1016/J.NRLENG.2018.01.004.

Rao, D.D. *et al.* (2009) 'siRNA vs. shRNA: Similarities and differences', *Advanced Drug Delivery Reviews*, 61(9), pp. 746–759. doi:10.1016/J.ADDR.2009.04.004.

Rejdak, K., Jackson, S. and Giovannoni, G. (2010) 'Multiple sclerosis: a practical overview for clinicians', *British Medical Bulletin*, 95(1), pp. 79–104. doi:10.1093/BMB/LDQ017.

Rice, J. and Cameron, M. (2017) 'Cannabinoids for Treatment of MS Symptoms: State of the Evidence', *Current Neurology and Neuroscience Reports*, 18(8), pp. 1–10. doi:10.1007/S11910-018-0859-X/TABLES/1.

Richardson, W.D., Kessaris, N. and Pringle, N. (2006) 'Oligodendrocyte wars', *Nature Reviews Neuroscience*, 7(1), pp. 11–18. doi:10.1038/NRN1826.

Van Rossum, D. and Hanisch, U.K. (2004) 'Microglia', *Metabolic Brain Disease 2004 19:3*, 19(3), pp. 393–411. doi:10.1023/B:MEBR.0000043984.73063.D8.

Satoh, J. *et al.* (2007) 'TROY and LINGO-1 expression in astrocytes and macrophages/microglia in multiple sclerosis lesions', *Neuropathology and Applied Neurobiology*, 33(1), pp. 99–107. doi:10.1111/J.1365-2990.2006.00787.X.

Schwarz, D.S. *et al.* (2006) 'Designing siRNA That Distinguish between Genes That Differ by a Single Nucleotide', *PLOS Genetics*, 2(9), p. e140. doi:10.1371/JOURNAL.PGEN.0020140.

Scott, N., Witt, K. and Schober, J.M. (2022) 'A simplified procedure for isolation of primary murine microglia', *BioTechniques*, 73(6), pp. 273–279. doi:10.2144/BTN-2022-0054/ASSET/IMAGES/LARGE/FIGURE4.JPEG.

Semizarov, D. *et al.* (2003) 'From the Cover: Specificity of short interfering RNA determined through gene expression signatures', *Proceedings of the National Academy of Sciences of the United States of America*, 100(11), p. 6347. doi:10.1073/PNAS.1131959100.

Serlin, Y. *et al.* (2015) 'Anatomy and physiology of the blood–brain barrier', *Seminars in Cell & Developmental Biology*, 38, pp. 2–6. doi:10.1016/J.SEMCDB.2015.01.002.

Serwanski, D.R., Jukkola, P. and Nishiyama, A. (2017) 'Heterogeneity of astrocyte and NG2 cell insertion at the node of Ranvier', *The Journal of comparative neurology*, 525(3), p. 535. doi:10.1002/CNE.24083.

Shapiro, L.A., Wang, L. and Ribak, C.E. (2008) 'Rapid astrocyte and microglial activation following pilocarpine-induced seizures in rats', *Epilepsia*, 49(SUPPL. 2), pp. 33–41. doi:10.1111/j.1528-1167.2008.01491.x.

Skaper, S.D. (2019) 'Oligodendrocyte precursor cells as a therapeutic target for demyelinating diseases', *Progress in Brain Research*, 245, pp. 119–144. doi:10.1016/BS.PBR.2019.03.013.

Sofroniew, M. V. (2015) ‘Astrocyte barriers to neurotoxic inflammation’, *Nature reviews. Neuroscience*, 16(5), pp. 249–263. doi:10.1038/NRN3898.

Sofroniew, M. V and Vinters, H. V (2010) ‘Astrocytes: biology and pathology’, *Acta Neuropathologica*, 119(1), p. 7. doi:10.1007/S00401-009-0619-8.

Speicher, A.M. *et al.* (2019) ‘Generating microglia from human pluripotent stem cells: Novel in vitro models for the study of neurodegeneration’, *Molecular Neurodegeneration*, 14(1), pp. 1–16. doi:10.1186/S13024-019-0347-Z/TABLES/3.

Suárez-Patiño, S.F. *et al.* (2019) ‘Semliki Forest Virus replicon particles production in serum-free medium BHK-21 cell cultures and their use to express different proteins’, *Cytotechnology*, 71(5), pp. 949–962. doi:10.1007/S10616-019-00337-Y/FIGURES/5.

Tan, H.B. *et al.* (2011) ‘Rho/ROCK pathway and neural regeneration: a potential therapeutic target for central nervous system and optic nerve damage’, *International Journal of Ophthalmology*, 4(6), p. 652. doi:10.3980/J.ISSN.2222-3959.2011.06.16.

Tata, M., Ruhrberg, C. and Fantin, A. (2015) ‘Vascularisation of the central nervous system’, *Mechanisms of Development*, 138, pp. 26–36. doi:10.1016/J.MOD.2015.07.001.

Tatsumi, K. *et al.* (2018) ‘Olig2-Lineage astrocytes: A distinct subtype of astrocytes that differs from GFAP astrocytes’, *Frontiers in Neuroanatomy*, 12(8), p. 312356. doi:10.3389/FNANA.2018.00008/BIBTEX.

Tickle, J. (2013) ‘The role of amphoterin-induced gene and open reading frame (AMIGO) family in myelination and neurodegeneration and Investigating the roles of mesenchymal and hematopoietic stem cell conditioned media on neutrophil recruitment in a model of inflammation’.

Trebst, C. *et al.* (2013) ‘Update on the diagnosis and treatment of neuromyelitis optica: Recommendations of the Neuromyelitis Optica Study Group (NEMOS)’, *Journal of Neurology 2013 261:1*, 261(1), pp. 1–16. doi:10.1007/S00415-013-7169-7.

Vasile, F., Dossi, E. and Rouach, N. (2017) 'Human astrocytes: structure and functions in the healthy brain', *Brain Structure and Function*, 222(5), pp. 2017–2029. doi:10.1007/S00429-017-1383-5/FIGURES/2.

Villoslada, P. (2016) 'Neuroprotective therapies for multiple sclerosis and other demyelinating diseases', *Multiple Sclerosis and Demyelinating Disorders 2016 1:1*, 1(1), pp. 1–11. doi:10.1186/S40893-016-0004-0.

Wake, H. *et al.* (2013) 'Microglia: actively surveying and shaping neuronal circuit structure and function', *Trends in Neurosciences*, 36(4), pp. 209–217. doi:10.1016/J.TINS.2012.11.007.

Waxman, S.G. and Swadlow, H.A. (1977) 'The conduction properties of axons in central white matter', *Progress in Neurobiology*, 8(PART 4), pp. 297–324. doi:10.1016/0301-0082(77)90009-0.

Wei, D.C. and Morrison, E.H. (2019) 'Histology, Astrocytes', *StatPearls* [Preprint]. Available at: http://europepmc.org/books/NBK545142 (Accessed: 30 June 2022).

Wiendl, H. *et al.* (2008) 'Basic and escalating immunomodulatory treatments in multiple sclerosis: Current therapeutic recommendations', *Journal of Neurology 2008 255:10*, 255(10), pp. 1449–1463. doi:10.1007/S00415-008-0061-1.

Williamson, J.M. and Lyons, D.A. (2018) 'Myelin dynamics throughout life: An ever-changing landscape?', *Frontiers in Cellular Neuroscience*, 12, p. 424. doi:10.3389/FNCEL.2018.00424/BIBTEX.

Willison, H.J., Jacobs, B.C. and van Doorn, P.A. (2016) 'Guillain-Barré syndrome', *The Lancet*, 388(10045), pp. 717–727. doi:10.1016/S0140-6736(16)00339-1.

Wingerchuk, D.M. *et al.* (2007) 'The spectrum of neuromyelitis optica', *The Lancet Neurology*, 6(9), pp. 805–815. doi:10.1016/S1474-4422(07)70216-8.

De Wit, J. *et al.* (2011) 'Role of leucine-rich repeat proteins in the development and function

of neural circuits', *Annual Review of Cell and Developmental Biology*, 27, pp. 697–729. doi:10.1146/annurev-cellbio-092910-154111.

de Wit, J. and Ghosh, A. (2014) 'Control of neural circuit formation by leucine-rich repeat proteins', *Trends in Neurosciences*, 37(10), pp. 539–550. doi:10.1016/J.TINS.2014.07.004.

Wojciak-Stothard, B. and Ridley, A.J. (2003) 'Shear stress–induced endothelial cell polarization is mediated by Rho and Rac but not Cdc42 or PI 3-kinases', *Journal of Cell Biology*, 161(2), pp. 429–439. doi:10.1083/JCB.200210135.

Wu, H.F. *et al.* (2013) 'The promotion of functional recovery and nerve regeneration after spinal cord injury by lentiviral vectors encoding Lingo-1 shRNA delivered by Pluronic F-127', *Biomaterials*, 34(6), pp. 1686–1700. doi:10.1016/J.BIOMATERIALS.2012.11.013.

Xie, Y. *et al.* (2024) 'Antagonizing LINGO-1 reduces activated microglia and alleviates dendritic spine loss in the hippocampus of APP/PS1 transgenic mice', *Neuroscience Letters*, 820, p. 137612. doi:10.1016/J.NEULET.2023.137612.

Yang, T. *et al.* (2020) 'Dissecting the Dual Role of the Glial Scar and Scar-Forming Astrocytes in Spinal Cord Injury', *Frontiers in Cellular Neuroscience*, 14, p. 515129. doi:10.3389/FNCEL.2020.00078/BIBTEX.

Yong, V.W. (2022) 'Microglia in multiple sclerosis: Protectors turn destroyers', *Neuron*, 110(21), pp. 3534–3548. doi:10.1016/J.NEURON.2022.06.023.

Young, E.A. *et al.* (2008) 'Imaging correlates of decreased axonal Na+/K+ ATPase in chronic multiple sclerosis lesions', *Annals of Neurology*, 63(4), pp. 428–435. doi:10.1002/ANA.21381.

Zhang, J.H. *et al.* (2005) 'Mechanisms of hyperbaric oxygen and neuroprotection in stroke', *Pathophysiology*, 12(1), pp. 63–77. doi:10.1016/J.PATHOPHYS.2005.01.003.

Zhang, Y. *et al.* (2014) 'An RNA-Sequencing Transcriptome and Splicing Database of Glia, Neurons, and Vascular Cells of the Cerebral Cortex', *Journal of Neuroscience*, 34(36), pp.

11929–11947. doi:10.1523/JNEUROSCI.1860-14.2014.

Zhang, Y. *et al.* (2015) ‘Inhibition of LINGO-1 promotes functional recovery after experimental spinal cord demyelination’, *Experimental Neurology*, 266, pp. 68–73. doi:10.1016/J.EXPNEUROL.2015.02.006.

Zhao, X. *et al.* (2018) ‘Lentiviral vector delivery of short hairpin RNA to NgR1 promotes nerve regeneration and locomotor recovery in injured rat spinal cord’, *Scientific Reports 2018 8:1*, 8(1), pp. 1–10. doi:10.1038/s41598-018-23751-2.

Zuchero, J.B. *et al.* (2015) ‘Article CNS Myelin Wrapping Is Driven by Actin Disassembly’, *Developmental Cell*, 34, pp. 152–167. doi:10.1016/j.devcel.2015.06.011.